

DYNAMIC ROLE OF THE CODON 72 P53 SINGLE NUCLEOTIDE POLYMORPHISM
IN MAMMARY TUMORIGENESIS IN A HUMANIZED MOUSE MODEL

A Dissertation

by

RAMESH THARINDU GUNARATNA

Submitted to the Office of Graduate and Professional Studies of
Texas A&M University
in partial fulfillment of the requirements for the degree of

DOCTOR OF PHILOSOPHY

Chair of Committee,	Robin S. Fuchs-Young
Committee Members,	Robert S. Chapkin
	J. Timothy Lightfoot
	Farida Sohrabji
Intercollegiate Faculty Chair,	Dorothy Shippen

May 2018

Major Subject: Genetics

Copyright 2018 Ramesh T Gunaratna

ABSTRACT

Female breast cancer (BrCa) is the most common noncutaneous cancer among women in the United States. Human epidemiological studies reveal that p53 codon 72 single nucleotide variants, encoding proline (P72) or arginine (R72), are associated with increased risk of several cancers, including BrCa. However, the molecular mechanisms by which these variants affect mammary tumorigenesis remain unresolved. To investigate the effects of this polymorphism on susceptibility to mammary cancer, we used a humanized p53 mouse model, homozygous for either P72 or R72. R72 mice had a significantly higher mammary tumor incidence and reduced latency in both DMBA-induced and MMTV-ErbB2/Neu mouse mammary tumor models. Our studies revealed that susceptible mammary glands of E-R72 mice developed a senescence-associated secretory phenotype (SASP), with influx of proinflammatory macrophages, ultimately resulting in chronic, pro-tumorigenic inflammation. Mammary tumors arising in E-R72 mice also had increased proliferation and influx of tumor-associated macrophages, contributing to angiogenesis and elevated tumor growth rates. These results demonstrate that the R72 variant increases susceptibility to aggressive BrCas through chronic inflammation, suggesting potential benefits of anti-inflammatory agents in the prevention or treatment of BrCa in women who are homozygous for the R72 variant.

DEDICATION

To my parents, and my wife for all their love, sacrifices and for shaping me to be the person who I am today.

ACKNOWLEDGEMENTS

There are many who were instrumental in completing the work described herewith and without their support, this work would not be possible. First, I sincerely thank my advisor, Dr. Robin Fuchs-Young for allowing a molecular entomologist to transition into the world of cancer research. I am thankful to her for the opportunities I had to present my work at various conferences/forums, for taking time and being patient to improve my writing, presentation skills and for her valuable advice and guidance.

I would like to thank my committee members, Dr. Farida Sohrabji, Dr. Tim Lightfoot and Dr. Robert Chapkin for serving on my committee amidst their busy schedules, for their helpful input regarding my work and for their kind words of encouragement. I am also thankful to you for asking me to write an off-topic proposal for my preliminary examination, which gave me a lot of confidence to push forward in graduate school. I would also like to thank Dr. Geoffrey Kapler at the department of Molecular and Cellular Medicine and Dr. Dorothy Shippen of the IDP in Genetics for supporting me financially, which has allowed me to focus on my research work. Some of the work reported in this dissertation would not have been possible without the generous support of Dr. David Threadgill and Dr. Weston Porter. They allowed me to use their instruments, reagents and even allowed their lab personnel to provide me with necessary training. While I thank all the members of their labs for welcoming me into their labs even during late hours and weekends, I like to thank especially, Bill Barrington, Danila Cuomo, Jessica Elswood and Scott Pearson for taking time off to train me, for answering myriad of questions I had, for reserving their instruments

for me to use, and for joyous and encouraging conversations. I wish to thank Dr. Claudio Conti at Universidad Carlos III de Madrid, Spain and Dr. Nagi at Baylor College of Medicine (BCM) for training me on mammary tumor pathology and for their prompt support in completing tumor histopathology, which is the heart of this work. I would also like to thank Dr. Alyssa Johnston at BCM for her generous and prompt support in establishing our collaboration with Dr. Nagi. I also wish to thank Dr. Andrew Ambrus for immunohistochemistry work and generously sharing antibodies with me to complete immunofluorescence experiments. I extend my gratitude to Brittany, Kelly and Rena Mao at histology cores of TAMU and BCM for all the histology work and their advice.

Thank you to all the members of the RFY group, past and present, for making it a great and an enjoyable atmosphere in the lab. I am grateful for Isabel Lambertz, Tom Berton, Andres Santos and Linjie Luo for training me on new techniques, for all the great conversations, and overall, for an enriching lab experience that indeed helped me mature as an individual as well as a scientist. I also like to thank Yuanning Zhang, Madison Spier and wonderful undergraduates; John, Kelsey, Daniel and Ali, for their willingness to help me whenever I needed, and for making the atmosphere in the lab more cheerful.

Throughout the graduate school, my friends in the IDP of Genetics, Sri Lankan Association of TAMU, Aggie Cricket Club of TAMU, Sri Lankan Lions Cricket Club in Houston, and my old college friends in the US have provided a much-needed respite from troubleshooting endeavors in the lab. I am grateful for the support, great times and all the memories. I would not be who I am today if not for a loving and a supportive family. I thank my parents who have endured and sacrificed many things in their lives always supporting me to reach beyond. I wish someday that I will have the strength to be as fearless and selfless

in life as you two. My wife, my best friend and at times, my elocution teacher, my mentor and my second mom, Randara; I thank you for guiding me through difficult times and for tolerating my clumsy ways. Your love has definitely made me a better individual and this would not be possible without you in my corner.

CONTRIBUTORS AND FUNDING SOURCES

This work was supervised by a dissertation committee consisting of Professor Robin S. Fuchs-Young (advisor) and Professors J. Timothy Lightfoot and Robert S. Chapkin of the Interdisciplinary Program in Genetics and Professor Farida Sohrabji of Department of Neuroscience and Experimental Therapeutics, Interdisciplinary Program in Neuroscience.

All work for the dissertation was completed by the student. Funding was provided by the grant R01 MD006228-01 from the National Institutes of Health, United States.

TABLE OF CONTENTS

	Page
ABSTRACT	ii
DEDICATION	iii
ACKNOWLEDGEMENTS	iv
CONTRIBUTORS AND FUNDING SOURCES.....	vii
TABLE OF CONTENTS	viii
LIST OF FIGURES.....	xi
LIST OF TABLES	xvii
CHAPTER I INTRODUCTION AND LITERATURE REVIEW	1
Female breast cancer (BrCa).....	1
Mutations and variants of p53 in cancer	1
Tumor suppressor p53.....	3
Functional domains of p53	4
Transactivation domain (TAD)	4
Proline-rich domain (PRD)	5
DNA binding domain (DBD).....	6
Oligomerization/tetramerization domain	7
Carboxy terminal domain (CTD)	7
Transactivation ability and selectivity of p53	8
Activation of p53.....	10
Biological processes regulated by p53	11
Apoptosis.....	11
Cell cycle arrest.....	13
Cellular senescence	14
Senescence-associated secretory phenotype (SASP)	15
p53 and regulated biological processes on tumorigenesis in mice.....	16
Modification of p53 function by codon 72 SNP	20
Current mouse models of codon 72 p53 SNP	26
Codon 72 p53 SNP and cancer risk.....	28

CHAPTER II MATERIALS AND METHODS	30
Maintenance and genotyping of transgenic mice	30
Tumorigenesis experiments.....	31
DMBA treatment of mice.....	31
Generation of MMTV- <i>ErbB2/Neu</i> codon 72 variant mice	32
Protein extraction and immunoblotting.....	32
RNA extraction and qRT-PCR.....	33
Chromatin immunoprecipitation of p53	34
Sudan Black B (SBB) staining of senescent cells	35
Immunohistochemistry of Ki67, CD31, IBA1 and CC3.....	35
Multiplex indirect immunofluorescence	36
Exposure of R72 and P72 mice to high-fat diet (HFD).....	37
Statistical analysis	37
 CHAPTER III EFFECT OF CODON 72 POLYMORPHIC VARIANTS ON MAMMARY TUMORIGENESIS.....	 39
Rationale.....	39
Results	40
Decreased mammary tumor latency and higher incidence in R72 mice.	40
Enhanced mammary tumor progression in E-R72 animals.....	44
Breast cancer prevention via early first full-term pregnancy (eFFTP)	48
Modeling pregnancy protection in rodents.....	49
Lack of pregnancy protection in codon 72 p53 mice	49
Discussion	52
 CHAPTER IV MOLECULAR MECHANISMS UNDERLYING DIFFERENTIAL MAMMARY TUMORIGENESIS IN MMTV-ERBB2/NEU CODON 72 P53 MICE	 55
Rationale.....	55
Results	55
Increased proportion of senescent cells in the susceptible mammary glands of E-R72 mice.....	55
Increased SASP, proinflammatory markers and angiogenesis in the susceptible mammary glands of E-R72 mice.....	60
Increased influx of proinflammatory macrophages in susceptible glands of E- R72 mice.....	64
Increased tumor-associated macrophages (TAMs) and blood vessels in mammary tumors from E-R72 mice.....	69
Increased association of R72 with the promoters of cell cycle arrest and inflammation genes.	72

CHAPTER V CONCLUSIONS AND FUTURE DIRECTIONS.....	75
REFERENCES.....	90

LIST OF FIGURES

	Page
Figure I-1. Protein structure of p53. Five major functional domains of p53 include, Transactivation domain (TAD), Proline-rich domain (PRD), DNA binding domain (DBD), Oligomerization domain (OD) and Carboxy-terminal domain (CTD).....	4
Figure I-2. Apoptosis triggered by transcription-dependent and -independent mechanisms regulated by p53.	12
Figure III-1. Kaplan-Meier curves, showing proportion of mammary tumor-free P72 (n=40) and R72 (n=39) mice, after DMBA treatment (*p<0.05). ...	41
Figure III-2. Percentage mammary tumor incidence in DMBA-treated R72 and P72 animals (*p<0.05).	41
Figure III-3. Percentage mammary tumor incidence in E-R72 and E-P72 animals (*p<0.05).	42
Figure III-4. MMTV-ErbB2/Neu mammary tumorigenesis. A) Kaplan-Meier curves of mammary tumor-free E-P72 (n=54) and E-R72 (n=56) animals (**p<0.01).....	43
Figure III-5. Representative H&E stained tumors of mammary adenocarcinoma found in E-P72 and E-R72 animals. Magnification 1.25X and 20X with scale bars 2.5 mm and 100 μm, respectively.	44
Figure III-6. Average growth rates (mm ³ per day) of mammary tumors in E-P72 (n=38) and E-R72 (n=48) animals. Error bars represent mean±SEM (*p<0.05).	45
Figure III-7. A) Representative IHC images of Ki67 stained mammary tumors from E-P72 and E-R72 animals, respectively. Magnifications, 20X and 40X, scale bar, 50 μm. B) Quantification of Ki67+ cells in mammary tumors from E-R72 and E-P72 animals. Values are standardized to the mean of E-P72 samples and shown as mean±SEM (n=5, *p<0.05).....	46

- Figure III-8. A) Representative IHC images of CC3 immunostaining in mammary tumors from E-P72 and E-R72 animals, respectively. Magnifications, 20X and 40X, scale bar, 50 μ m. E) Quantification of CC3+ cells in tumors from E-R72 and E-P72 animals. The values are standardized to the mean of E-P72 samples and shown as mean \pm SEM (n=5, *p<0.05)..... 47
- Figure III-9. qRT-PCR of mRNAs of *ErbB2* and *p53* genes in tumors of E-P72 (black bars) and E-R72 (grey bars) animals (n=4). Results shown as relative mRNA expression of specified genes normalized to corresponding *Tbp* levels. The expression values are standardized to the mean of E-P72 samples and shown as mean \pm SEM..... 48
- Figure III-10. Mammary tumor incidence in DMBA-treated parous and nulliparous R72 and P72 mice. Percentage mammary tumor incidence in parous and virgin P72 and R72 animals (*p<0.05, Fisher's exact test). Mammary tumor incidence is indicated at the top of the bar (animals that prematurely died or were sacrificed without mammary tumors, were excluded from the mammary tumor incidence calculations). 50
- Figure III-11. DMBA-induced mammary tumorigenesis in parous and virgin P72 and R72 animals. Kaplan-Meier curves of mammary tumor-free parous and virgin P72 (n=42 and 40, respectively) and R72 (n=35 and 39, respectively) animals exposed to six weekly doses of 1 mg of DMBA dissolved in corn oil. Mammary tumor latencies of R72 and P72 animals were 21 days vs 71 days post DMBA dosing, respectively. Log rank test was used for statistical comparison of tumorigenesis curves. Different letters indicate that the curves are statistically significant (p<0.05)..... 51
- Figure IV-1. Apoptosis in susceptible mammary glands of E-R72 and E-P72 mice. A) Quantitative RT-PCR of mRNAs of p53-regulated proapoptotic genes in the mammary glands from age-matched E-P72 (black bars) and E-R72 (grey bars) animals. Relative mRNA expression of specified genes is normalized to corresponding *Tbp* levels. The expression values are standardized to the mean of E-P72 samples and shown as mean \pm SEM (n=6). B) Representative western blot image of CC3 and the loading control, GAPDH, in the protein extracted from mammary glands of age-matched E-P72 (black bars) and E-R72 (grey bars) animals (n=4). Densitometry of the CC3 bands normalized to corresponding GAPDH levels, and standardized to the mean of E-P72 samples shown as mean \pm SEM. 56

Figure IV-2. Representative IHC images of CC3 stained mammary tumors found in E-P72 and E-R72 animals, respectively. 20X, 40X magnification, scale bar, 50 μ m. 57

Figure IV-3. Cell cycle arrest and senescence in susceptible mammary glands of E-R72 and E-P72 mice. A) Quantitative RT-PCR of mRNAs of cell cycle arrest and senescence effectors, *p21* and *p16^{INK4A}* in the mammary glands of age-matched E-P72 and E-R72 animals. Results shown as relative mRNA expression of specified genes normalized to corresponding *Tbp* levels. The expression values are standardized to the mean of E-P72 samples and shown as mean \pm SEM (n=6, *p<0.05). B) Representative western blot image of p21, phosphorylated RB (P-RB) and the loading control, GAPDH, in mammary glands from age-matched E-P72 and E-R72 animals. Densitometry of the p21 and P-RB bands normalized to corresponding GAPDH levels and standardized to the mean of E-P72 samples shown as mean \pm SEM (n=5, *p<0.05, **p<0.01)..... 58

Figure IV-4. Representative images of Sudan Black B stained susceptible mammary glands of age-matched E-P72 (black bars) and E-R72 (grey bars) animals, respectively. Magnification 40X, scale bar 50 μ m. Quantification of relative proportion of Sudan Black B (SBB)-positive cells in susceptible mammary glands of age-matched E-R72 and E-P72 animals. Results show counts of six high power fields per animal (more than 9000 cells in total). Proportions are standardized to the mean of E-P72 samples shown as mean \pm SEM (n=3, *p<0.05). ... 59

Figure IV-5. Representative western blots of P-p65 (Ser536) and the loading control, GAPDH, in mammary glands from age-matched E-P72 (black bars) and E-R72 (grey bars) mice. Densitometry of P-p65 bands normalized to corresponding GAPDH levels and standardized to the mean of E-P72 samples shown as mean \pm SEM (n=4, *p<0.05). ... 61

Figure IV-7. Representative western blots of TNFA, and the loading control, GAPDH, in the protein extracted from mammary glands of age-matched E-P72 (black bars) and E-R72 (grey bars) animals. Densitometry of the western blots normalized to corresponding GAPDH levels and standardized to the mean of E-P72 samples shown as mean \pm SEM (n=4, *p<0.05)..... 62

Figure IV-6. Quantitative RT-PCR of mRNAs of SASP genes in mammary glands from age-matched E-P72 and E-R72 mice. Relative mRNA expression is normalized to corresponding *Tbp* levels, and expression values are standardized to the mean of E-P72 samples and expressed as mean \pm SEM (n=6, *p<0.05)..... 62

- Figure IV-8. Representative images of CD31 stained mammary glands from age-matched E-P72 and E-R72 mice, respectively. Magnifications, 20X and 40X, scale bar, 50 μ m. Quantification of CD31+ blood vessels surrounding mammary epithelia per high power field in mammary glands from age-matched E-P72 and E-R72 mice. Values are standardized to the mean of E-P72 samples and shown as mean \pm SEM (n=5, *p<0.05)..... 63
- Figure IV-9. A) Quantitative RT-PCR of *Ccl2* mRNA in the mammary glands from age-matched E-P72 (black bars) and E-R72 (grey bars) animals. Relative mRNA expression is normalized to corresponding *Tbp* levels, and values are standardized to the mean of E-P72 samples and expressed as mean \pm SEM (n=9, *p<0.05). B) Representative western blots of CCL2 and GAPDH in extracts of mammary glands from age-matched E-P72 and E-R72 animals. Densitometry of the CCL2 western blot normalized to corresponding GAPDH levels and standardized to the mean of E-P72 samples shown as mean \pm SEM (n=4, *p<0.05)..... 64
- Figure IV-10. Influx of macrophages into susceptible glands of E-R72 and E-P72 mice. A) Representative IHC images of IBA1 stained mammary glands of age-matched E-P72 and E-R72 animals, respectively (n=5). Magnifications, 20X and 40X, scale bar, 50 μ m. B-D) Quantification of IBA1+ macrophages per 100 epithelial cells (B), 100 adipocytes (C), and CLSs per animal (D) in mammary glands of age-matched E-P72 and E-R72 animals. The values are standardized to the mean of E-P72 samples and shown as mean \pm SEM (n=5, *p<0.05)..... 65
- Figure IV-11. qRT-PCR of mRNAs of *Il1 β* and *iNos* markers in the mammary glands of age-matched E-P72 and E-R72 animals. Results shown as relative mRNA expression of specified genes normalized to corresponding *Tbp* levels. The expression values are standardized to the mean of E-P72 samples and shown as mean \pm SEM (n=4, *p<0.05, ***p<0.001). 66
- Figure IV-12. A) Representative images of indirect multiplex immunofluorescence using Hoechst dye (blue), IBA1 (red) and IL1 β (green) in the mammary glands of age-matched E-P72 and E-R72 animals, respectively. Magnifications, 20X and 40X, scale bar 50 μ m. Arrows point to IBA1+IL1 β + macrophages. B-C) Quantification of relative number of IBA1+IL1 β + macrophages per 100 epithelial cells (B), and adipocytes (C) mammary glands of age-matched E-P72 and E-R72 animals. The values are standardized to the mean of E-P72 samples and represent mean \pm SEM (n=5, *p<0.05). 67

Figure IV-13. Representative crown-like structure (CLS) stained with Hoechst (blue), IBA1 (red) and IL1 β (green) found in the susceptible mammary glands of E-R72 mouse. Magnification 40X, scale bar 50 μ m. Magnified IBA1+IL1 β + macrophages are shown in the lower-right inset. White square on the merged image identifies the magnified area of the image.....	68
Figure IV-15. qRT-PCR of mRNAs of <i>Vegfa</i> in the tumors age-matched E-P72 and E-R72 animals. Results shown as relative mRNA expression of specified genes normalized to corresponding <i>Tbp</i> levels. The expression values are standardized to the mean of E-P72 samples and shown as mean \pm SEM (n=5, *p<0.05).....	70
Figure IV-14. Representative IHC images of IBA1 stained tumors harvested from E-P72 and E-R72 animals. Magnifications, 20X and 40X, scale bar, 50 μ m. Quantification of number of IBA1+ macrophages in tumors harvested from E-P72 and E-R72 animals. The values are standardized to the mean of E-P72 samples and shown as mean \pm SEM (n=4, *p<0.05).....	70
Figure IV-16. Representative IHC images of CD31 stained mammary tumors in E-P72 and E-R72 animals, respectively. Magnifications, 20X and 40X, scale bar, 50 μ m. Quantification of CD31+blood vessels per high power field of view (FOV). The values are standardized to the mean of E-P72 samples and shown as mean \pm SEM (n=5, *p<0.05).....	71
Figure IV-17. A) Diagram of the <i>p21</i> gene with the distal p53 response element (RE). The start of exon 1 is denoted as +1, and the locations of potential p53 REs are shown relative to the start of exon 1. B) Chromatin immunoprecipitation of p53 in mammary glands harvested from E-P72 and E-R72 age-matched animals. Input DNA and immunoprecipitated DNA were analyzed by qPCR using primers flanking p21 p53 RE. The expression values are standardized to the mean of E-P72 samples and shown as mean \pm SEM (n=3, *p<0.05).....	73

Figure IV-18. A) Diagram of the *Tnfa* gene with p53 RE. The start of exon 1 is denoted as +1, and the locations of potential p53 REs are shown relative to the start of exon 1. B) Chromatin immunoprecipitation of p53 in mammary glands harvested from E-P72 and E-R72 age-matched animals. Input DNA and immunoprecipitated DNA were analyzed by qPCR using primers flanking *Tnfa* p53 response element. The expression values are standardized to the mean of E-P72 samples and shown as mean±SEM (n=3, *p<0.05). C). Diagram of the *Ccl2* gene with p53 response elements. The start of exon 1 is denoted as +1, and the locations of potential p53 REs are shown relative to the start of exon 1. D) Chromatin immunoprecipitation of p53 in mammary glands harvested from E- P72 and E-R72 age-matched animals. Input DNA and immunoprecipitated DNA were analyzed by qPCR using primers flanking *Ccl2* p53 response elements. The expression values are standardized to the mean of E-P72 samples and shown as mean±SEM (n=3, *p<0.05). 74

Figure V-1. Weekly body weights of male R72 (Red) and P72 (Blue) animals fed HFD (*p<0.05). 82

Figure V-2. Average food intake per male R72 and P72 animal fed HFD (*p<0.05). 82

Figure V-3. Weekly body weights of female R72 (Red) and P72 (Blue) animals fed HFD. 84

Figure V-4. Average food intake per female R72 or P72 animal fed HFD. 84

Figure V-5. Diagram of the proposed model of how R72 variant increase mammary tumor incidence and proliferation. Accumulation of senescent cells in the mammary glands of E-R72 animals contributed to increased chronic inflammation in the mammary tissue milieu through upregulation of proinflammatory SASP which, elevates influx of proinflammatory macrophages and angiogenesis. Increased influx of macrophages leads to mutagenic tissue environment by increasing oxidative stress via RNS, which may elevate cellular transformation and in turn, tumor incidence. R72 is likely to play a direct role in upregulating *p21*, *Ccl2* and *Tnfa* expression *via* higher affinity to the respective p53 REs. In addition to prosurvival functions of chronic inflammation, higher influx of macrophages may increase TAMs that enhance tumor vasculature contributing to increased tumor proliferation observed in the tumors arising in E-R72 mice. 89

LIST OF TABLES

	Page
Table I-1. Common subtypes of BrCa with associated intrinsic markers and general trends of the selected clinical parameters	3
Table I-2. Allele and genotypic frequencies of codon 72 p53 SNP in populations of African, European, Asian and South American ancestries (1000 Genomes project)	22
Table II-1. qRT-PCR primer sequences used in SYBR green reactions.....	34
Table II-2. ChIP qRT-PCR primer sequences used in SYBR green reactions.....	35
Table II-3. Composition of the defined high-fat diet	37

CHAPTER I

INTRODUCTION AND LITERATURE REVIEW

Female breast cancer (BrCa)

Female breast cancer (BrCa) affects more than 2.2 million women each year, and is the cause of more than 500,000 estimated mortalities worldwide.¹ BrCa is a heterogeneous disease, which presents clinically in at least five different subtypes depending on the expression of estrogen receptor (ER), progesterone receptor (PR), human epidermal growth factor receptor-2 (HER2) and Claudin. Table 1 summarizes the histological markers, their expression, general trends of prognosis and relapse-free survival of the specific subtypes. Etiology of BrCa is heterogeneous and include both non-genetic and genetic factors. Only 5-10% of the BrCa cases are hereditary,² which indicates that majority of the BrCa cases occur due to genetic susceptibilities of the host in responding to environmental stimuli. Both environmental, reproductive and genetic factors such as exposure to carcinogens, education, access to healthcare, obesity, age at first full-term pregnancy (FFTP), age at menarche, menopausal status and family history play an important role in BrCa etiology, progression, metastasis, response to therapy and survival.³⁻⁵

Mutations and variants of p53 in cancer

Mutations in the p53 gene have been reported at varying frequencies in almost all cancer types. In order to better predict cancer susceptibility, progression and relapse-free survival, research efforts have been focused on identifying genetic biomarkers such as mutations and variants.⁶ While next-generation sequencing of human tumor samples has

enabled discovering gene mutations that are associated with significant risk of developing cancer, genome-wide association studies (GWAS) have led the efforts to uncover highly- and modestly-penetrant common germline single nucleotide polymorphisms that are significantly associated with risk of cancer.⁷ A recent comprehensive genetic analysis of 165 GWAS studies on multiple cancer types showed that the p53 pathway genes are more enriched with causal mutations and common SNPs that are significantly associated with cancer risk. Among 67 genes in the p53 pathway, 15 genes included at least one causal mutation which resulted in a 11.15-fold enrichment of causal mutations over the rest of the 24,553 genes analyzed. Similarly, cancer-associated SNPs in the genes of the p53 pathway were 6.77-fold enriched compared to the other genes analyzed. Together, these findings demonstrated that causal mutations and cancer-associated SNPs are found at a higher percentage in genes of the p53 pathway. Moreover, these findings indicate the vulnerability of genes in the p53 pathway to undergo somatic mutations that alter the functions of p53.⁸

Similarly, the Cancer Genome Atlas Network recently reported a higher proportion of p53 somatic mutations in breast cancer.⁹ In this study, breast tumors from 510 female patients were subjected to whole exome sequencing. Results showed that the frequency of *p53* mutations was dependent on the BrCa subtype. Luminal subtypes showed the fewest p53 mutation frequencies; 12% of luminal A cases and 29% of luminal B cases. In contrast, 72% of HER2 cases and 80% of basal-like, mostly triple-negative, cases showed p53 mutations.⁹ As given in table 1, while luminal A cases tend to have a better prognosis and relapse-free survival, basal-like and HER2 subtypes often present as poorly differentiated, aggressive with a poor prognosis and both relapse-free and overall survival.¹⁰

Table I-1. Common subtypes of BrCa with associated intrinsic markers and general trends of the selected clinical parameters

Subtype	Prevalence	Histological markers and their occurrence	Tumor Grade	Prognosis
Luminal A	50-60%	ER+, PR+, HER2-, K8+, K18+	Low	Good
Luminal B	10-20%	ER+/low and/or PR+, HER2-/+ , K8+, K18+	Intermediate	Intermediate/Poor
HER2-enriched	10-15%	ER-, PR-, HER2+(high)	High	Poor
Basal-like	10-20%	ER-, PR-, HER2-, K5+, K6+	High	Poor
Claudin-low	12-14%	ER-, PR-, HER2-, Claudin-/low, K5+, K6+	High	Poor

+: present, -: absent, (high): overexpressed/amplified

Tumor suppressor p53

Immunoprecipitation of p53 with the large T antigen of SV40 tumor virus oncoprotein in transformed mouse cell lines led to initial speculation that p53 was an oncoprotein.^{11, 12} This notion was further supported by the finding that overexpression of clones of murine *p53* together with oncoprotein *Ras*, transformed normal rat embryonic fibroblasts.¹³⁻¹⁵ However, several lines of evidence contradicted the oncogenic role of p53. Missense mutations were found in the sequences of p53 clones used in the experiments that succeeded in transforming rat embryonic fibroblasts.^{16, 17} Also, Finlay et al. showed that overexpressing a wild-type copy of p53 greatly reduced number of foci due to *Ras* or mutant p53 plus *Ras* transformation of rat embryo fibroblasts.¹⁸ In another study, Li-Fraumani

patients who inherited germline p53 mutations had 100% cancer onset by 70 years of age and were often diagnosed with sarcomas, lymphomas, lung cancer and breast cancer.¹⁹ Additionally, identification of p53 mutations in mouse tumors, human cell lines and colon tumors of humans provided further evidence for the tumor suppressive role of p53.²⁰

Functional domains of p53

The *p53* gene consists of 11 exons and 10 introns that span across approximately 19200 nucleotides. Ten exons encode for five functionally important domains enabling transactivation of target genes through sequence-specific binding and oligomerization to form functionally important p53 tetramers (Figure I-1).²⁰



Figure I-1. Protein structure of p53. Five major functional domains of p53 include, Transactivation domain (TAD), Proline-rich domain (PRD), DNA binding domain (DBD), Oligomerization domain (OD) and Carboxy-terminal domain (CTD).

Transactivation domain (TAD)

The transactivation domain lies in the loosely-structured amino-terminus (amino acid residues 1-60) and consists of two subdomains, TAD-I and TAD-II. To investigate the involvement of TADs in the transcription capacity of p53, Attradi et al. generated mouse models carrying inactivating mutations in the TAD-I (L25Q, W26S – $p53^{25,26}$) or TAD-II (F53Q, F54S – $p53^{53,54}$) or in both ($p53^{25,26,53,54}$).²¹⁻²³ The mouse model of $p53^{25,26}$ showed significantly impaired transactivation of *p21*, a major effector of cell cycle arrest as well as

of proapoptotic genes *Puma*, *Noxa* and *Perp* upon DNA damage. Interestingly, p53^{53,54} showed no transactivation impairment of *p21* or other proapoptotic genes. However, p53^{25,26,53,54} significantly decreased the transactivation capability of p53.²²

Proline-rich domain (PRD)

The Proline-rich domain (PRD) is located between the transactivation domain and the DNA binding domain (amino acid residues 61-97) and contains 12 proline residues. Most of the proline residues are found in PXXP (P-proline, X-any amino acid) motifs in this region, resulting in a left-handed type-II helix which creates a binding site for proteins containing SH3 (Src homolog 3) domains.²⁴ Deletion mutants of p53 that lack PRDs are shown to not affect transactivation of *p21* and *Bax* in multiple cancer cell lines. While cell cycle arrest remains intact, in Lovo colon carcinoma cells, deletion of PRD significantly reduced the level of apoptosis.²⁵ In contrast, work by Walker and Levine in p53-deficient HT1299 lung carcinoma and Sao2 osteosarcoma cell lines shows that deletion mutants of p53 that lack PRD significantly reduces growth suppression when exposed to geneticin in comparison to wild type p53.²⁴ This was further supported by the lack of DNA damage-induced cell cycle arrest and attenuated apoptotic response in MEFs derived from PRD knockout mouse model.²⁶

The ability of proteins carrying PXXP motifs to bind to transcription coactivator, p300 led Doran et al. to investigate the interaction of p300 with PRD of p53 in Sao2 and HCT116 cell lines.²⁷ Studies prior had already established that the transcription coactivator p300 acetylates p53 bound to DNA in the C-terminal domain.^{28, 29} In the Doran study, while p300 interacted with p53, deletion of PRD prevented p53-p300 interaction. The deletion

mutant was shown to bind to the p53 response element (RE) of p21 but did not form p53-DNA-p300 complex or acetylate p53 lacking PRD.²⁷

Prolyl isomerase PIN1 (Protein interacting with NIMA-1) is also found to interact with phosphorylated p53 *via* PRD. PIN1 is a peptidyl-prolyl cis/trans isomerase which catalyzes isomerization of peptidyl-prolyl peptide bonds and PIN1 does so in a phosphorylation-dependent manner at phosphorylated Serine/Threonine followed by a proline residue.³⁰⁻³² Conformation change of p53 due to PIN1 stabilizes p53 by reducing interaction with its negative regulator MDM2.^{33,34} In HCT116 cells, PIN1 is recruited to p53 REs at p21 promoter upon exposure to UV or etoposide induced DNA damage and this is significantly reduced by removal of PIN1 interacting sites on p53. RNAi knockdown of PIN1 significantly reduces interaction of p300 with DNA-bound p53 and acetylation of L373 and L382 residues of p53. Additionally, PIN1 stimulates dissociation of iASPP (inhibitor of apoptosis-stimulating protein of p53) from p53 which has been shown to induce apoptosis.³⁵

DNA binding domain (DBD)

Central DBD constitutes the largest portion of p53 and spans from amino acid residues 100 to 300. DBD consists mainly of two antiparallel β sheets that are connected by two large loops and a loop-sheet-helix motif. A zinc ion provides stability to the large loops and are important for proper conformation. This enables binding to the major and minor grooves of p53 response elements (REs) in a sequence-specific manner. Given the role of transcription factor, approximately 86% of somatic mutations are found in the DBD of p53.³⁶ Most frequent, hotspot mutations are located at residues that make contacts with DNA or stabilize the conformation of binding sites. Hence, p53 mutants are categorized into contact (S241, R248, R273 and C277) or structural mutants (R175, C176, H179, C242, G245, R249

and R282), respectively.³⁷ X-ray crystallography studies reveal that contact mutants do not affect the DBD conformation of p53 but may prevent DNA binding. In contrast, structural mutants, such as the zinc-binding mutants, affect the conformation of DBD.³⁸⁻⁴¹

Oligomerization/tetramerization domain

Monomers of p53 interact *via* the oligomerization domain (amino acid residues 324–355) to form a tetramer that makes the functional unit of p53 in terms of transactivation of genes.^{42, 43} During this process, the nuclear export signal of p53 is masked, increasing the isolation of p53 in the nucleus for enhanced transactivation of target genes.⁴⁴ Tetramers of p53 predominantly bind to the canonical p53 response element (RE), which consists of two consensus nucleotide sequences of RRRCWWGYYY (R = purine, W = A or T, and Y = pyrimidine), on either side of a spacer sequence (0–13 nucleotides).^{45, 46} However, other rare noncanonical p53 REs are seen in the promoter regions of *Pig3*, *Aqp3* and *Mdr1*.⁴⁷ In the majority of the target genes, REs are found in the 5' region upstream of the transcription initiation site (TIS) (e.g. *p21*). However, early intronic and even exonic REs are found on target genes such as *Puma (Bbc3)* and *miR-34a*, respectively.⁴⁷

Carboxy terminal domain (CTD)

The carboxy terminal domain (CTD) (amino acid residues 364–393) contains signals for nuclear localization as well as export, and is the region where most of the post-translational modifications (PTMs) occur.⁴⁸ PTMs in this region include phosphorylation, acetylation, methylation, SUMOylation and neddylation. These modifications affect protein stability and activation, which enable/modify functions of p53, nuclear import and export of the protein.⁴⁹

Transactivation ability and selectivity of p53

Transactivation ability of p53 is dependent on factors both intrinsic and extrinsic to the molecule. In general, distance from TIS to RE negatively affects the potential of transactivation. In addition, affinity of p53 towards target DNA is critical to its transactivation ability. Hainut and Milner showed that three cysteine residues (at 176, 238 and 242) in the DBD of p53 are critical to DNA binding as mutations in these sites resulted in impaired binding and transactivation. Further, DBD of p53 imparts a favorable steric change to DNA showing that flexible DNA conformations facilitate p53 tetramer binding.⁵⁰ This is partly due to histone modification through acetylation after p53 recruitment to REs. Several studies have shown that histone acetyltransferases such as p300/CBP, pCAF, GCN5 and TIP60 acetylate histones close to p53 REs in a p53 dependent manner.⁴⁷

Acetylation of several lysine residues located in the CTD of p53 has been shown to correlate with enhanced transactivation potential. Truncation of the CTD significantly reduces binding to chromatin-like DNA templates and REs in a physiologically relevant *in vivo* setting, showing that CTD plays a key role in DNA binding of p53 and transactivation of target genes.^{51, 52} Similar to histone acetyl transferases (HATs), hematopoietic zinc finger protein (HZF) interacts with p53 directly and affect p53 RE selection, resulting in enhanced transactivation of genes involved in growth arrest such as *p21*.⁵³ In contrast to HATs, the chromosome segregation 1-like protein (CSE1L) protein complex modifies histones to relax chromatin in a p53 independent manner. Chromatin relaxation at p53 REs by CAS/CSE1L increases transactivation of select proapoptotic genes such as *p53Aip1* and *Pig3*, showing a unique way of supporting p53 transactivation ability.⁵⁴

Also, p53 is capable of modifying the preinitiation complex formation in the basic transcription machinery of RNAPII, through recruitment of TBP as well as TAF1, which is a TFIID subunit.⁴⁷ In addition, Espinosa et al showed that REs of certain p53 target genes are poised with prerecruited basal components of the transcription machinery. This was seen on the p53 RE of the *p21* gene and was postulated to reduce the activation barrier to initiate transcription.⁵⁵ Recent *in vivo* studies show that the E177 (E180 in humans) residue of p53 plays a critical role in formation of p53 tetramers. Mutation of the negatively-charged glutamic residue to positively-charged arginine (E177R) disrupts salt bridges between E177 and R178 in interacting monomers of p53, thereby destabilizing H1 helix interactions that form p53 tetramers. Interestingly, p53^{E177R} results in selective inhibition of proapoptotic gene transactivation but not *p21* or genes involved in metabolism such as *Gls2*, *Aldh4*, *Sesn1/2* and *Dram1*.⁵⁶ Similarly, Li and colleagues recently generated mice with mutations at three lysine residues, K117, K161 and K162 (K120, K164 and K165 in humans) in the DBD of p53 (p53^{3KR}) that significantly reduced transactivation of apoptosis, cell cycle arrest and senescence associated genes, thereby impairing these processes. However, these mutations did not affect transactivation of metabolism-related *Gls2*, *Tigar* and *Gpx*, as both the level of gene expression and promoter occupancy of p53^{3KR} was comparable to those of the wild type p53, further indicating how PTMs could affect promoter selectivity.⁵⁷ Therefore, these studies show that as DBD and CTD of p53 play important roles in promoter selectivity and transactivation of p53 target genes, TAD and PRD modify p53 transactivation capacity.

Activation of p53

In healthy cells, protein levels of p53 are kept at a low level through polyubiquitination-mediated degradation by its negative regulators; Human Double Minute 2 (HDM2, mouse ortholog MDM2) and HDMX (MDMX).⁵⁸⁻⁶⁰ Upon DNA damage, damage sensing complexes such as MRN (consisted of MRE11, RAD50, NBN) and 9-1-1 (consisted of RAD9, RAD1, HUS1) are recruited to damaged sites, depending on whether it's double strand break (DSB) or a single strand break (SSB), respectively.^{61, 62} These complexes phosphorylate and activate signal transducing sensory kinases, Ataxia-telangiectasia mutated (ATM) and ATM and Rad3-related (ATR), respectively. Activated sensory kinases phosphorylate and activate downstream kinases and effector proteins.^{63, 64} As a result, p53 is rapidly phosphorylated in the amino terminus by several stress-sensing kinases such as ATM, ATR, DNA-dependent protein kinase (DNA-PK), CHK1/2 relieving p53 of the negative regulation by HDM2 or HDMX.^{22, 65, 66} Redundancy of kinases capable of phosphorylating p53 is postulated to indicate the critical nature of the process. Findings in mouse models with mutations at 18th (S18) and 23rd (S23) serine residues (15th and 20th in humans) of p53, show that abrogation of both S18 and S23 phosphorylation significantly reduces p53 stability as well as its transactivation ability.⁶⁷ In addition, p53 undergoes post-translational covalent modifications such as acetylation, methylation, SUMOylation, ubiquitination and neddylation that can significantly modify the stability, transactivation potential and protein interactions of p53. Hence, it can be seen that type of PTM could dictate the function of p53.⁵¹

Biological processes regulated by p53

Traditionally, p53 is known to regulate cellular processes such as apoptosis, cell cycle arrest, cellular senescence and DNA repair. Additionally, recent findings show glucose as well as lipid metabolism and immunity are under the umbrella of cellular processes regulated by p53.^{48, 57, 68-71} In the context of suppressing cancer development, p53 has been reported to act against tumor microenvironment signaling, invasion, metastasis, reprogramming of metabolism, accumulation of reactive oxygen species and self-renewal of stem cells. Recent ChIP-seq and RNA-seq expression analyses have revealed more genes regulated by p53, expanding the intricate network of p53 regulation. This suggests that p53 possesses the ability to respond to numerous insults in a context dependent manner.⁴⁸

Apoptosis

p53 can trigger apoptosis through intrinsic or extrinsic signaling pathways. Upon severe or irreparable DNA damage, p53 is phosphorylated at S46 by HIPK2 or DYRK2,^{72, 73} and acetylated at K120 by TIP60 or hMOF.^{74, 75} These have been shown to be critical PTMs that trigger p53-mediated apoptosis.⁷⁶ The activation of the intrinsic apoptosis pathway is determined by the balance between the levels of proapoptotic proteins and prosurvival BCL2 family members on the mitochondrial membrane.⁷⁷ Prosurvival BCL2 family members include BCL2, BCLXL and MCL1. In a damaged cell, proapoptotic BAX and BAK oligomerize on the outer membrane of the mitochondria. As a result, pores are formed, permeating the mitochondrial membrane (MOMP), thereby leading to Cytochrome C release into the cytoplasm. This activates the Caspase cascade to induce apoptosis. Transactivation of *Puma*, *Noxa* and *Bax* by p53 tilts the balance between prosurvival BCL2

members and proapoptotic proteins in favor of apoptosis as PUMA and NOXA bind to BCL2 members.⁴⁸

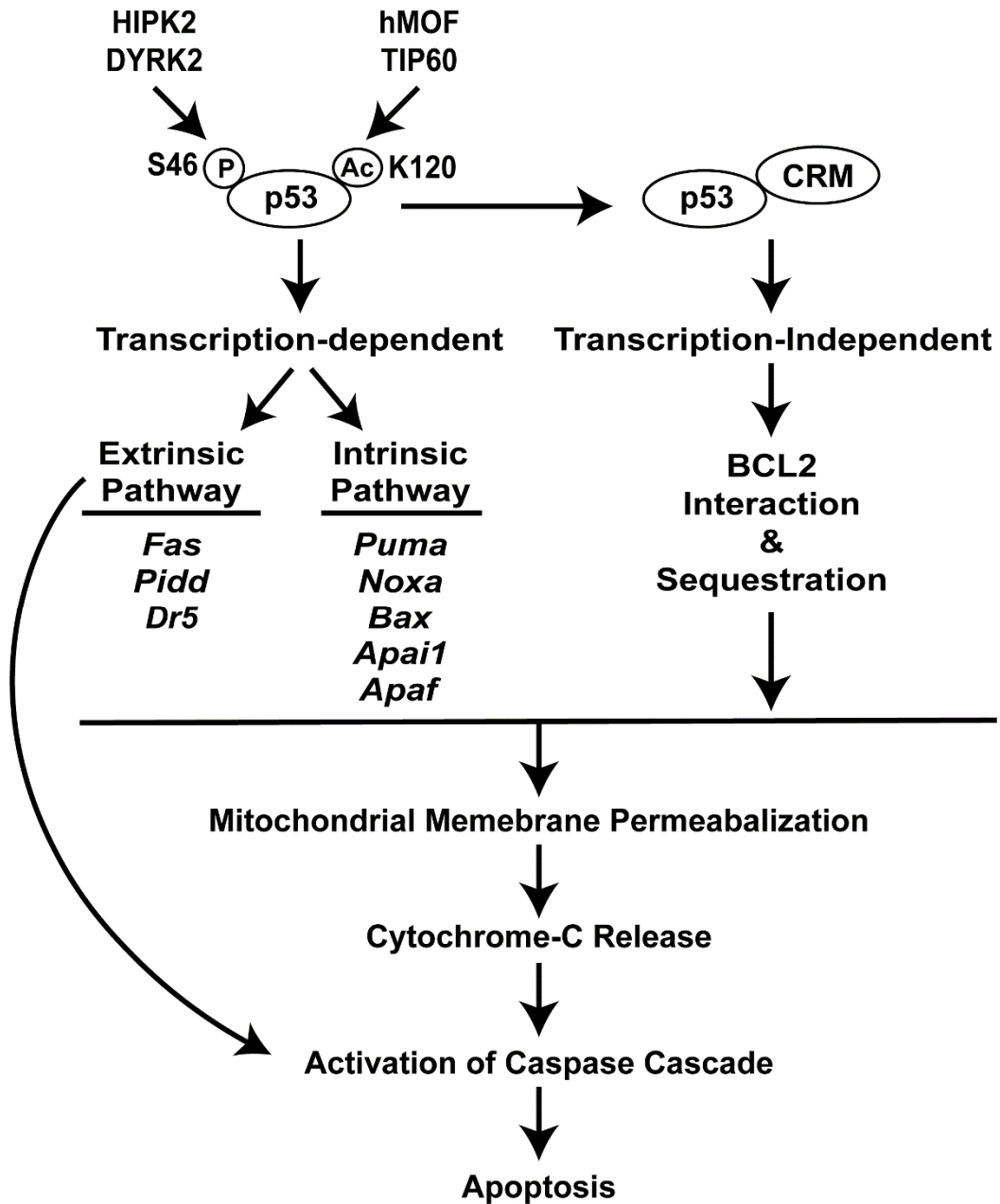


Figure I-2. Apoptosis triggered by transcription-dependent and -independent mechanisms regulated by p53.

In addition, findings by Leuet al. show that p53 can bind to BCL2 triggering MOMP-mediated apoptosis.⁷⁸ Apart from transactivating BH3-only BCL2 members, p53 also transactivates *p53aip1*, which mediates depolarization of the mitochondrial membrane potential, aiding Cytochrome C release. Additionally, p53 transactivates *Apaf* that binds to released Cytochrome C to form the apoptosome complex, activating the Caspase cascade. Consequently, Caspase-activated DNAses digest genomic material resulting in apoptosis.⁴⁷

The extrinsic pathway of apoptosis encompasses reception of death signals *via* death receptors that also results in the activation of the Caspase cascade. p53 participates in this pathway by transactivating genes encoding death receptors such as *Dr5/Killer*, *Pidd* and *Fas*.⁷⁹ In addition to transactivation of the host of genes involved in the intrinsic and extrinsic pathways, p53 transactivates *Perp*, which is a tetraspan membrane protein that has been shown to play a role in apoptosis and in maintaining epithelial integrity. However, the exact mechanism of action on how *Perp* contributes to p53-mediated apoptosis is not clear.⁸⁰⁻⁸²

Cell cycle arrest

Checkpoint mechanisms are evolved to survey and respond to errors in genetic material by preventing cell cycle progression allowing DNA repair. This safeguards the genetic integrity and in turn, plays a tumor suppressive role by preventing proliferation of cells with damaged DNA.⁸³ Upon DNA damage-induced activation, p53 inhibits cell cycle progression by transactivating genes involved in cell cycle arrest. Cyclin/CDK (Cyclin-dependent kinase) complexes drive cell cycle progression past G1/S checkpoint by phosphorylating RB (Retinoblastoma). This results in derepression of the E2F transcription factors that transactivate genes involved in DNA replication.^{84, 85} p53 transactivates one of the major effectors of cell cycle arrest, p21 (CDKN1A) which halts cell cycle at G1/S

checkpoint.⁸⁶ Mouse embryonic fibroblasts (MEFs) derived from *p21*^{-/-} mice show impaired DNA damage-induced G1 cell cycle arrest.⁸⁷ p21 binds to CDK2 inhibiting the kinase activity of CDK2 complexes inducing cell cycle arrest.⁸⁸ In addition, p53 transactivates genes involved in G2/M cell cycle arrest preventing passage of genetic material with errors following DNA replication. These genes include *14-3-3 sigma*, *Gadd45*, *Reprimo*, that disrupt activity and nuclear localization of Cyclin B/CDC2 complex that is essential for G2/M transition.⁸⁹⁻⁹²

Cellular senescence

Senescence is a cellular stress response that halts proliferation through irreversible cell cycle arrest. Irreparable DNA damage, telomere attrition due to replication exhaustion and oncogene activation have been shown to initiate cellular senescence.⁹³ Cellular senescence was first observed by Hayflick and Moorhead in cultured human fibroblasts when the cells failed to divide after a limited number of passages.⁹⁴ The most prominent characteristic of senescent cell is permanent cell cycle arrest. Constitutive upregulation of cell cycle arrest mediators, *p21* and *p14*^{ARF} (*p19*^{ARF} in mice) as well as *p16*^{INK4a} encoded by CDKN2A locus are shown to trigger cellular senescence. *p14*^{ARF} stabilizes p53 by degrading MDM2 and in turn, promoting p53-driven p21 expression.⁹⁵ Upregulation of p21 disrupts CDK2 complexes while *p16*^{INK4a} inhibit CDK4/6 complexes to trigger cell cycle arrest at G1/S checkpoint.^{86, 96} As a result, the cellular levels of phosphorylated RB protein are maintained at a lower level. Hypophosphorylated RB is shown to bind and inhibit E2F transcription factors, repressing genes that are necessary for cell cycle progression.^{85, 93, 97-}
¹⁰⁰ In addition to permanent cell cycle arrest, senescent cells are shown to increase in size and present a flat morphology *in vitro*. Senescent cells also accumulate lipofuscin,

aggregates of oxidized proteins, and lysosomal β -galactosidase enzyme that are currently utilized to identify senescent cells.^{101, 102}

Senescence-associated secretory phenotype (SASP)

Senescent cells remain metabolically active despite existing under permanent cell cycle arrest. Recent evidence shows that senescent cells secrete an array of factors, a phenomenon known as the senescence-associated secretory phenotype (SASP).¹⁰³ This was first reported while investigating the transcriptional profiles of senescent cells.¹⁰⁴⁻¹⁰⁶ Transcription of SASP factors are regulated by NF- κ B (nuclear factor of kappa light) and C/EBP β (CCAAT/enhancer-binding protein- β) transcription factors that are shown to be upregulated during senescence.¹⁰⁷⁻¹¹⁰ Supporting evidence was shown by Acosta et al. where authors were able to show that inhibition of I κ B kinases that activate NF κ B pathway, and depletion of C/EBP β mRNA using shRNA significantly down regulates SASP factors in human fibroblasts.¹⁰⁷ Additionally, Lujambio et al. have shown that NF κ B pathway is significantly upregulated in senescent hepatic stellate cells, and shRNA against p65 significantly reduces SASP factors.¹¹⁰ SASP is regulated predominantly through DNA damage response (DDR)-dependent mechanisms. However, DDR -independent mechanisms such as p38 activation and PTEN-loss have been shown to induce SASP.¹¹¹ DDR-dependent mechanism involves DDR kinase, ATM as depletion of ATM has been shown to attenuate SASP factors.^{112, 113} A recent study shows mechanistic evidence to link DDR and SASP. Kang et al. have shown that in senescent cells, activation of DDR kinases, ATM and ATR in turn, activates GATA4 leading to induction of TRAF3IP2 (tumor necrosis factor receptor-associated factor interacting protein 2) and IL1A (interleukin 1A), which activates NF- κ B to initiate and maintain the SASP.¹¹⁴ In addition, several regulators of SASP are described.

These include NEMO (IKBK κ G; inhibitor of kappa light polypeptide gene enhancer in B-cells, kinase gamma), RIG1 (retinoic acid-inducible gene I), Klotho, MacroH2A1, HMGB1 (high mobility group box 1) and HMGB2. However, mechanistic link between these regulators and SASP is yet to be elucidated.¹¹⁵

SASP factors include proinflammatory cytokines, chemoattractants, growth factors, angiogenic factors and matrix metalloproteases (MMPs). SASP components have been shown to reinforce senescence in both autocrine and paracrine manner. Plasminogen activation inhibitor-1 (PAI1), and activation of inflammasome through IL1A which leads to DDR have been shown to induce senescence in neighboring cells.^{107, 116-119} In addition, SASP factors extend the functional repertoire of cellular senescence beyond growth arrest-mediated tumor suppression to embryonic development, tissue remodeling, wound healing, aging and even, tumor promotion and epithelial-mesenchymal-transition (EMT).^{93, 97-99}

p53 and regulated biological processes on tumorigenesis in mice

Donehower et al. first demonstrated the tumor suppressor ability of p53 using a *p53*-null mouse model, where all the animals rapidly developed spontaneous tumors. Majority of the tumors are lymphomas specifically, CD4+CD8+ T-cell lymphomas, along with some carcinomas and sarcomas.¹²⁰ In a separate study, a phenotype similar to Li-Fraumeni syndrome seen in humans is observed in *p53*^{+/-} mice where the p53 level is halved and the other allele gathers mutations in some animals resulting in a wide array of cancers. Compared to mice with wild type *p53*, both *p53*^{-/-} and *p53*^{+/-} are significantly poor in survival due to susceptibility to tumorigenesis.^{121, 122} These observations clearly demonstrate the importance of wild type *p53* and the level of expression in tumor suppression and survival. Since these pioneering studies, numerous *p53* mouse models have been used to investigate

how intrinsic properties of p53 and the regulated biological processes affect tumorigenesis.⁴⁸ Brady et al. used *p53*^{25,26}, *p53*^{53,54} and *p53*^{25,26,53,54} to investigate the effect of transactivation ability of p53 on mouse models with different tumor etiologies.²² These included *Kras*^{G12D}-induced non-small-cell lung cancers, *Eμ-Myc*-driven B cell lymphomas, spontaneous T cell lymphomas and medulloblastomas triggered by inactivation of *Patched*. Mice with *p53*^{25,26} and *p53*^{53,54} showed significantly suppressed tumorigenesis while those with *p53*^{25,26,53,54}, which lacks transactivation capacity, succumbed to tumorigenesis. These results show that the transactivation potential of p53 plays a critical role in suppressing tumorigenesis.

The importance of p53-driven apoptosis in tumorigenesis has been shown in a B-cell lymphoma susceptible Eμ–Myc mouse model that overexpresses c-Myc, using enhancer μ (Eμ).^{123, 124} The majority of pre-B cell and B cell lymphomas found in these animals showed mutated p53 or loss of p53 and lack of apoptosis. To dissect the contribution of apoptosis in tumor development, Schmitt et al. impaired apoptosis through overexpression of BCL-2 or dominant negative Caspase-9 (C9DN) in tumors arising in Eμ-Myc animals, where wild type copies of *p53* were present. Similar to lymphomas with p53 loss, lymphomas generated by overexpression of BCL2 and C9DN showed significantly low apoptotic cells, indicating that disruption of apoptosis is critical to tumor development in this setting.¹²⁵

Interestingly, mouse models in which individual genes involved in cell cycle arrest are knocked-down, have shown that animals that are *Gadd45a*- or *Pml*-null are not susceptible for spontaneous tumorigenesis.⁴⁸ However, *p21*-null animals developed spontaneous tumors after an average latency of 5 months, which was significantly higher compared to *p53*^{-/-} tumor susceptibility.¹²⁶ A recent tumorigenesis study using *p53*^{E177R} mice in which apoptosis was severely compromised, but cell cycle arrest, senescence or

antioxidant defense were not, showed that $p53^{E177R}$ significantly delayed survival compared to both spontaneous tumorigenesis in $p53^{-/-}$ or $E\mu$ -*Myc*-driven lymphoma mouse models.¹²⁷ These results indicated that intact cell cycle arrest, senescence and antioxidant defense mechanisms are important in tumor suppression possibly, in a context-dependent manner.

As discussed before, the $p53^{3KR}$ mouse model fails to trigger apoptosis, cell cycle arrest or senescence. Yet, these mice are not susceptible to early onset spontaneous tumors as seen in $p53^{-/-or+/-}$ animals. Li et al. showed that these animals have an intact p53-regulated antioxidant defense and energy metabolism as shown by doxorubicin-induced transactivation of *Tigar*, *Gls2*, *Gpx* and *Gss* in $p53^{3KR}$ to levels similar to corresponding levels in $p53^{+/+}$ animals. Transformation of H1299 cells with $p53^{3KR}$ and *Gls2* significantly reduced colony formation *in vitro*, providing compelling evidence to support the important roles played by non-traditional functions regulated by p53.⁵⁷

From a tumorigenesis perspective, elimination of senescent cells has been shown to be tumor suppressive while accumulation of senescent cells have been shown to induce chronic inflammation that promotes tumorigenesis.^{97, 115} Recent work shows that clearance or accumulation of senescent cells are determined by immune cells such as natural killer (NK) cells, macrophages and T cells. SASP factors include chemoattractants and activating cytokines that are responsible for recruiting immune cells.^{111, 115} In hepatocellular carcinoma (HCC) mouse model, Xu et al. has shown that restoration of p53 in H-Ras^{K12V}-expressing hepatoblasts resulted in induction of senescence and tumor regression. Pharmacological inhibition of NK cells delayed tumor regression showing that NK cells play an important role in removing senescent cells.¹²⁸ In a follow-up study, Sagiv et al. showed that tumor regression is mediated by NK cells expressing the receptor NKG2D. These NK cells remove

senescent tumor cells that express a NK ligand, RAE1 ϵ (retinoic acid early inducible 1 ϵ).¹²⁹ In a different HCC model where N-RasG12V oncogene was overexpressed in the epithelial cells, senescence was shown to limit onset of tumor development. In this model, SASP activated CD4⁺ T helper type 1 (T_H1) cells which played a critical role in clearing senescent premalignant cells. However, this was accomplished together with monocytes/macrophages and NK cells as removal of senescent cells were compromised in an immunodeficient mouse model that lacked NK cells and monocytes/macrophages.¹³⁰ In a diethylnitrosamine (DEN)-induced HCC model, Lujambio et al. showed that p53-mediated senescence in hepatic stellate cells (HSCs) led to enrichment of M1-polarized macrophages and reduced tumor development. In contrast, ablation of p53 resulted in increased number of M2-polarized macrophages and tumorigenesis. Using conditioned media (CM) from senescent hepatic stellate cells (HSCs), authored showed SASP-derived factors resulted in M1-polarization of bone marrow-derived macrophages (BMDMs) that had increased ability to clear senescent cells *in vitro*. In contrast, SASP factors in CM from non-senescent proliferating HSCs polarized the BMDMs towards M2 phenotype that promoted proliferation of premalignant HSCs. Study concluded that SASP factors from senescent HSCs with intact p53 promoted M1 polarization of macrophages that limited tumor development.¹¹⁰

In contrast to beneficial effects of SASP, tumor promoting effects are also seen in several cancer models. In contrast to the findings in DEN-induced HCC model, Yoshimoto et al. showed that senescent HSCs induced DMBA (7,12-dimethylbenz(a)anthracene)-induced HCC in obese mice. Obese livers were shown to accumulate senescent HSCs as a result of chronic activation of DDR by deoxycholic acid, a product of gut microbiota. Regulation of SASP via IL1 β -mediated inflammasome was critical for tumor development

as inhibition of SASP in IL1 β -null mice reduced number and size of tumors.¹³¹ In a prostate cancer model, deletion of PTEN significantly induced senescence in the initiated epithelium. As a result, senescent tumor cells created an immunosuppressive tissue environment through activation of JAK2/STAT3 signaling, which led to tumor progression and resistance to docetaxel therapy.¹³² In a colorectal cancer model, Pribluda et al. showed that deletion of CSNK1A1 and p53 in the gut epithelium resulted in induction of senescence-associated inflammatory response, which promoted tumor growth and invasiveness.¹³³ In addition, Jackson et al. showed that SASP activation in MMTV-Wnt1 mammary adenocarcinoma tumors, with wild type p53, promoted cell proliferation and cancer relapse following doxorubicin treatment. In these tumors, activation of STAT3 signaling was observed in senescent cells adjacent to Ki67-positive proliferative cells indicating paracrine tumor promoting effects of SASP.¹³⁴ Considering current findings, it is postulated that composition of SASP seems to vary depending on the cell/tissue type, senescence inducer and the cellular context, resulting in different functional outcomes.¹¹¹

Modification of p53 function by codon 72 SNP

Frequent mutation of *p53* in human cancers shows the importance of p53 and the regulated processes in cancer susceptibility and progression. Therefore, single nucleotide polymorphisms that affect p53-regulated biological processes can play a significant role in modifying cancer risk. The *p53* gene has estimated 85 polymorphisms, which is a relatively high number within the length of the gene.^{8, 135}

Among the array of SNPs found on p53, rs1042522 is one of the most well-studied polymorphisms of p53. Located at codon 72 within exon 4 of p53, rs1042522 shows a non-synonymous substitution of 'C' to 'G', changing the encoded amino acid from a proline

(CCC) to an arginine (CGC) within the polyproline region between TAD and DBD. In 1994, the codon 72 SNP of *p53* (P72R) first came to limelight as a study concluded that higher abundance of the proline-coding variant (P72) of P72R in African populations was speculated to play a role in providing protection from sunlight.¹³⁶ As shown in Table 2, higher prevalence of P72 in African populations is further corroborated by recent findings of the 1000Genome study.¹³⁷ This study further showed that European populations that are farther from the equator, have higher prevalence of the arginine-coding variant of P72R (R72).¹³⁸ Similar to European populations, American populations have higher prevalence of R72. In contrast, Asian populations do not show preference to a particular allele or homozygous variant genotype. Recent comparative analysis of genes associated with cancer among primates by Puente et al. shows that P72 is exclusively found in non-human primates, but not R72. This provides evidence to support that P72 is the ancestral version and R72 may have coincided with the human migration to higher latitudes. Moreover, several hypotheses have been proposed to explain the abundance of R72 in higher altitudes where the climate is colder. Increased transactivation of the implantation factor LIF by R72 has been shown to provide an advantage in implantation, reproduction as well as tolerance to colder climates.¹³⁹ R72 has also been shown to increase lipid accumulation and weight gain that has been suggested to provide an adaptive advantage in colder climates and during famines.^{140, 141}

Table I-2. Allele and genotypic frequencies of codon 72 p53 SNP in populations of African, European, Asian and South American ancestries (1000 Genomes project)

African Population	C allele (%)	no. of Individuals	G allele (%)	no. of Individuals	CC (%)	no. of Individuals	GC (%)	no. of Individuals	GG (%)	no. of Individuals
Barbados	66%	126	34%	66	46%	44	40%	38	15%	14
Southwest US	60%	73	40%	49	33%	20	54%	33	13%	8
Esan, Nigeria	68%	135	32%	63	46%	45	46%	45	9%	9
Gambia	71%	160	29%	66	55%	62	32%	36	13%	15
Kenya	75%	148	25%	50	53%	52	44%	44	3%	3
Sierra Leon	61%	104	39%	66	37%	31	49%	42	14%	12
Yoruba, Nigeria	64%	138	36%	78	42%	45	44%	48	14%	15
Total	67%	884	33%	438	45%	299	43%	286	12%	76
<hr/>										
European Population	C allele (%)	no. of Individuals	G allele (%)	no. of Individuals	CC (%)	no. of Individuals	GC (%)	no. of Individuals	GG (%)	no. of Individuals
Utah	24%	48	76%	150	5%	5	38%	38	57%	56
Finland	30%	60	70%	138	11%	11	51%	50	38%	38
Great Britain	31%	56	69%	126	8%	7	46%	42	46%	42
Spain	30%	64	70%	150	8%	8	48%	51	45%	48
Italy	28%	59	72%	155	6%	6	51%	54	44%	47
Total	29%	287	72%	719	7%	37	42%	213	50%	253

Table I-2. Continued.

Asian Population	C allele (%)	no. of Individuals	G allele (%)	no. of Individuals	CC (%)	no. of Individuals	GC (%)	no. of Individuals	GG (%)	no. of Individuals
Xishuangbanna, China*	47%	88	53%	98	22%	20	52%	48	27%	25
Beijing, China*	45%	93	55%	113	18%	18	55%	57	27%	28
Southern, China*	40%	84	60%	126	15%	16	50%	52	35%	37
Tokyo, Japan	32%	66	68%	142	14%	14	37%	38	50%	52
Ho Minh City, Vietnam	43%	86	57%	112	19%	19	49%	48	32%	32
Bengali, India	42%	73	58%	99	16%	14	52%	45	31%	27
Gujarati, India [†]	42%	87	58%	119	18%	19	48%	49	34%	35
Telugu, India [‡]	54%	110	46%	94	28%	28	53%	54	20%	20
Punjabi, Pakistan [▯]	52%	100	48%	92	26%	25	52%	50	22%	21
Tamil, Sri Lanka [‡]	54%	111	46%	93	32%	33	44%	45	24%	24
Total	45%	898	55%	1088	21%	206	49%	486	30%	301

*Dan population, *Han population, [†]living in Houston, USA, [‡]living in the United Kingdom, [▯]living in Lahore, Pakistan

Table I-2. Continued.

American Population	C allele (%)	no. of Individuals	G allele (%)	no. of Individuals	CC (%)	no. of Individuals	GC (%)	no. of Individuals	GG (%)	no. of Individuals
Medellin, Columbia	28%	53	72%	135	7%	7	42%	39	51%	48
Mexico [€]	31%	40	69%	88	11%	7	41%	26	48%	31
Lima, Peru	37%	62	64%	108	14%	12	45%	38	41%	35
Puerto Rico	31%	65	69%	143	8%	8	47%	49	45%	47
Total	32%	220	68%	474	10%	34	43%	152	46%	161

[€]living in Los Angeles, USA

Molecular mechanistic data associated with P72R are predominantly based on *in vitro* studies where P72 and R72 are expressed under non-endogenous promoters within *p53*-null human cancer cell lines.^{142, 143} One of the obvious differences between the two variant *p53* proteins is the migration pattern on an immunoblot under native or denaturing conditions. In this assay, R72 migrates further than P72, suggesting that P72R imparts structural differences to p53. This was further supported by the differences in the banding pattern observed by Ozeki and colleagues following digestion of variant *p53* forms.¹⁴⁴

Several functional differences between these polymorphic variants have also been described. Specifically, upon DNA damage, the P72 variant preferentially binds to the p53 RE of *p21* upregulating the transcription, which has been shown to promote cell cycle arrest at G1/S¹⁴⁵ and senescence¹⁴⁶ compared to R72.¹⁴⁵⁻¹⁴⁷ Siddique and Sabapathy showed that P72 significantly upregulated UV-induced DNA repair by enhanced transactivation of *Gadd45a* and *p53r2* that led to better resolution of dipyrimidine photoproduct cyclobutane pyrimidine and enhanced unscheduled DNA synthesis in H1299 (lung cancer) and UISO (melanoma) cells.¹⁴⁸ In contrast, several studies have demonstrated that the R72 variant shows greater ability to induce apoptosis by transcription-dependent and -independent mechanisms.¹⁴³ Transcription-dependent mechanisms include enhanced transactivation of proapoptotic p53 target genes such as *Puma*, *Noxa*, *Bax*, *Perp* by R72. Dumont et al. demonstrated that R72 show increased binding to CBP, which enable translocation of R72 onto the mitochondrial membrane, inducing apoptosis.^{149, 150} PIN1 is previously shown to interact with the PRD of p53 and important in inducing apoptosis. In a study to investigate whether codon 72 variants affect interaction of PIN1 and apoptosis, Mantovani et al. showed that PIN1 interacts better with R72 than P72 and dissociate iASPP, a negative regulator of

apoptosis, from p53 allowing acetylation of p53 by p300 leading to enhanced apoptosis. In addition, Kung et al. showed that R72 binds to SUMO-ligase, TRIML2 preferentially in human fibroblasts homozygous for the variants. TRIML2 interaction increased SUMOylation of p53 which resulted in increased transactivation of proapoptotic p53 target genes P53-Induced Death Domain Protein 1 (PIDD), P53-Inducible Protein 3 (PIG3), and P53-Inducible Protein 6 (PIG6).¹⁵⁰

Current mouse models of codon 72 p53 SNP

There are currently two mouse models that have been utilized to understand the role of codon 72 p53 SNPs *in vivo*. Both mouse models are generated by replacing portions of mouse p53 with human p53 as mouse p53 codes for an alanine residue at codon 72. Murphy et al. developed the first codon 72 mouse model using human p53 knock-in (Hupki) mice having C57/B6 genetic background. In this model, exon 4-9 of mouse p53 is replaced with the equivalent region of human p53.^{138, 151, 152} In contrast to the Hupki model, Johnson et al. developed the second codon 72 p53 mouse model by replacing only the exon 4 of p53 and these mice had FVB/NJ genetic background.¹⁵² Recent studies using these models have explored the *in vivo* effects of codon 72 variants on p53-mediated biological processes and their functional outcomes.¹⁴³ To investigate whether variants modify apoptosis *in vivo*, Azzam et al. exposed P72 and R72 homozygous Hupki mice to 10 Gy of gamma radiation and analyzed apoptosis in radio-sensitive thymus, small intestine and spleen. Interestingly, P72 mice showed a significant induction of apoptosis in the thymus while the opposite was true for small intestine as R72 mice had more apoptotic cells. However, in the spleen, there was no observable difference in level of apoptosis between the two variant mice. Together, results showed that the apoptotic response modified by the variants in a tissue-specific

manner.¹⁵³ In the same animal model, Kung et al. recently showed that R72 increased obesity, metabolic dysfunction and inflammation when animals were fed with a high-fat diet. Ability of R72 variant to transactivate *Tnfa* and *Npc1l1* were shown to play a critical role in promoting fat accumulation and inflammation in the livers as pharmacological inhibition of TNF α and NPC1L1 significantly reduced fat accumulation and inflammation.¹⁴⁰ In a separate study, Frank et al. showed that in MEFs derived from Hupki codon 72 variant mice, P72 variant significantly increased cell cycle arrest and senescence when exposed to DNA damaging agent, etoposide or H-Ras was overexpressed. Codon 72 Hupki mice were also challenged with lipopolysaccharide (LPS) to investigate how the variants would affect immune response. Findings showed that inflammation was significantly upregulated in the livers of P72 Hupki mice compared to R72 counterparts. P72 Hupki mice showed increased levels of p53 target genes, *Caspase-4/11* and *Gdf15* as well as NF-kB pathway that was concluded to mediate the increased inflammation. Effect of R72 and P72 variants were also explored in *E μ -Myc*-driven B cell lymphoma using homozygous P72 and R72 Hupki mice overexpressing *E μ -Myc*. Mice carrying the P72 variant showed a modest increase in latency, which was attributed to increased ability to induce senescence. However, the tumor spectrum or survival was not different between the R72 and P72 mice.¹⁴⁶ In the FVB model of codon 72 p53, exposure to different DNA damaging agents induced apoptosis better in R72 MEFs than in P72 MEFs through transcription-dependent and -independent manner. Same study showed that the polymorphic variants did not have differential effects on chronic UV-induced skin carcinogenesis in homozygous variant mice backcrossed into SKH background. Together, results to-date show that the variants affect p53-regulated biological

processes in a context-dependent manner with a minimal impact on tumorigenesis in the contexts of *Eμ-Myc*-driven B cell lymphoma and chronic UV-induced skin carcinogenesis.

Codon 72 p53 SNP and cancer risk

Among the various polymorphisms found in the p53 gene, rs1042522, is widely studied in human populations for association with cancer risk. While association of increased cancer susceptibility of p53 polymorphic variants to many human cancers have been shown in literature, the findings show modest correlation with cancer susceptibility.^{142, 154} This may be attributed to the complexity of cancer in terms of incomplete penetrance of risk alleles and interaction with the environmental factors.^{142, 155} Yet, an increased risk association with many types of cancers, including skin, squamous cell carcinoma of the head and neck (SCCHN), lung, cervix, colon, colorectal, prostate and breast has been reported.^{142, 143, 156-163}

The role of codon 72 p53 variants in cancer is accentuated by the findings of several studies. These showed that P72 allele is lost while R72 allele is more frequently mutated and retained in tumors of codon 72 heterozygous patients with breast, SCCHN and colon cancer.^{143, 156, 158, 159, 164} In these studies, breast as well as head and neck cancer patients with mutations in the R72 allele showed significantly poor sensitivity to chemotherapy, disease-free and overall survival.^{157, 158} In this head and neck cancer patient cohort, Bergamaschi et al. showed that mutant R72 was able to bind to p73.¹⁵⁷ Previous *in vitro* findings by Marin et al. showed that mutant R72 is capable of binding to p73 and inhibit induction of apoptosis.¹⁶⁴ Therefore, it is likely that inhibition of p73-mediated induction of apoptosis by mutant R72 may play a role in observed chemoresistance and poor survival.

Despite these findings, major challenges remain in translating these associations into clinical applications. For example, discerning the functional consequences of the variant, as

well as the genes and molecular pathways connecting the variant with disease, have proved extremely challenging. This limited understanding of the biology behind these significant associations has clearly constrained the ability to integrate SNP biomarkers into the proper genetic, cellular and clinical context to maximize their effective use in the clinic.⁸

The work reported in this dissertation extends the understanding of the important role of the codon 72 p53 single nucleotide polymorphism on mammary tumorigenesis. Chapter III describes investigations on the risk modifying effect of the codon 72 variants on mammary tumorigenesis using DMBA- and MMTV-*ErbB2/Neu* mouse models, while chapter IV provides mechanistic details thereof.

CHAPTER II

MATERIALS AND METHODS

Maintenance and genotyping of transgenic mice

Transgenic FVB mice that were homozygous for the proline (P72), or for the arginine variant (R72) were used in the study (received from Dr. David Johnson at M.D. Anderson Cancer Center, Smithville, TX). PCR-based genotyping of mice was performed as previously described (22). All the study mice were generated from genotype-confirmed parents. Genotypes of random study mice were verified using both the PCR- and a qRT-PCR-based characterization method. The PCR-based method is described previously (22). The qRT-PCR-based method was a custom SNP allelic discrimination assay (Assay ID: AH89RLW) provided by Applied Biosystems. The qRT-PCR genotyping was performed in ABI7900HT real-time PCR instrument (Applied Biosystems, Thermo Fisher Scientific Inc.).

All mice were fed standard chow ad libitum, except during tumorigenesis studies, with free access to water and were housed in our Association for Assessment and Accreditation of Laboratory Animal Care-certified, temperature- and humidity-controlled facilities, with a 12-hour light/12-hour dark cycle. All procedures were performed according to the protocols approved by the Institutional Animal Care and Use Committee at Texas A&M University, College Station, TX.

Tumorigenesis experiments

DMBA treatment of mice

To generate parous study animals, a total number of P72 (46) and R72 (41) mice were harem bred at 6 weeks of age. Litters were weaned at 3 weeks of age and the mammary glands of parous study animals were allowed to involute for 3 weeks. Mice were gavaged 1 mg of DMBA (dissolved in 100 uL of corn oil) orally once a week for six weeks. For the nulliparous arms of the study, 16 weeks old P72 (39) and R72 (40) mice were gavaged 1 mg of DMBA (dissolved in 100 uL of corn oil) orally once a week for six weeks similar to the parous mice.

All study mice of both tumorigenesis studies were fed AIN76A diet after weaning and palpated twice weekly for tumors. Tumor latency was recorded as the day a palpable mammary tumor was detected. Mice were sacrificed when the tumor reached approx. 1 cm in any direction. Tumors were sliced and fixed in 10% *Neutral* buffered formalin (NBF) for histology. Intact solid tumors were sliced and a slice was frozen in OCT and the rest of the tumor was snap frozen for molecular analyses. Glands with no observable tumors/abnormal growths were fixed in 10% NBF and snap-frozen for molecular analyses.

Tumors histology was analyzed by two pathologists to confirm mammary gland origin and subsequent features displayed. The Kaplan-Meier method was used to generate percentage mammary tumor free versus latency curves of DMBA-treated variant mice and E-P72R mice (Graph Pad Software).

Generation of MMTV-*ErbB2*/*Neu* codon 72 variant mice

FVB/N-Tg(MMTV*Neu*)202Mul/J mice were purchased from Jackson Laboratories and bred with p53 polymorphic mice to generate bigenic mice that were hemizygous for *ErbB2* and homozygous for the p53 variants (E-P72R). *ErbB2* copy number was determined by qRT-PCR using a TaqMan assay (Applied Biosystems, Inc., Assay ID: Mm00658541_m1). A total of 54 E-P72 and 56 E-R72 female mice were used for this study.

Animals were monitored daily for health status and tumors. Mice were palpated twice weekly for tumors throughout the study and were sacrificed when the tumor reached 1.5 cm in any direction. Mice were sacrificed by CO₂ asphyxiation and mammary tumors were measured and tissues harvested for later analyses.

Tumor histology was analyzed by two pathologists to confirm diagnosis and characterization.

Protein extraction and immunoblotting

Proteins were extracted from mammary glands using boiling 2X Laemmli sample buffer. Protein concentrations were determined using the BCA protein assay kit (Cat#: 23225, Thermo Fisher Scientific, MA) according to the manufacturer's protocol. Equal amounts of total protein (40 ug) were resolved by SDS-PAGE and transferred to PVDF membranes. Membranes were probed with following primary antibodies: from Cell Signaling Technologies (CST): CCL2 (1:1000, 2029) GAPDH (1:5000, 2118), Phospho-RB (1:1000, 8516), Phospho-p65 (Ser536) (1:1000, 3033), TNF α (1:1000, 11948), from Santa Cruz Technologies: p53 (1:500, sc-6243) and p21 (1:500, sc-397).

All blots except GAPDH were incubated with goat anti-rabbit HRP-conjugated secondary antibody (1:2000, CST 7074) and developed using ECL Prime reagents (GE

Healthcare). The images were captured using a FluorChem M imager (ProteinSimple, San Jose, CA) and quantified with AlphaView software (ProteinSimple, San Jose, CA). GAPDH blots were incubated with iRDye800CW secondary antibody (1:5000, 925-3211) and developed and imaged using the Odyssey Li-COR system (LI-COR Biotechnology, NE).

RNA extraction and qRT-PCR

Mammary glands were homogenized with a Brinkmann Polytron bench-top homogenizer and RNA was extracted with Maxwell® 16 LEV simplyRNA Tissue Kit using the Maxwell® 16 Instrument according to the SimplyRNA tissue protocol (Promega Corporation, WI). To validate the quality of extracted RNA, samples were randomly checked for the quality of RNA using 2200 TapeStation instrument following manufacturer's protocol (Agilent Technologies, Inc.). Total RNA was then reverse transcribed as previously described.¹⁶⁵

Reverse transcription was performed using the epMotion 5075t automated liquid handling system (Eppendorf North America, NY). The ABI Prism 7900HT sequence detection system was used for the qRT-PCR analyses, and TaqMan gene expression assays for *p53* (Mm01731290_g1), *p21* (Mm04205640_g1) were purchased from Applied Biosystems, Inc. Previously published qRT-PCR primers for SYBR green reactions of *Erb2*, *Il6*, *Il8*, *p16^{INK4a}*, *Pai1*, *Tnfa*, *Ccl2*, *Vegfa*, *Mmp3*, *Mmp9*, *Il1 β* and *iNos* were used to determine the target gene expression.^{57, 140, 166-170} Each sample was normalized to corresponding TATA box binding protein (*Tbp*) gene expression, using TaqMan assay (Assay ID: Mm00446973_m1) for TaqMan reactions, and previously published qRT-PCR primers for SYBR green reactions (Table II-1).^{57, 140, 166-170} All the samples were run in

triplicates per gene. Quantification of target gene expression was performed using the delta delta Ct (relative quantification) method.

Table II-1. qRT-PCR primer sequences used in SYBR green reactions

Gene	Forward Primer (5' to 3')	Reverse Primer (5' to 3')
<i>Ccl2</i>	CCCAATGAGTAGGCTGGAGA	TCTGGACCCA TTCCTTCTTG
<i>Ccl4</i>	CCCACCTTCTGCTGTTTCTC	GTCTGCCTCTTTTGGTCAGG
<i>Erbb2</i>	GCAAGCACTGTCTGCCATGC	GGGCACAAGCCTCACACTGG
<i>Il1β</i>	GTGTGGATCCAAAGCAATAC	GTCTGCTCATTTCATGACAAG
<i>Il6</i>	AGTCAATTCCAGAAACCGCTATGA	TAGGGAAGGCCGTGGTTGT
<i>Il8</i>	CCATGGGTGAAGGCTACTGT	AGAGGCTTTTCATGCTCAACA
<i>iNos/Nos2</i>	GTCAACTGCAAGAGAACGGAGA	CTGAGAACAGCACAAGGGGTT
<i>Mmp3</i>	CGATGATGAACGATGGACAG	AGCCTTGGCTGAGTGGTAGA
<i>Mmp9</i>	TGAATCAGCTGGCTTTTGTG	GTGGATAGCTCGGTGGTGT
<i>p16</i>	GTCGTACCCCGATTCAAGT	ACCAGCGTGTCCAGGAAG
<i>Pai1</i>	TTGTCCAGCGGGACCTAGAG	AAGTCCACCTGTTTCACCATAGTCT
<i>Tbp</i>	GGAATTGTACCGCAGCTTCAAA	GATGACTGCAGCAAATCGCTT
<i>Tnfa</i>	CCCCAAAGGGA TGAGAAGTT	CACTTGGTGGTTTGCTACGA
<i>Vegfa</i>	AGGCTGCTGTAACGATGAAG	TCTCCTATGTGCTGGCTTTG

Chromatin immunoprecipitation of p53

Chromatin from the mammary glands was isolated as described previously.¹⁷¹ In brief, approximately 300mg of tissue was minced in cold PBS and cross-linked in 1% freshly-made paraformaldehyde-PBS for 10 min. Cross-linking was quenched by adding glycine to a final concentration of 125mM, and homogenized with a Dounce homogenizer in cold cell lysis buffer (10mM Tris-Cl, pH 8.0, 10mM NaCl, 3mM MgCl₂, 1% NP-40) supplemented with protease inhibitors (Roche, #04693159001) to generate a single cell suspension. Cells were incubated on ice, and centrifuged at 1,000g for 10 min at 4°C to pellet

nuclei. The pellet was then resuspended in nuclear lysis buffer. Chromatin was sheared by sonication to an average size of 200 to 1000bp using a Bioruptor (Diagenode, NJ), and insoluble debris were removed by centrifugation. Immunoprecipitation was performed using 10ug of p53 (FL393) antibody (sc-6243). Primer pairs used for ChIP analysis of p53 RE are given in Table II-2. Primers used for qRT-PCR to measure *Tnfa* and *Ccl2* p53 REs are previously published.¹⁴⁰

Table II-2. ChIP qRT-PCR primer sequences used in SYBR green reactions

Gene with p53 RE	Forward Primer (5' to 3')	Reverse Primer (5' to 3')
<i>Ccl2</i> -RE1	CAGGAAATGCTTGGATGACA	GGTGGAAAGGACCAGACTCA
<i>Ccl2</i> -RE2	CATAGCCAAGCCACTGTGAA	GACCTCCATGCTGAAGTGCT
<i>Tnfa</i> -RE	GCCTCTCCTACCCTGTCTCC	CAGGAGGACCAGACCCATTA
<i>p21</i> -RE	AAAATCGGAGCTCAGCAGGCCT	ATCAGGTCTCCACCACCTGC

Sudan Black B (SBB) staining of senescent cells

SBB staining was performed at the histology core, College of Veterinary, Texas A&M using Sudan Black B Histochemical Stain Kit following manufacturer's protocol (American MasterTech, KTSBBPT).

Immunohistochemistry of Ki67, CD31, IBA1 and CC3

The Immunohistochemistry Core, Texas A&M or Pathology core at Baylor College of Medicine, performed IHC using standard protocols. Briefly, FFPE tissue sections were deparaffinized in xylene (VWR, MK866802) and rehydrated in ethanol (100%-95%) and then distilled water. Antigen retrieval was performed in 0.1M Tris-HCl, pH 9.0 for 15

minutes. Endogenous peroxidase activity was quenched with 3% hydrogen peroxide (VWR, BDH7540-2). Sections were blocked in 10% bovine serum albumin in PBST. Tissue sections were incubated for 45 min with primary antibody, and 1 hour with HRP-conjugated anti-rabbit IgG secondary antibody (Abcam). Color was developed by adding the substrate and chromogen 3,3'-diaminobenzidine (DAKO). Primary antibodies used in IHC staining include Ki67 (1:500, Abcam, 15580), CC3 (1:200, CST, 9664), IBA1 (1:500, WAKO, 019-19741) and CD31 (1:200, Abcam, ab28364). Sections were counterstained with hematoxylin (VWR, RC353032) before visualization using automated upright microscope (LeicaDM5500B, Leica Biosystem, Germany). Quantification of images was performed using Immuneration application¹⁷² in Fiji software¹⁷³⁻¹⁷⁵ or blinded manual counting in at least six high power fields.

Multiplex indirect immunofluorescence

Slides with FFPE 5 µm sections of mammary glands were de-paraffinized in xylene (VWR, MK866802) and re-hydrated in ethanol (100%-95%-70%) and then 1X PBS. Antigen retrieval was performed by boiling in sodium citrate solution, pH 6.0 for 10 minutes. After washing in PBST, sections were blocked with 10% horse serum in PBST for 1 hour. Tissue sections were incubated overnight at 4°C with primary antibodies, washed, and incubated with Alexa dye-conjugated anti-goat/anti-rabbit IgG for 1 hour at RT. Primary antibodies used included: IBA1 (1:100, WAKO, 019-19741) and IL1β (1:50, R&D Systems, AF-401-NA). Sections were visualized using A1R HD confocal microscope (NIKON Instruments Inc., NY). Images was captured using NIS elements software and blindly quantified in six high power fields.

Exposure of R72 and P72 mice to high-fat diet (HFD)

The defined HFD was purchased from Research Diets, Inc. (cat#D04011601). The composition of the diet is given in Table II-3. Both male and female homozygous R72 and P72 mice at the age of 10 weeks were fed HFD for 13 weeks. Animal weight and food intake were recorded weekly during the experiment.

Table II-3. Composition of the defined high-fat diet

Ingredient	Weight (g)	% of calories
Casein	200	20%
L-Cystine	3	
Cornstarch	0	
Maltodextrin	100	10%
Sucrose	245.6	24%
Cellulose	50	
Soybean oil	25	6%
Lard	177.5	39%
Minerals	45	
Vitamin mix	10	
Choline bitartrate	2	
Energy	4.728 kcal/g (45% of calories from fat)	

Statistical analysis

Log-rank test for trend was performed to compare the K-M curves statistically. Fisher's exact test and chi-square tests were performed to compare tumor incidence. Unpaired Student's t test was used to compare tumor growth rates and any two groups in

qRT-PCR, IHC and densitometry analyses. All the statistical analyses were performed in GraphPad Prism software (version 6). P value less than 0.05 was considered statistically significant ($P < 0.05^*$, $P < 0.01^{**}$ and $P < 0.001^{***}$).

CHAPTER III
EFFECT OF CODON 72 POLYMORPHIC VARIANTS ON MAMMARY
TUMORIGENESIS

Rationale

Codon 72 p53 variants have been demonstrated to differentially-regulate p53-regulated mechanisms such as apoptosis, cell cycle arrest, senescence and inflammation.¹⁴³ In addition, human epidemiological data show increased risk association with many types of cancers, including skin, squamous cell carcinoma of the head and neck (SCCHN), lung, cervix, colon, colorectal, prostate and breast has been reported.^{135, 136, 149-156} To date, the mechanisms by which codon 72 p53 variants differentially affect mammary tumorigenesis remain unresolved since none of the *in vitro* and *in vivo* experiments on codon 72 variants has been performed in a setting relevant to breast cancer. Traditionally, rats and mouse models have been used successfully to model mammary tumorigenesis using potent carcinogens such as 7,12-dimethylbenz[a]anthracene (DMBA), or overexpression of oncogenes such as MMTV-ErbB2/Neu in genetically engineered mouse models.¹⁷⁶⁻¹⁷⁹ Therefore, we investigated how codon 72 p53 variants affect mammary tumorigenesis in a physiologically relevant *in vivo* setting, using a previously characterized human p53 exon 4 knock-in mouse model, carrying the polymorphic variants.¹⁵²

Results

Decreased mammary tumor latency and higher incidence in R72 mice.

Our initial investigations focused on the impact of the codon 72 p53 variants on mammary tumor development in two distinct models. We initially used 7,12-dimethyl benz(a)anthracene (DMBA) to induce mammary carcinomas.²³ As shown in Figure III-1, mice with the arginine variant, R72 (n=39), had significantly reduced mammary tumor latency compared to those with the proline variant, P72 (n=40) (Log-rank test; p=0.049). Mammary tumors first appeared at 21 days post-DMBA in R72 mice, 50 days earlier than in P72 animals. R72 mice also had 50% higher mammary tumor incidence compared to P72 animals (Figure III-2). Histopathological analysis revealed multiple mammary cancer phenotypes, with mammary adenocarcinomas with squamous metaplasia being the most common (data not shown).

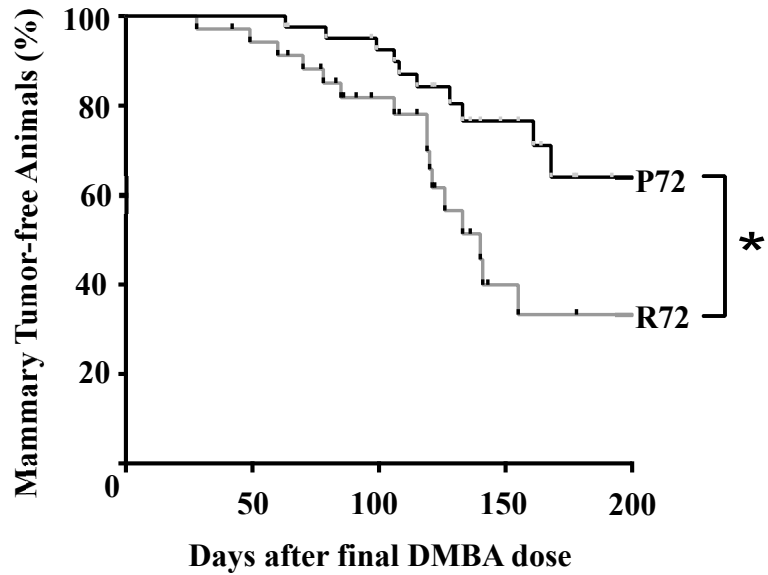


Figure III-1. Kaplan-Meier curves, showing proportion of mammary tumor-free P72 (n=40) and R72 (n=39) mice, after DMBA treatment (*p<0.05).

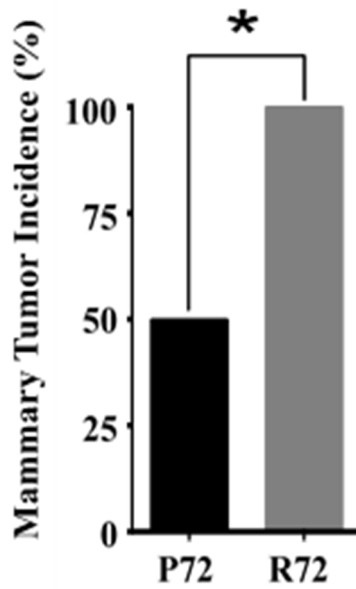


Figure III-2. Percentage mammary tumor incidence in DMBA-treated R72 and P72 animals (*p<0.05).

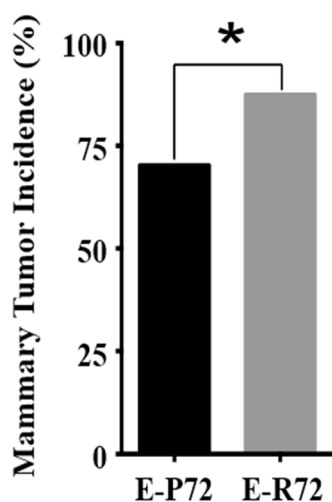


Figure III-3. Percentage mammary tumor incidence in E-R72 and E-P72 animals (* $p < 0.05$).

Next, we investigated the impact of *p53* polymorphic variants on mammary tumorigenesis in the *MMTV-ErbB2/Neu* FVB mouse model.¹⁸⁰ We generated F3 animals that were homozygous for codon 72 variants and hemizygous for *MMTV-ErbB2/Neu* transgene. Similar to the carcinogenesis study, mammary tumor incidence was increased by 17% in E-R72 animals compared to E-P72 animals ($p = 0.004$, Figure III-3). In addition, E-R72 mice had significantly reduced mammary tumor latency compared to E-P72 (Log-rank test, $p = 0.004$, Figure III-4). Mammary tumors appeared in E-R72 animals as early as 122 days of age, while in E-P72 animals they appeared at 173 days of age, a difference of 51 days. At the stage of 50% mammary tumor-free, tumor latency of E-R72 mice was 227 days compared to 250 days of E-P72 mice.

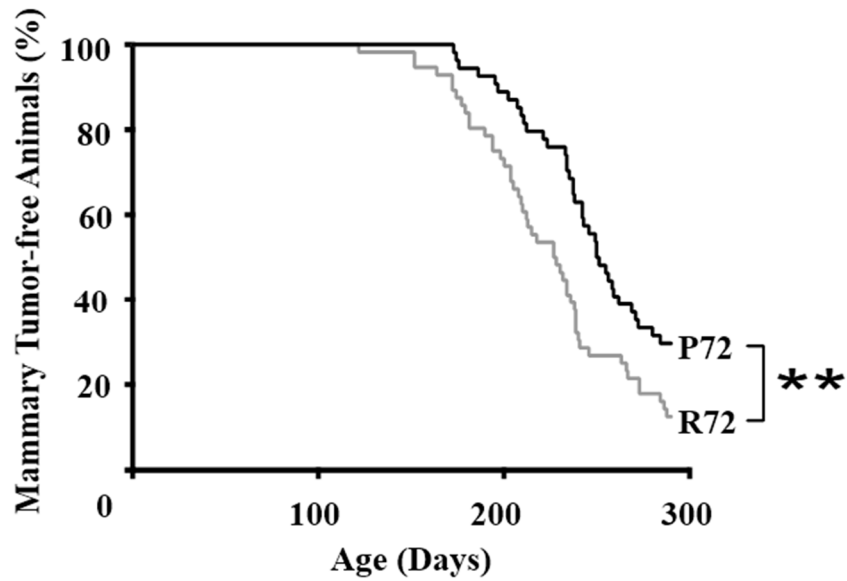


Figure III-4. MMTV-*ErbB2/Neu* mammary tumorigenesis. A) Kaplan-Meier curves of mammary tumor-free E-P72 (n=54) and E-R72 (n=56) animals (**p<0.01).

As previously observed in *MMTV-ErbB2/Neu* mice with a FVB background¹⁸⁰, histopathological assessment revealed that all tumors found in E-R72 and E-P72 mice were mammary adenocarcinomas with central necrosis (Figure III-5). Together, results demonstrate that codon 72 p53 variants modified mammary tumor development in the context of either DMBA- or MMTV-*ErbB2/Neu*-induced mammary tumorigenesis.

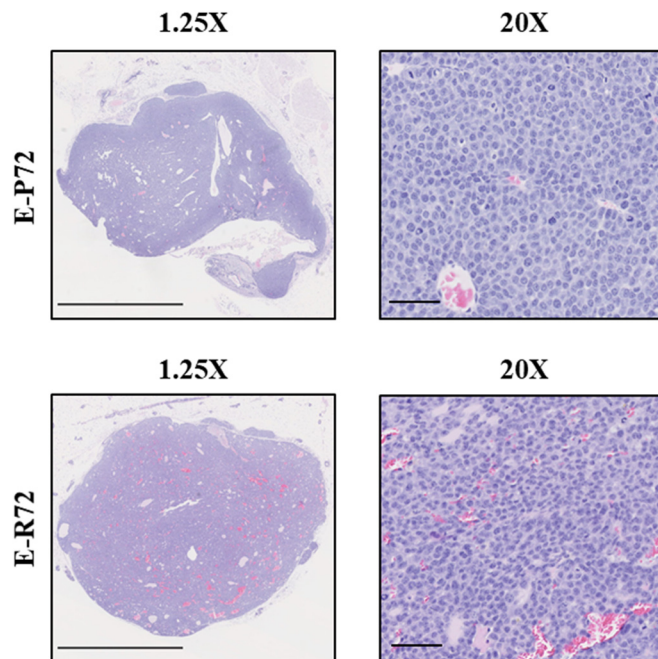


Figure III-5. Representative H&E stained tumors of mammary adenocarcinoma found in E-P72 and E-R72 animals. Magnification 1.25X and 20X with scale bars 2.5 mm and 100 μ m, respectively.

Enhanced mammary tumor progression in E-R72 animals.

The observed reduction in tumor latency in mice carrying R72 prompted us to assess tumor growth rates. Mammary tumors appeared in DMBA-treated animals grew fast, which did not allow us to determine the tumor growth rates of all tumors. Additionally, the tumors were of different histopathologies, which makes comparison of growth rates uninformative. In contrast, mammary tumors found in MMTV-*ErbB2/Neu* mice had similar tumor histopathology (mammary adenocarcinoma) and the growth rates were determined for all tumors. As shown in Figure III-6, tumors arising in E-R72 animals showed a significantly higher average growth rate (37.8 ± 5.1 mm³ per day) compared to tumors that developed in E-P72 mice (22.8 ± 5.0 mm³ per day). This indicated that a R72-mediated mechanism

provided proliferative advantage to mammary tumors found in E-R72 mice compared to E-P72 counterparts.

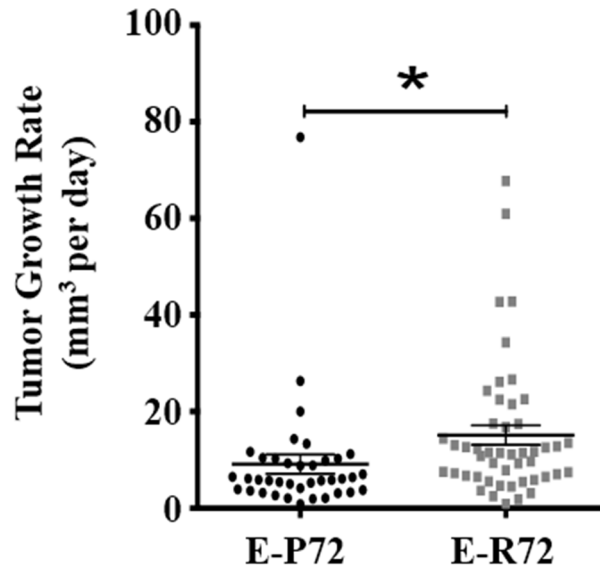


Figure III-6. Average growth rates (mm³ per day) of mammary tumors in E-P72 (n=38) and E-R72 (n=48) animals. Error bars represent mean \pm SEM (*p<0.05).

Expression analysis of Ki67, a marker of cell proliferation¹⁸¹, showed that tumors from E-R72 animals had a significantly higher percentage of Ki67-positive cells compared to those in E-P72 animals (Figures III-7A and B). The proportions of cleaved Caspase-3 positive cells, albeit in very low levels, were similar in tumors from E-R72 and E-P72 mice, indicating no difference in apoptosis (Figures III-8A and B). Together, results showed that the increased growth rate is a consequence of increased prosurvival/proliferation advantage rather than a reduction in cell turnover in the tumors of E-R72 mice compared to that of E-P72 counterparts.

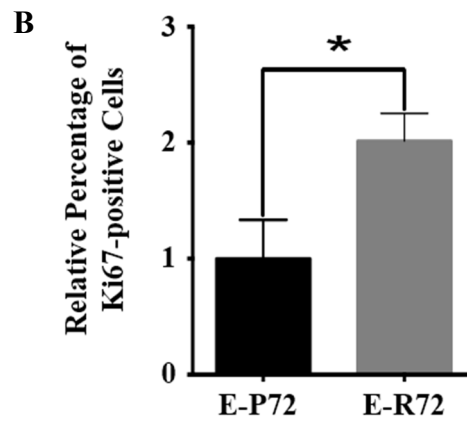
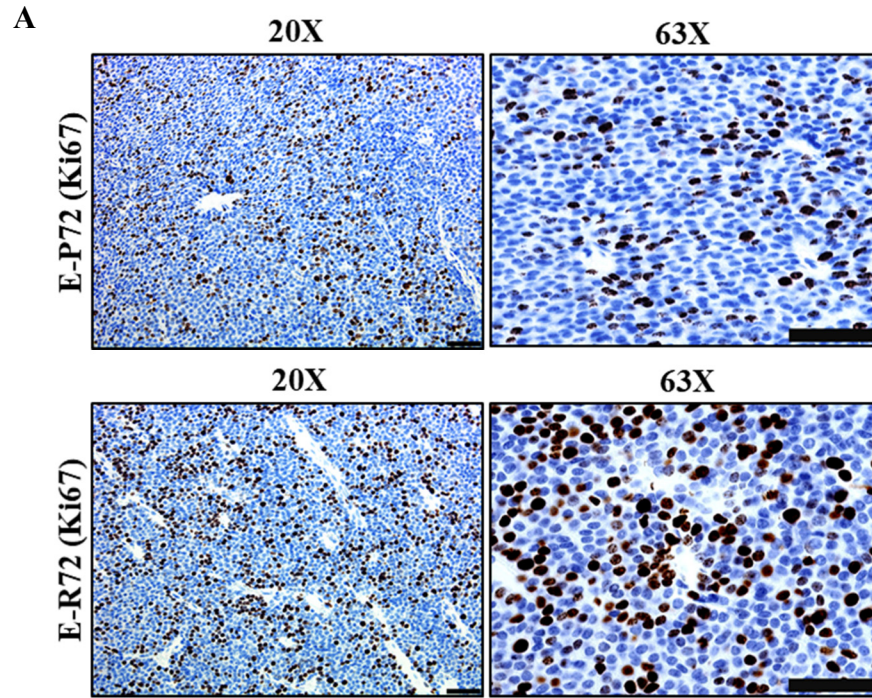


Figure III-7. A) Representative IHC images of Ki67 stained mammary tumors from E-P72 and E-R72 animals, respectively. Magnifications, 20X and 40X, scale bar, 50 μ m. B) Quantification of Ki67+ cells in mammary tumors from E-R72 and E-P72 animals. Values are standardized to the mean of E-P72 samples and shown as mean \pm SEM (n=5, *p<0.05).

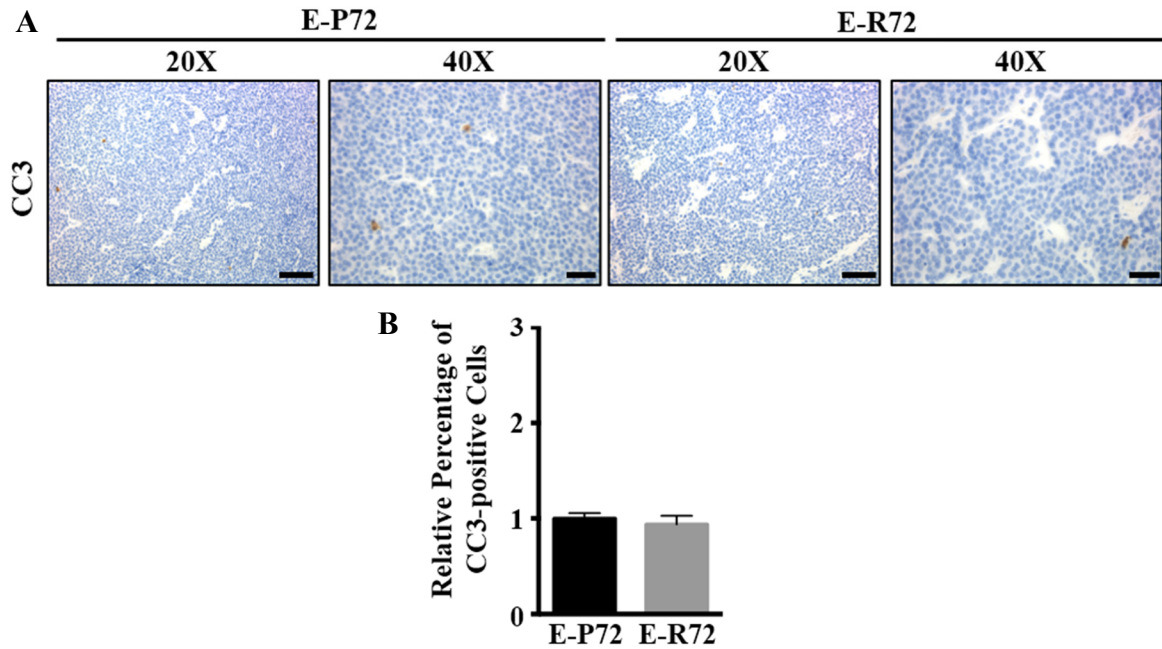


Figure III-8. A) Representative IHC images of CC3 immunostaining in mammary tumors from E-P72 and E-R72 animals, respectively. Magnifications, 20X and 40X, scale bar, 50 μ m. E) Quantification of CC3+ cells in tumors from E-R72 and E-P72 animals. The values are standardized to the mean of E-P72 samples and shown as mean \pm SEM (n=5, *p<0.05).

Level of p53 is important to instigate p53-mediated biological processes⁴⁸ and these processes are important for MMTV-*ErbB2/Neu*-driven tumor growth as loss of *p53* allele and mutations that disrupt p53-regulated processes have been shown to provide growth advantage.^{182, 183} In addition, previous studies show that the level of *ErbB2/Neu* affects tumor growth.¹⁸⁰ Therefore, we determined the gene expression levels of *p53* and *ErbB2* in the tumors from MMTV-*ErbB2/Neu* mice carrying P72 and R72. The qRT-PCR results showed that the gene expression of *ErbB2* and *p53* were similar between the two genotypes

indicating that the differences mediated by expression of *ErbB*.

y tumors were not

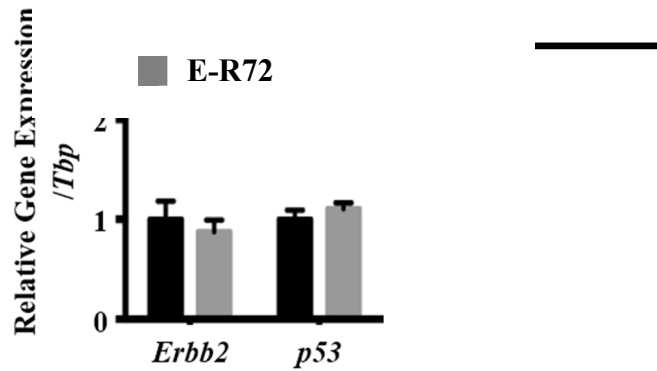


Figure III-9. qRT-PCR of mRNAs of *ErbB2* and *p53* genes in tumors of E-P72 (black bars) and E-R72 (grey bars) animals (n=4). Results shown as relative mRNA expression of specified genes normalized to corresponding *Tbp* levels. The expression values are standardized to the mean of E-P72 samples and shown as mean±SEM.

Breast cancer prevention via early first full-term pregnancy (eFFTP).

Among new BrCa patients more than 90% are above the age of 45 years and women aged between 55 - 64 years are more prone to the disease.³ Among many reproductive risk factors of BrCa, an eFFTP provides a breast cancer protection later in life. Epidemiological studies show that an eFFTP before the age of 20 years result in 50% reduction in a life-long risk of breast cancer relative to nulliparous women.¹⁸⁴⁻¹⁸⁶ However, pregnancy is followed by a transient increase in breast cancer risk.¹⁸⁷ However, the window of breast cancer risk is minimal in women younger than 25 years at FFTP benefitting from the significant protective effect of pregnancy later in life.¹⁸⁸ Several epidemiological studies show that the protective

effect of eFFTP reduces the incidence of hormone receptor-positive luminal BrCa, which is the most common among older BrCa patients.^{189, 190}

Modeling pregnancy protection in rodents.

Pregnancy-mediated breast cancer protection was replicated in rodent, both rat and mouse, models where carcinogen treatment resulted in more than 40% reduction in mammary tumorigenesis in parous animals compared to the age-matched nulliparous.^{177, 179, 191} In addition, mammary tumorigenesis studies in these models demonstrated that a mimicry of pregnancy, by administration of high doses of estrogen (E₂) and progesterone (P) for 21 days, was capable of providing a similar protection. Mammary glands of parous mice, and mice exposed to higher doses of E₂ and P shows elevated levels of *p53* in comparison to age-matched nulliparous and non-treated mice, respectively.^{177, 178, 191} Medina and Kittrel showed that the pregnancy protection was absent in mice carrying transplanted *p53*^{-/-} mammary epithelia demonstrating that *p53* is a critical contributor to pregnancy-mediated protection from BrCa.¹⁹¹

Lack of pregnancy protection in codon 72 p53 mice.

Given the critical role played by *p53* in pregnancy protection, we first investigated whether the proline (P) and arginine (R) variants of *p53* have different effects on pregnancy-induced protection. To this extent, we used 7,12-dimethyl benz(a)anthracene (DMBA) to induce mammary tumors in parous as well as virgin R72 and P72 mice. Surprisingly, pregnancy did not significantly affect mammary tumor incidence (Figure III-10) or latency (Figure III-11) in parous P72 or R72 mice treated with DMBA, compared to nulliparous counterparts. Interestingly, pregnancy actually increased mammary tumor incidence by

12.5% in mice homozygous for the P72 variant, and decreased incidence by 20% in homozygous R72 animals, these changes did not reach statistical significance, even though groups included ≥ 35 animals. Analysis of histopathology of mammary tumors revealed most common (data not shown). This was similar multiple tumor types, with mammary adenocarcinomas with squamous metaplasia being the to the profiles of previous DMBA-induced tumor studies.^{176, 192}

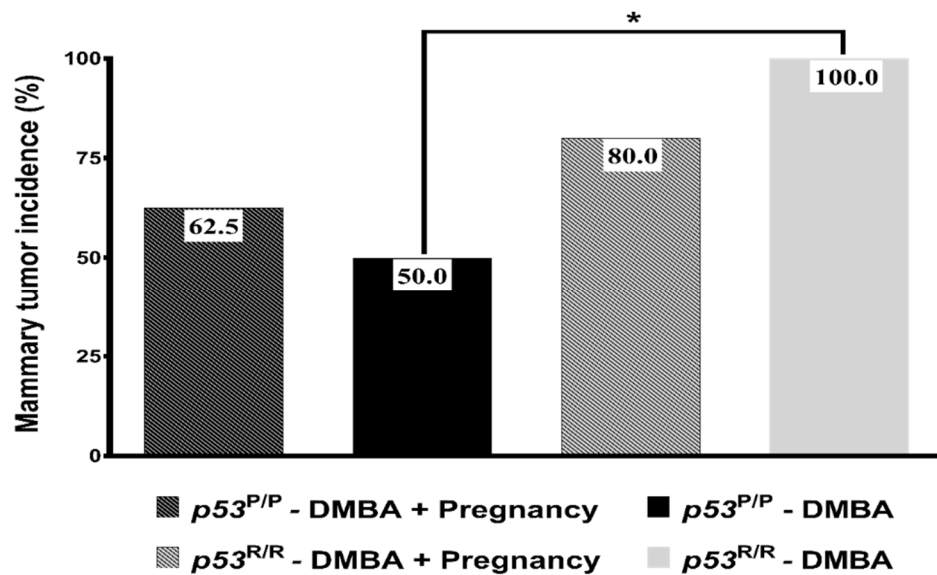


Figure III-10. Mammary tumor incidence in DMBA-treated parous and nulliparous R72 and P72 mice. Percentage mammary tumor incidence in parous and virgin P72 and R72 animals (* $p < 0.05$, Fisher's exact test). Mammary tumor incidence is indicated at the top of the bar (animals that prematurely died or were sacrificed without mammary tumors, were excluded from the mammary tumor incidence calculations).

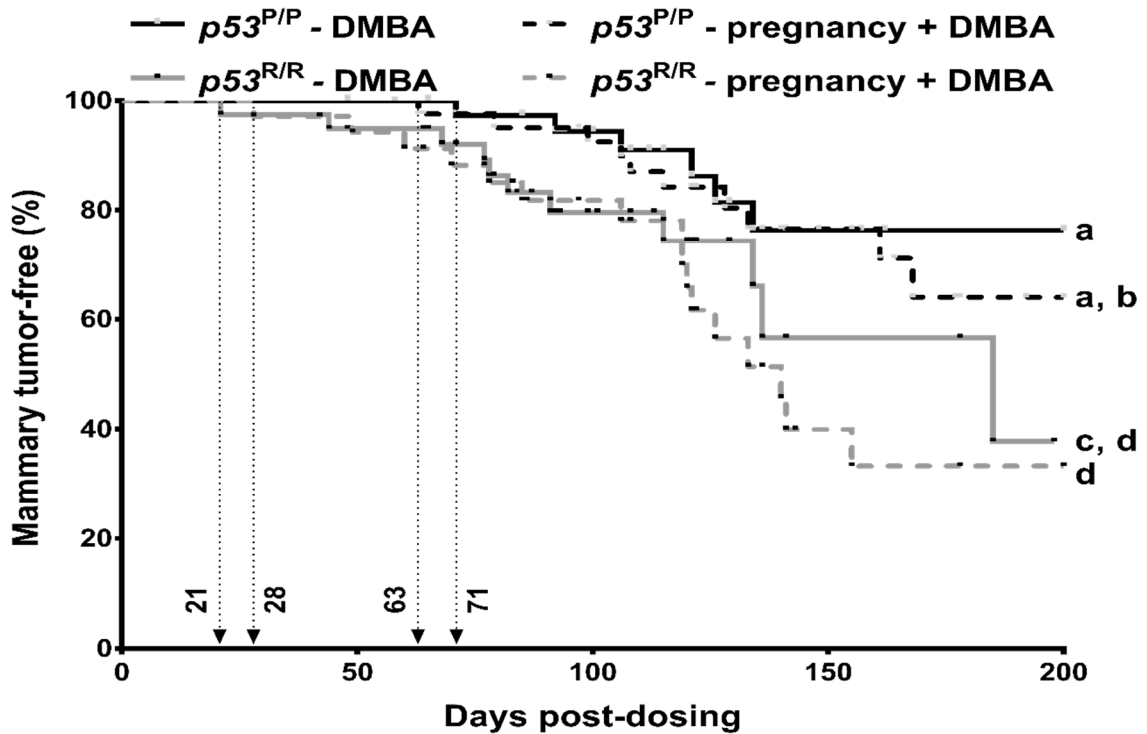


Figure III-11. DMBA-induced mammary tumorigenesis in parous and virgin P72 and R72 animals. Kaplan-Meier curves of mammary tumor-free parous and virgin P72 (n=42 and 40, respectively) and R72 (n=35 and 39, respectively) animals exposed to six weekly doses of 1 mg of DMBA dissolved in corn oil. Mammary tumor latencies of R72 and P72 animals were 21 days vs 71 days post DMBA dosing, respectively. Log rank test was used for statistical comparison of tumorigenesis curves. Different letters indicate that the curves are statistically significant ($p < 0.05$).

Discussion

We conducted mammary tumorigenesis studies in R72 and P72 transgenic mice to study the effect of codon 72 variants on mammary tumor development, which has not been resolved so far. In addition, we investigated the effect of codon 72 variants on pregnancy-mediated protective mechanism on mammary tumorigenesis that has been successfully modeled in previously in rat models and two mouse strains.¹⁷⁹ Results demonstrated that the codon 72 p53 polymorphism modifies mammary tumor susceptibility and latency in both the DMBA- and MMTV-*ErbB2/Neu*-induced mammary tumorigenesis models that are of distinct tumor etiologies. R72 variant was associated with higher tumor susceptibility and reduced tumor latency compared to P72. However, pregnancy did not reduce tumor incidence or latency in R72 and P72 mice exposed to DMBA.

Several aspects of our carcinogenesis study may explain the lack of pregnancy protection, including the use of a different mouse strain, timeline of DMBA treatment, and duration of lactation and involution. Medina and Smith utilized BD2fF1 (F1 animals of a cross between C57BL and DBA/2f-F1) and C3H/Sm mouse strains¹⁹³ in contrast to the inbred FVB/NJ strain used in our study. In the Medina study, parous mice lactated for only 1 week before they allowed mammary glands to involute for 3 (in BD2fF1 mice) or 4 (in C3H/Sm mice) weeks. In contrast, our *p53* variant animals lactated for 3 weeks until pups are normally weaned, which is physiologically more relevant, and glands were allowed to involute for 3 weeks. Our variant mice were 16 weeks of age at the beginning of the DMBA administration, compared to 12 or 15 weeks in the Medina study. However, we believe the most important difference was likely the background strain.

While the differences mentioned above could explain the observed lack of pregnancy protection, recent findings by Katz et al. (2015) may also be informative. In this study, parous and nulliparous FVB/NJ mice lactated for 21 days and mammary glands were allowed to undergo involution for 4 weeks. Animals were euthanized 4 weeks (at the age of 125 days) or 6.5 months (at the age of 315 days) post-involution, and genomic DNA was subjected to a massive parallel targeted sequencing approach in order to analyze differentially methylated regions across the genome.¹⁹⁴ Their findings showed that while 446 genes are hypermethylated after 4 weeks of involution, there was an approximately five-fold increase in the number of hypermethylated genes (2,260) 315 days post-involution. Many of the members of the IGF-1 pathway that play key roles in mammary development and pregnancy, lactation, and involution, such as *Igf1*, *Irs1*, *Irs2*, *Igfbp4*, *Ghr*, *Akt1* and *Akt2*, are hypomethylated after 4 weeks of involution, but are hypermethylated 315 days post-involution. These results indicate that the methylation of important IGF-1 pathway genes is altered over time following pregnancy and involution. Since the precise time frame for these changes in expression regulation is unknown, it is possible that the effects of pregnancy can be altered by epigenetic mechanisms that may be affected by protocol differences.

Even though the pregnancy protection was not recapitulated in our model, findings of DMBA- and MMTV-*ErbB2/Neu*-driven mammary tumorigenesis in codon 72 mice showed that mice with R72 variant had increased tumor incidence and shorter tumor latency compared to P72 counterparts. This suggests that R72 variant may increase the risk of mammary tumorigenesis despite distinct tumor etiologies, chemical- or genetic-driven. Increased tumor proliferation, as assessed by higher number of Ki67⁺ tumor cells, and similar levels of apoptosis, determined by CC3⁺ tumor cells, which was significantly low,

showed that tumors found in E-R72 mice have higher proliferative/survival advantage than tumors in E-P72 mice. In addition, this may also explain the reduction in tumor latency observed in E-R72 animals. Similar expression levels of *ErbB2* and *p53* showed that the differences in tumor incidence and latency were not a result of *ErbB2* and/or *p53* expression levels.

CHAPTER IV

**MOLECULAR MECHANISMS UNDERLYING DIFFERENTIAL MAMMARY
TUMORIGENESIS IN MMTV-ERBB2/NEU CODON 72 P53 MICE**

Rationale

The milieu in susceptible tissues can play a critical role in initiation and progression of tumors.^{195, 196} Previous studies have shown that the 72 variants of p53 differ significantly in their ability to regulate biological processes such as apoptosis, cell cycle arrest and senescence that not only directly regulate cell survival, but can also modulate the tissue environment.^{48, 196, 145, 146, 149, 197} Therefore, we examined apoptosis, cell cycle arrest and senescence in the mammary glands of adult E-P72 and E-R72 mice, to determine whether codon 72 variants differentially regulate processes that modify susceptibility to mammary tumorigenesis.

Results

Increased proportion of senescent cells in the susceptible mammary glands of E-R72 mice.

First, we assessed the expression of p53-regulated proapoptotic genes that trigger mitochondrial permeabilization leading to Caspase cleavage and apoptosis. As shown in Figure IV-1A, expression of *Puma*, *Noxa* and *Bax* were similar in E-P72 and E-R72 animals. Interestingly, *Perp* showed significantly higher gene expression levels in the susceptible

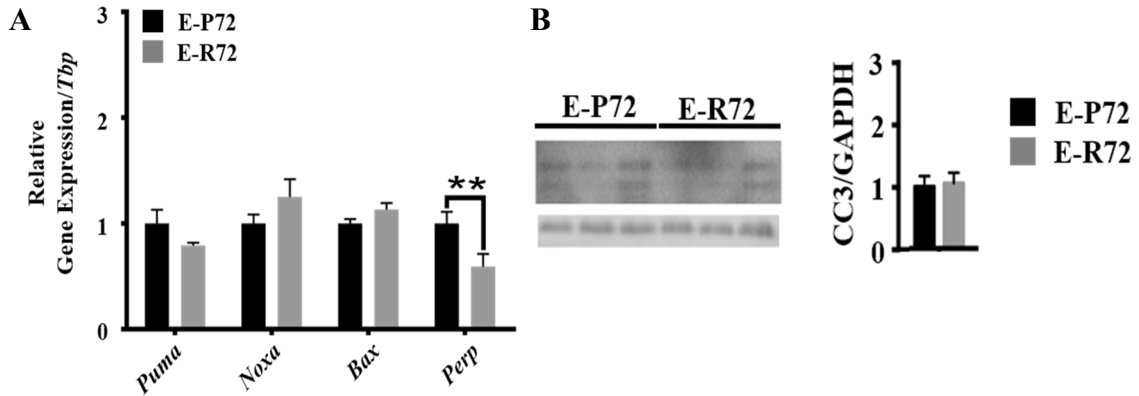


Figure IV-1. Apoptosis in susceptible mammary glands of E-R72 and E-P72 mice. A) Quantitative RT-PCR of mRNAs of p53-regulated proapoptotic genes in the mammary glands from age-matched E-P72 (black bars) and E-R72 (grey bars) animals. Relative mRNA expression of specified genes is normalized to corresponding *Tbp* levels. The expression values are standardized to the mean of E-P72 samples and shown as mean±SEM (n=6). B) Representative western blot image of CC3 and the loading control, GAPDH, in the protein extracted from mammary glands of age-matched E-P72 (black bars) and E-R72 (grey bars) animals (n=4). Densitometry of the CC3 bands normalized to corresponding GAPDH levels, and standardized to the mean of E-P72 samples shown as mean±SEM.

mammary glands of E-P72 mice. Interestingly, *Perp* showed significantly higher gene expression levels in the susceptible mammary glands of E-P72 mice. However, as determined by protein densitometry (Figure IV-1B) and immunohistochemistry (Figure IV-2), similar levels of cleaved Caspase-3 showed that apoptosis was not significantly different in the susceptible glands of E-R72 and E-P72 mice.

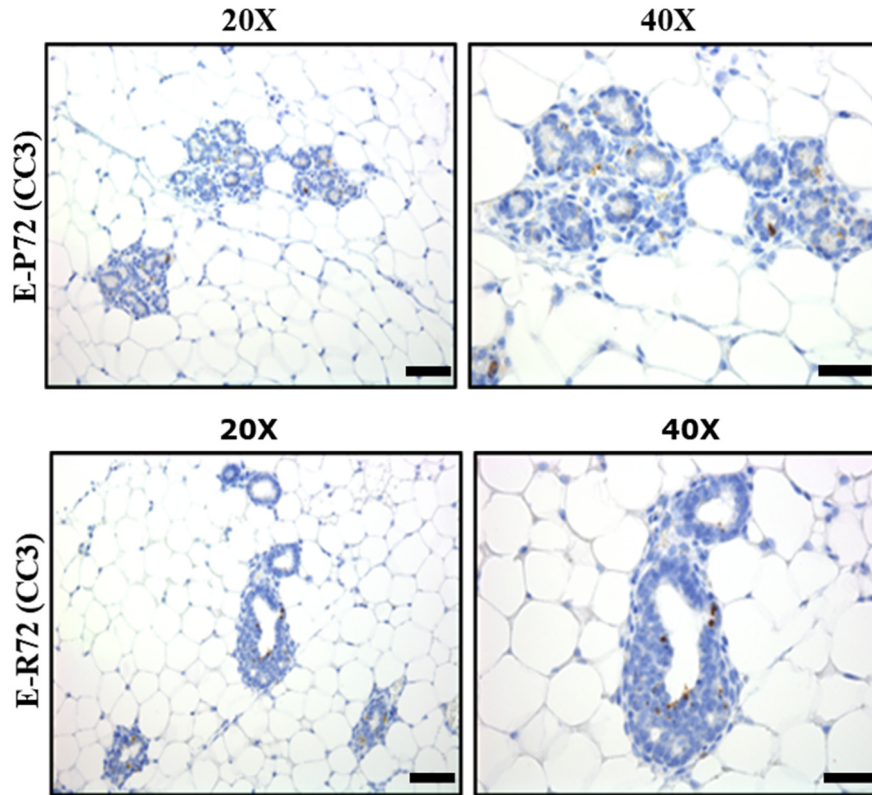


Figure IV-2. Representative IHC images of CC3 stained mammary tumors found in E-P72 and E-R72 animals, respectively. 20X, 40X magnification, scale bar, 50 μ m.

We then measured the expression of two major effectors of cell cycle arrest and senescence, *p21* and *p16^{INK4a}*.^{100, 103} These genes induce cell cycle arrest by disrupting the formation of Cyclin-CDK complexes and activating RB via hypophosphorylation.⁸⁵ The active form of RB binds to members of the E2F family, repressing expression of cell cycle progression genes.¹⁹⁸ As shown in Figure IV-3A, the expression levels of *p21* and *p16^{INK4a}* mRNA were two and three times higher, respectively, in the glands of E-R72 animals compared to E-P72 animals ($p < 0.05$). Protein expression of p21 was also upregulated in the

mammary glands of E-R72 animals (Figure IV-3B). In addition, glands from E-R72 animals had a significant decrease in levels of phosphorylated RB (P-RB) (Figure IV-B).

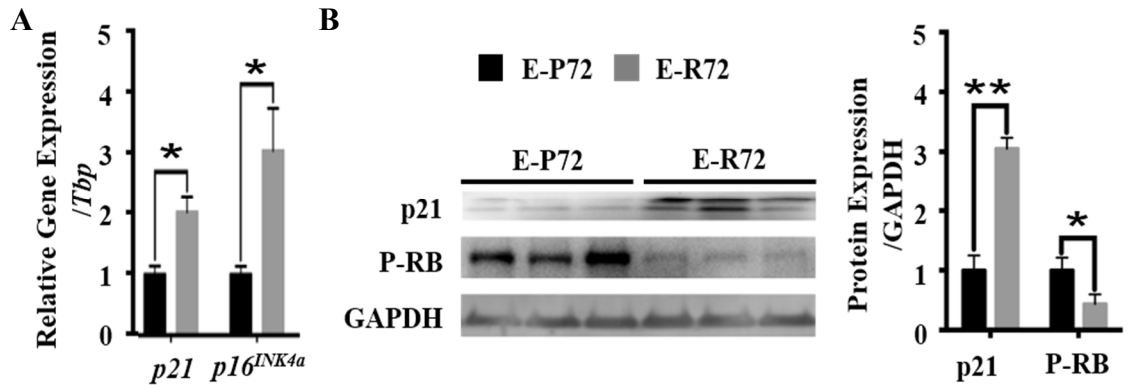


Figure IV-3. Cell cycle arrest and senescence in susceptible mammary glands of E-R72 and E-P72 mice. A) Quantitative RT-PCR of mRNAs of cell cycle arrest and senescence effectors, *p21* and *p16^{INK4A}* in the mammary glands of age-matched E-P72 and E-R72 animals. Results shown as relative mRNA expression of specified genes normalized to corresponding Tbp levels. The expression values are standardized to the mean of E-P72 samples and shown as mean±SEM (n=6, *p<0.05). B) Representative western blot image of p21, phosphorylated RB (P-RB) and the loading control, GAPDH, in mammary glands from age-matched E-P72 and E-R72 animals. Densitometry of the p21 and P-RB bands normalized to corresponding GAPDH levels and standardized to the mean of E-P72 samples shown as mean±SEM (n=5, *p<0.05, **p<0.01).

Sudan Black B (SBB) identifies senescent cells by binding to lipofuscin, an aggregate of oxidized and cross-linked proteins.¹⁰² As shown in Figure IV-4, the proportion of SBB+ cells was higher in mammary glands of E-R72 compared to E-P72 animals. These results show that mammary tumor incidence and proliferation were increased in E-R72 mice,

while the mammary glands from these animals also had an increased proportion of senescent cells.

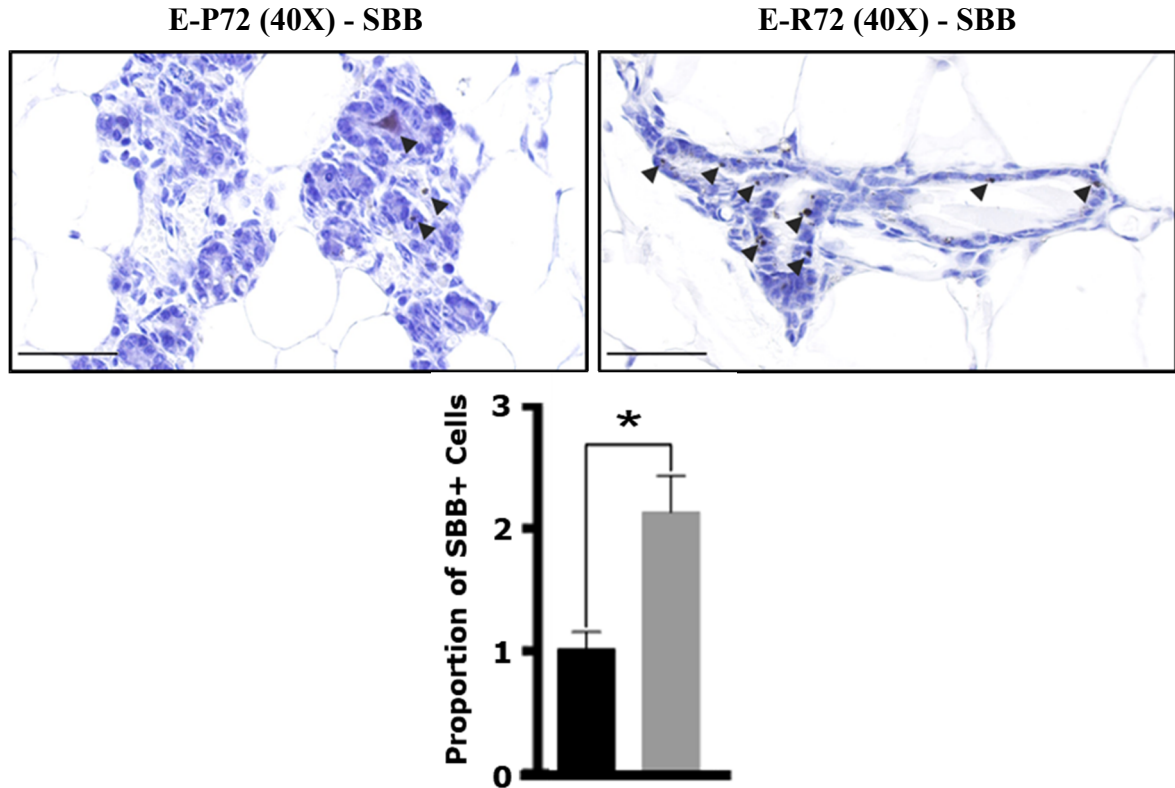


Figure IV-4. Representative images of Sudan Black B stained susceptible mammary glands of age-matched E-P72 (black bars) and E-R72 (grey bars) animals, respectively. Magnification 40X, scale bar 50 μ m. Quantification of relative proportion of Sudan Black B (SBB)-positive cells in susceptible mammary glands of age-matched E-R72 and E-P72 animals. Results show counts of six high power fields per animal (more than 9000 cells in total). Proportions are standardized to the mean of E-P72 samples shown as mean \pm SEM (n=3, *p<0.05).

Increased SASP, proinflammatory markers and angiogenesis in the susceptible mammary glands of E-R72 mice.

Traditionally, permanent cell cycle arrest, a pre-requisite of cellular senescence, has been thought to inhibit tumorigenesis by preventing expansion of transformed cells. However, recent studies provide strong evidence for the contrary, demonstrating that senescent cells can acquire a senescence-associated secretory phenotype (SASP), which is proinflammatory and protumorigenic. SASP is characterized by secretion of a mixture of proinflammatory cytokines, growth and matrix remodeling factors and chemoattractants that contribute to chronic tissue inflammation.^{103, 119, 199} In turn, chronic inflammation promotes cancer initiation and tumor progression, due to its mutagenic and proliferative signals, respectively.^{200, 201}

RelA (p65), one of 5 transcription factors in the NFκB signal transduction pathway, is phosphorylated in response to stress, and translocates into the nucleus to regulate the transcription of factors that contribute to the inflammatory SASP.^{109, 113} As shown in Figure IV-5, levels of phosphorylated p65 (serine 536) were significantly higher in the glands from E-R72 compared to E-P72 mice, demonstrating differential activation of the NFκB pathway.

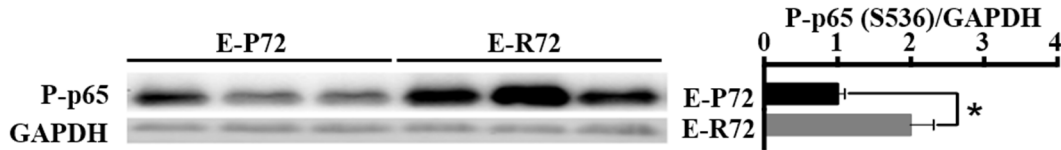


Figure IV-5. Representative western blots of P-p65 (Ser536) and the loading control, GAPDH, in mammary glands from age- matched E-P72 (black bars) and E-R72 (grey bars) mice. Densitometry of P-p65 bands normalized to corresponding GAPDH levels and standardized to the mean of E-P72 samples shown as mean \pm SEM (n=4, *p<0.05).

In addition to activation of the of the NFkB pathway, differential acquisition of the SASP in glands from E-R72 mice is demonstrated by increased expression of genes that regulate multiple aspects of the secretory phenotype. Expression of Pail, an angiogenic factor that also contributes to sustained cellular senescence,¹¹⁶ was elevated in the glands of E-R72 mice compared to E-P72 (Figure IV-6). The matrix remodeling protease gelatinase-B (MMP9) has also been associated with breast cancer risk specifically,²⁰² and Mmp9, but not Mmp3, was also elevated in glands from R72 mice. Proinflammatory cytokines Tnfa and Il6, but not Il8, were also significantly increased in mammary glands of E-R72 mice compared to their E-P72 counterparts (Figure IV-6). TNF α in the mammary glands of E-P72R mice. As shown in Figure IV-7, immunoblots revealed that TNF α protein levels were upregulated by two-times in the mammary glands of E-R72 mice, providing further evidence of increased NFkB pathway activation.

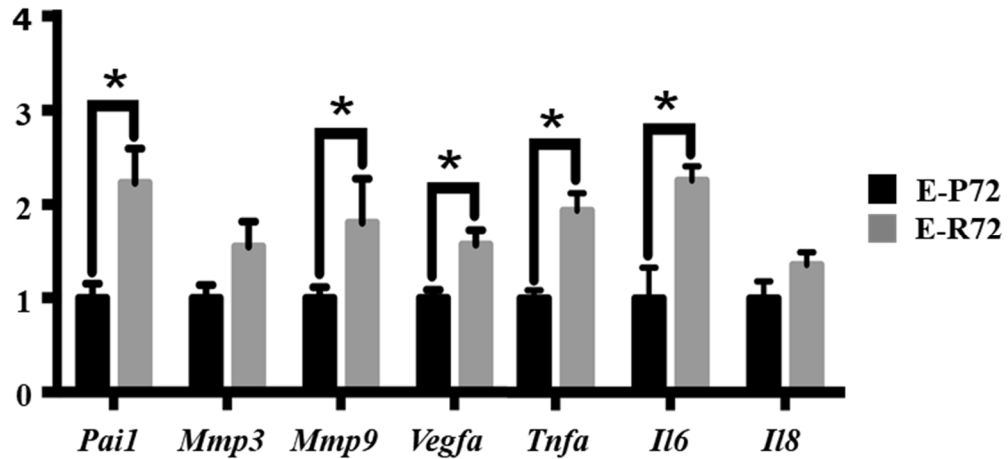


Figure IV-6. Quantitative RT-PCR of mRNAs of SASP genes in mammary glands from age-matched E-P72 and E-R72 mice. Relative mRNA expression is normalized to corresponding *Tbp* levels, and expression values are standardized to the mean of E- P72 samples and expressed as mean±SEM (n=6, *p<0.05).

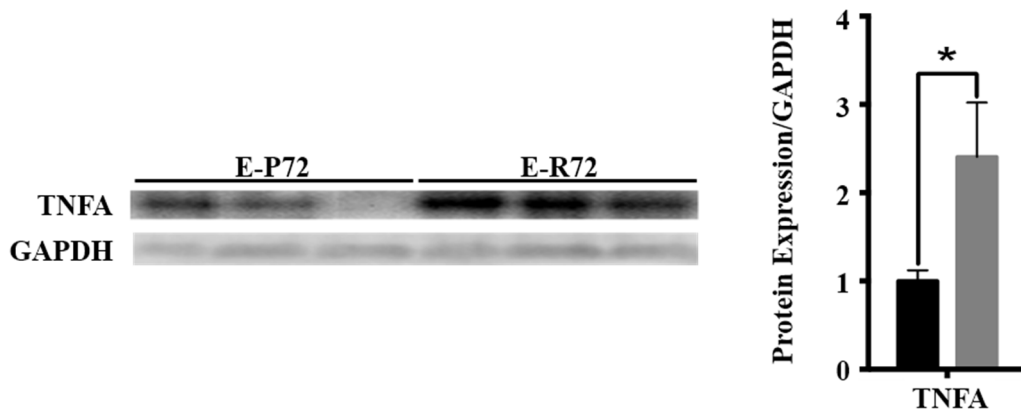


Figure IV-7. Representative western blots of TNFA, and the loading control, GAPDH, in the protein extracted from mammary glands of age-matched E-P72 (black bars) and E-R72 (grey bars) animals. Densitometry of the western blots normalized to corresponding GAPDH levels and standardized to the mean of E-P72 samples shown as mean±SEM (n=4, *p<0.05).

Inflammation also stimulates vascular dilation and increased capillary density as part of the immune response.^{203, 204} VEGF is one of the most studied angiogenic factors, and variants of this gene have been associated with increased risk of a variety of different cancers.^{205, 206} Since a significant increase in *Vegfa* expression was observed in the glands of E-R72 mice (Figure IV-6), mammary angiogenesis was also assessed by immunolocalization of the endothelial cell marker CD31.²⁰⁷ As shown in Figure IV-8, a significant increase in CD31+ blood vessels was observed in the mammary epithelia of E-R72 mice.

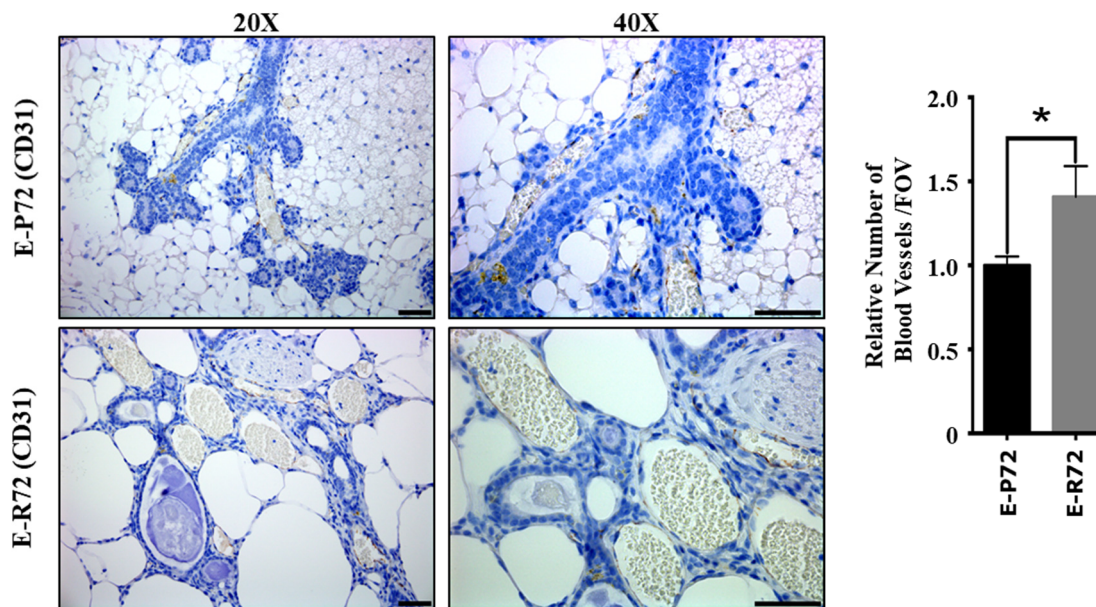


Figure IV-8. Representative images of CD31 stained mammary glands from age-matched E-P72 and E-R72 mice, respectively. Magnifications, 20X and 40X, scale bar, 50 μ m. Quantification of CD31+ blood vessels surrounding mammary epithelia per high power field in mammary glands from age-matched E-P72 and E-R72 mice. Values are standardized to the mean of E-P72 samples and shown as mean \pm SEM (n=5, *p<0.05).

Increased influx of proinflammatory macrophages in susceptible glands of E-R72 mice.

The influx and persistence of proinflammatory macrophages are also critical indicators of and contributors to chronic tissue inflammation.²⁰⁸ CCL2 is a major driver of macrophage infiltration that has been shown to promote tumor progression in multiple cancer models.²⁰⁹ Expression of a major macrophage chemoattractant, CCL2 was increased in mammary glands of E-R72 animals, by 3.3 times at the message level (Figure IV-9A), and 1.5 times at the protein level (Figure IV-9B).

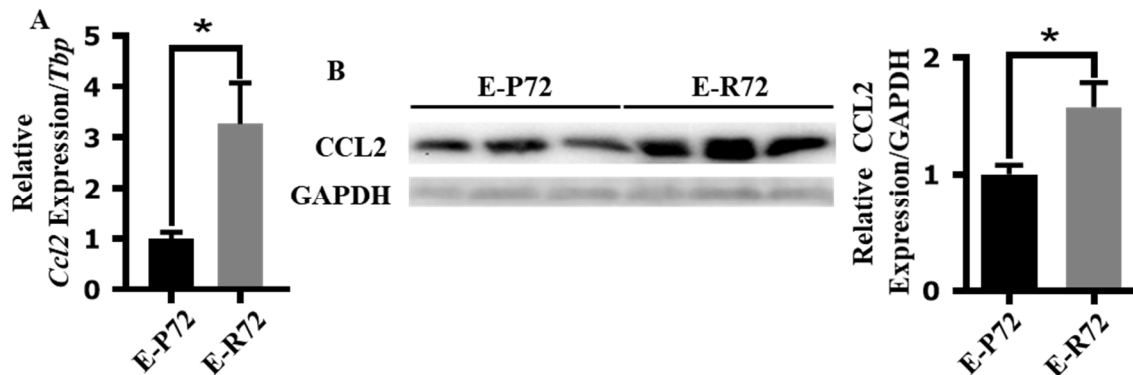


Figure IV-9. A) Quantitative RT-PCR of *Ccl2* mRNA in the mammary glands from age-matched E-P72 (black bars) and E-R72 (grey bars) animals. Relative mRNA expression is normalized to corresponding *Tbp* levels, and values are standardized to the mean of E-P72 samples and expressed as mean \pm SEM (n=9, *p<0.05). B) Representative western blots of CCL2 and GAPDH in extracts of mammary glands from age-matched E-P72 and E-R72 animals. Densitometry of the CCL2 western blot normalized to corresponding GAPDH levels and standardized to the mean of E-P72 samples shown as mean \pm SEM (n=4, *p<0.05).

Macrophage influx into mammary glands of E-P72R animals was evaluated using the pan-macrophage marker, IBA1. Immunohistological localization of IBA1 revealed significantly more macrophages surrounding the ducts (Figures IV-10A and B) and within the white adipose tissue (WAT) (Figure-10A and C) of susceptible mammary glands from E-R72 compared to E-P72 mice.

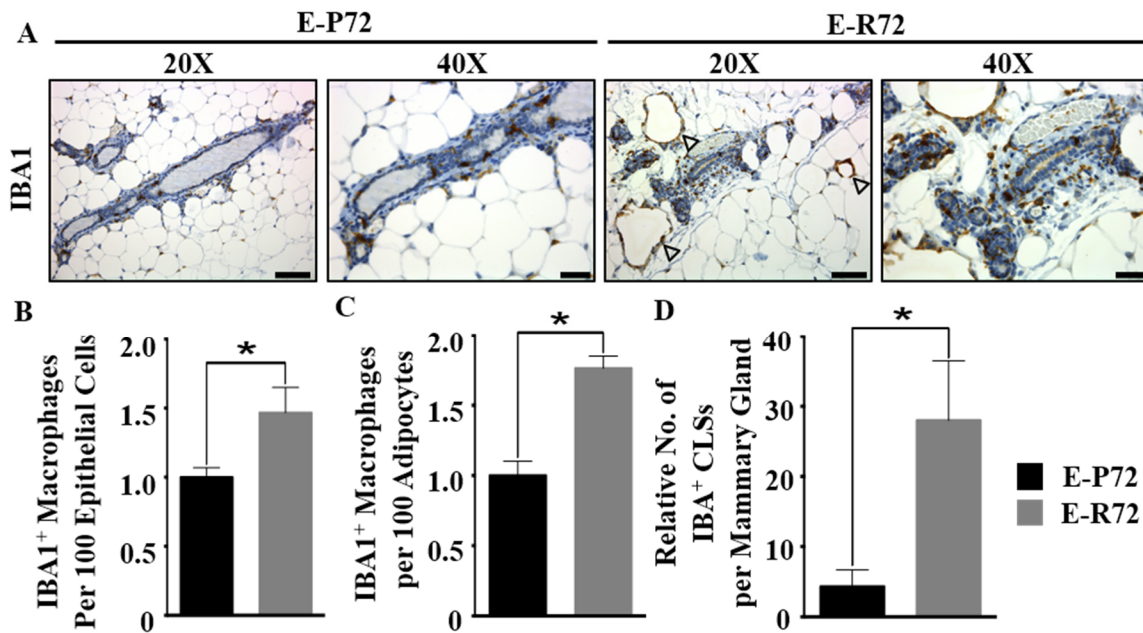


Figure IV-10. Influx of macrophages into susceptible glands of E-R72 and E-P72 mice. A) Representative IHC images of IBA1 stained mammary glands of age-matched E-P72 and E-R72 animals, respectively (n=5). Magnifications, 20X and 40X, scale bar, 50 μ m. B-D) Quantification of IBA1⁺ macrophages per 100 epithelial cells (B), 100 adipocytes (C), and CLSs per animal (D) in mammary glands of age-matched E-P72 and E-R72 animals. The values are standardized to the mean of E-P72 samples and shown as mean \pm SEM (n=5, *p<0.05).

Proinflammatory macrophages produce cytokines such as IL1 β and, through upregulation of iNOS (inducible nitric oxide synthase), reactive nitrogen species.^{166, 210} Expression of *Il1 β* and *iNos* were significantly upregulated in mammary glands of E-R72 animals compared to E-P72s (Figure IV-11). Dual immunofluorescent staining of IBA1 and IL1 β revealed a significant increase of proinflammatory macrophages around mammary epithelia (Figures IV-12A and B) and adipose tissue (Figures IV-12A and C) in glands of E-R72 compared to E-P72 mice.

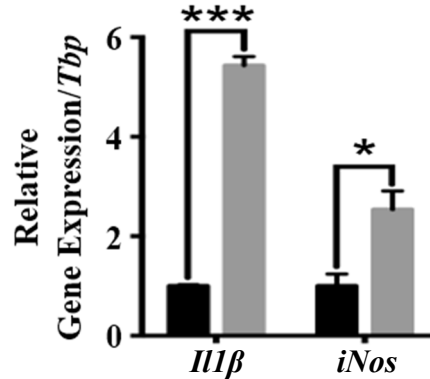


Figure IV-11. qRT-PCR of mRNAs of *Il1 β* and *iNos* markers in the mammary glands of age-matched E-P72 and E-R72 animals. Results shown as relative mRNA expression of specified genes normalized to corresponding *Tbp* levels. The expression values are standardized to the mean of E-P72 samples and shown as mean \pm SEM (n=4, *p<0.05, ***p<0.001).

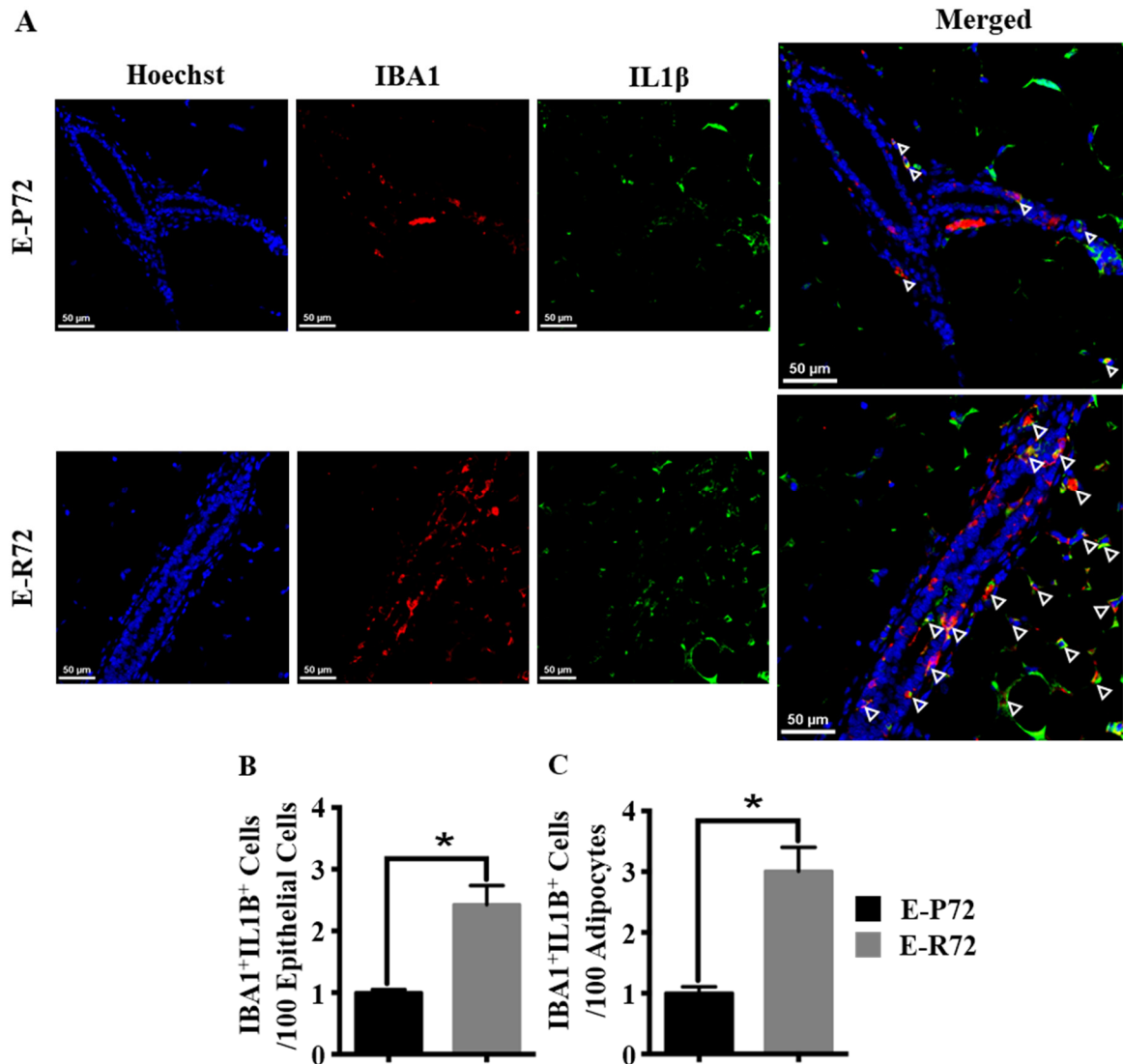


Figure IV-12. A) Representative images of indirect multiplex immunofluorescence using Hoechst dye (blue), IBA1 (red) and IL1 β (green) in the mammary glands of age-matched E-P72 and E-R72 animals, respectively. Magnifications, 20X and 40X, scale bar 50 μ m. Arrows point to IBA1⁺IL1 β ⁺ macrophages. B-C) Quantification of relative number of IBA1⁺IL1 β ⁺ macrophages per 100 epithelial cells (B), and adipocytes (C) mammary glands of age- matched E-P72 and E-R72 animals. The values are standardized to the mean of E-P72 samples and represent mean \pm SEM (n=5, *p<0.05).

An increased number of crown-like structures (CLSs), formed when macrophages surround adipocytes, was also detected in glands from E-R72 animals (Figures IV-10A and D). CLSs are hallmarks of inflammation, and are often observed in chronically inflamed breast tissue of obese women and mice,²¹¹⁻²¹³ and women with breast cancer.²¹⁴ As shown in Figure IV-13, macrophages in CLSs expressed high levels of IL1 β , providing further evidence of persistent inflammation in the susceptible glands of E-R72 compared to E-P72 mice.

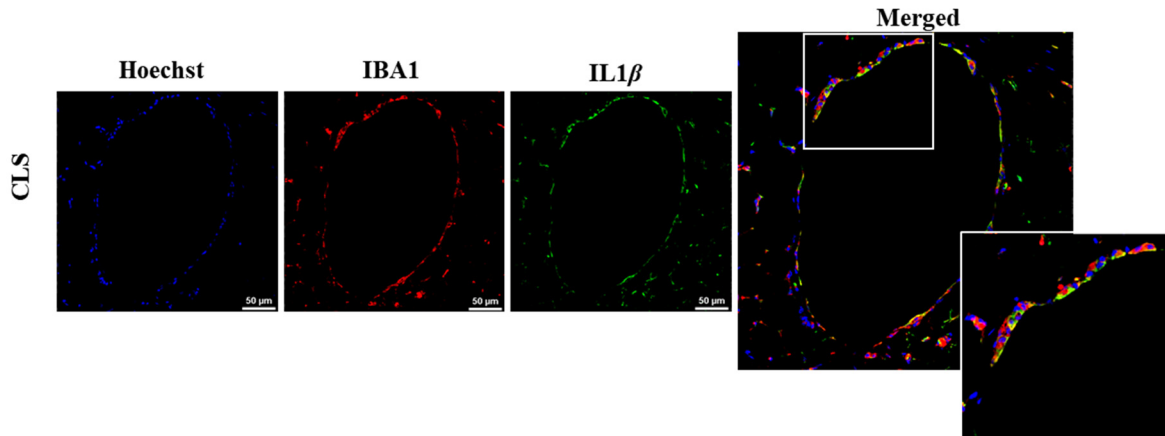


Figure IV-13. Representative crown-like structure (CLS) stained with Hoechst (blue), IBA1 (red) and IL1 β (green) found in the susceptible mammary glands of E-R72 mouse. Magnification 40X, scale bar 50 μ m. Magnified IBA1+IL1 β + macrophages are shown in the lower-right inset. White square on the merged image identifies the magnified area of the image.

Increased tumor-associated macrophages (TAMs) and blood vessels in mammary tumors from E-R72 mice.

CCL2 is a major chemoattractant that recruits TAMs to primary tumor sites, where they promote an immunosuppressive and angiogenic environment that further stimulates tumor growth and progression.^{215, 216} Inhibition of CCL2 reduces macrophage infiltration and tumor growth in MMTV-PyMT mice.²¹⁷ Since elevated levels of CCL2 and resulting macrophage influx were observed in susceptible mammary glands of E-R72 mice (Figures IV-9 and 10), we also assessed expression in mammary tumors. Examination of tumor sections by IHC revealed a significant increase in IBA1⁺ macrophages in tumors from E-R72 compared to E-P72 mice (Figure IV-14).

Angiogenesis has been shown to play a critical role in tumor progression as depletion of tumor vasculature significantly decrease tumor progression.²¹⁵ Previous work shows that TAMs promote angiogenesis by secreting VEGFA.^{166, 216} Interestingly, expression of *Vegfa* was significantly elevated in the tumors of E-R72 mice compared to E-P72 indicating increased angiogenesis in the tumors of E-R72 mice (Figure IV-15).

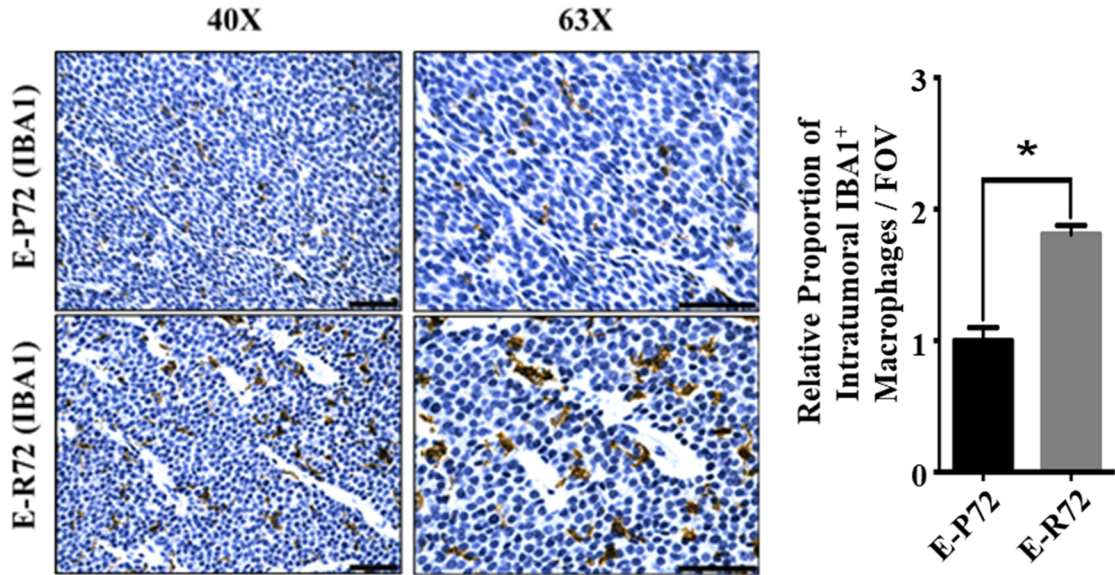


Figure IV-14. Representative IHC images of IBA1 stained tumors harvested from E-P72 and E-R72 animals. Magnifications, 20X and 40X, scale bar, 50 μ m. Quantification of number of IBA1+ macrophages in tumors harvested from E-P72 and E-R72 animals. The values are standardized to the mean of E-P72 samples and shown as mean \pm SEM (n=4, *p<0.05).

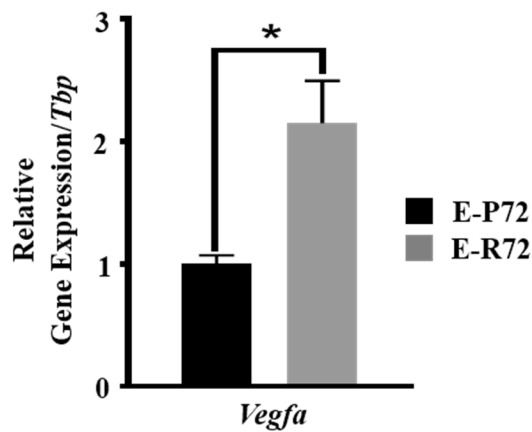


Figure IV-15. qRT-PCR of mRNAs of *Vegfa* in the tumors age-matched E-P72 and E-R72 animals. Results shown as relative mRNA expression of specified genes normalized to corresponding *Tbp* levels. The expression values are standardized to the mean of E-P72 samples and shown as mean \pm SEM (n=5, *p<0.05).

Through secretion of VEGFA, TAMs also promote angiogenesis that supports tumor progression.^{166,216} As shown in Figure IV-15, expression of *Vegfa* was significantly elevated in tumors of E-R72 compared to E-P72 mice. Density of intratumoral blood vessels, assessed by the immunolocalization of CD31, was elevated in mammary tumors from E-R72 animals (Figure IV-16). Together, these results show that influx of TAMs, resulting in elevated levels *Vegfa* and angiogenesis, contributed to the enhanced progression of tumors in E-R72 mice.

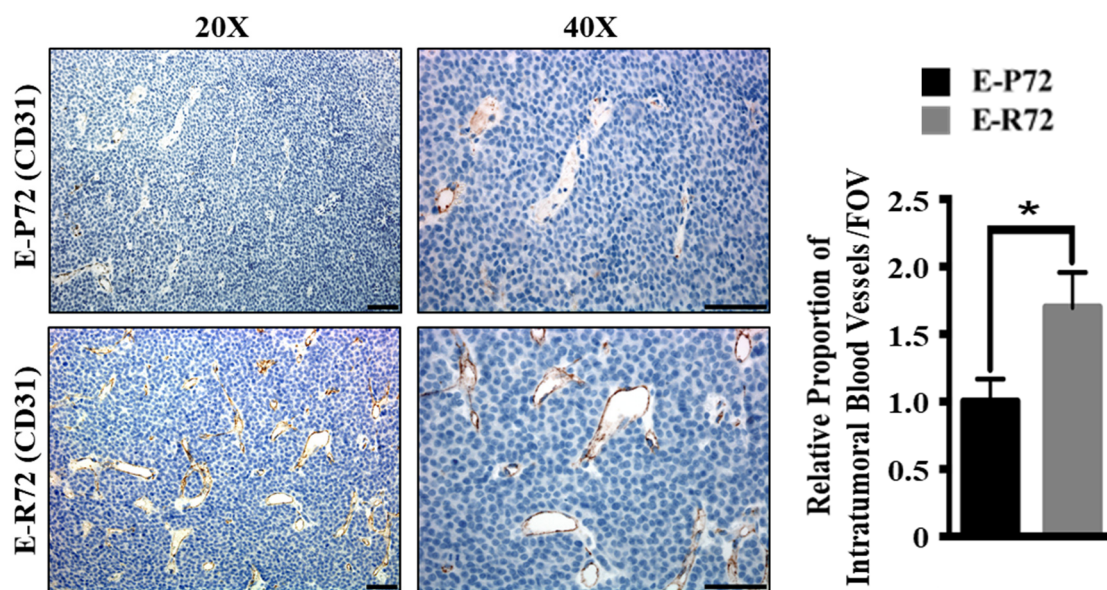


Figure IV-16. Representative IHC images of CD31 stained mammary tumors in E-P72 and E-R72 animals, respectively. Magnifications, 20X and 40X, scale bar, 50 μ m. Quantification of CD31+blood vessels per high power field of view (FOV). The values are standardized to the mean of E-P72 samples and shown as mean \pm SEM (n=5, *p<0.05).

Increased association of R72 with the promoters of cell cycle arrest and inflammation genes.

p53 directly transactivates *Tnfa*, *Ccl2* and *p21* by binding to p53 response elements (REs) in the respective promoter regions.^{140, 218} Since these genes are critical effectors of inflammation and cellular senescence and their expression was significantly upregulated in susceptible mammary glands from E-R72 animals (Figures IV-3 and IV-6), we next examined the association of R72 and P72 with the gene promoters using ChIP-qPCR. ChIP assay revealed significantly higher enrichment of p53 REs of *p21* (Figure IV-17A and B), *Tnfa* (Figure IV-18A and B) and *Ccl2* (distal element) (Figure IV-18C and D) in the susceptible mammary glands of E-R72 mice compared to E-P72 showing increased association of R72 to the respective p53 REs compared to P72. These results describe a mechanism by which R72 directly contributed to the differences in the expression of *p21*, *Tnfa* and *Ccl2*, resulting in increased cellular senescence, chronic inflammation and macrophage influx compared to P72 variant.

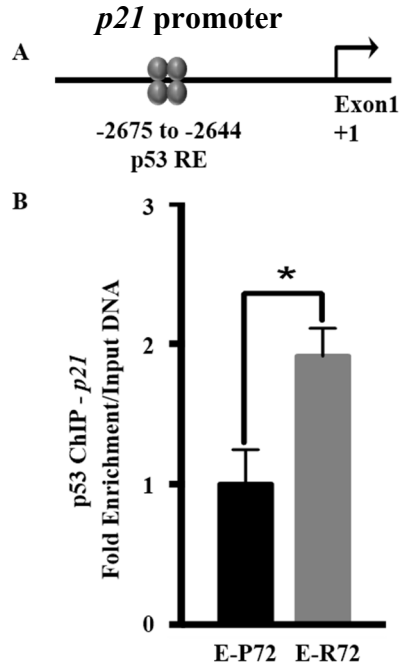


Figure IV-17. A) Diagram of the *p21* gene with the distal p53 response element (RE). The start of exon 1 is denoted as +1, and the locations of potential p53 REs are shown relative to the start of exon 1. B) Chromatin immunoprecipitation of p53 in mammary glands harvested from E-P72 and E-R72 age-matched animals. Input DNA and immunoprecipitated DNA were analyzed by qPCR using primers flanking p21 p53 RE. The expression values are standardized to the mean of E-P72 samples and shown as mean±SEM (n=3, *p<0.05).

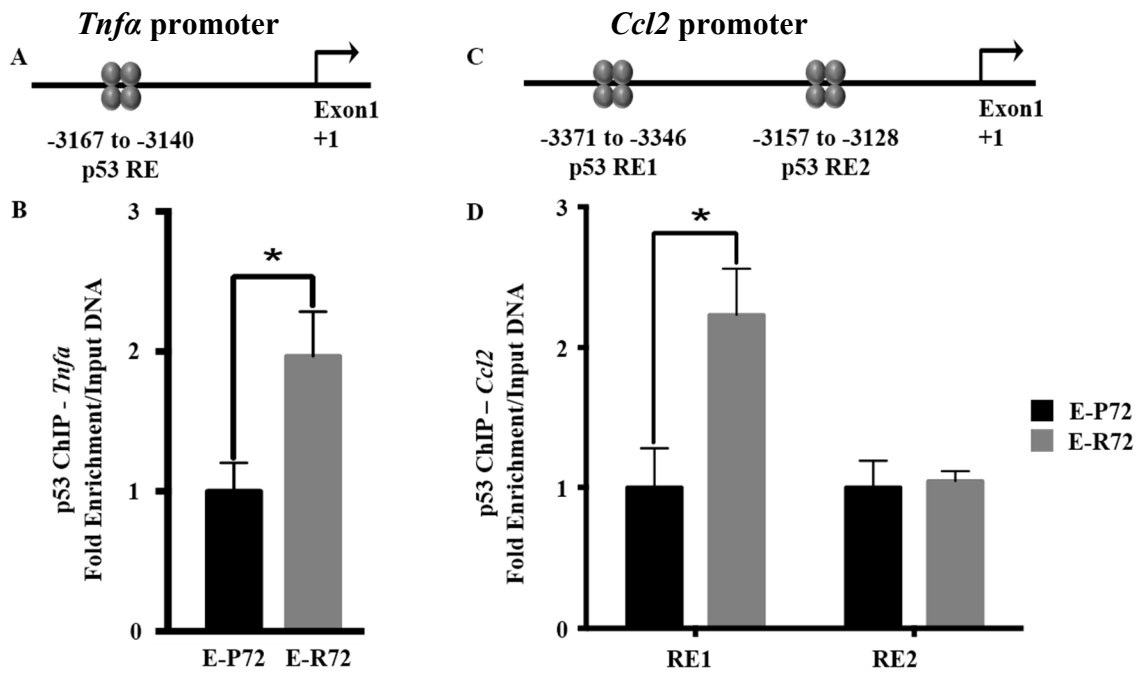


Figure IV-18. A) Diagram of the *Tnfa* gene with p53 RE. The start of exon 1 is denoted as +1, and the locations of potential p53 REs are shown relative to the start of exon 1. B) Chromatin immunoprecipitation of p53 in mammary glands harvested from E-P72 and E-R72 age-matched animals. Input DNA and immunoprecipitated DNA were analyzed by qPCR using primers flanking *Tnfa* p53 response element. The expression values are standardized to the mean of E-P72 samples and shown as mean±SEM (n=3, *p<0.05). C). Diagram of the *Ccl2* gene with p53 response elements. The start of exon 1 is denoted as +1, and the locations of potential p53 REs are shown relative to the start of exon 1. D) Chromatin immunoprecipitation of p53 in mammary glands harvested from E- P72 and E-R72 age-matched animals. Input DNA and immunoprecipitated DNA were analyzed by qPCR using primers flanking *Ccl2* p53 response elements. The expression values are standardized to the mean of E-P72 samples and shown as mean±SEM (n=3, *p<0.05).

CHAPTER V

CONCLUSIONS AND FUTURE DIRECTIONS

Numerous human epidemiological studies investigating cancer risk association have shown modest, yet persistent association of codon 72 p53 variants with incidence of several types of cancers including breast. Studies report R72 is more frequently mutated, thereby, providing a proliferative advantage to cancers of the breast, head and neck, and colon.^{143, 158} BrCa patients with mutations in the R72 allele has been shown to have significantly poor sensitivity to chemotherapy and survival.^{157, 158, 142, 154} To investigate whether codon 72 p53 variants affect mammary tumorigenesis differentially, we explored this question in a physiologically relevant *in vivo* setting, using a previously characterized human p53 exon 4 knock-in mouse model, carrying the polymorphic variants.¹⁵² Results demonstrated that the codon 72 p53 polymorphism modifies mammary tumor susceptibility and latency in both the DMBA- and MMTV-*ErbB2/Neu*-induced mammary tumorigenesis models that are of distinct tumor etiologies. R72 variant was associated with higher tumor susceptibility and reduced tumor latency compared to P72. Our work showed chronic tissue inflammation to be the key factor governing differences in MMTV-*ErbB2/Neu* mammary tumor incidence and latency. Based on our results, increase in persistent cellular senescence observed in the mammary glands of E-R72 animals could explain the SASP-mediated elevation of chronic tissue inflammation. Increased chronic inflammation was further supported by significantly higher influx of proinflammatory macrophages in the susceptible mammary glands of E-R72 mice.

Findings of current work contradict many *in vitro* findings where the P72 variant is found to increase cell cycle arrest and senescence while the R72 variant is better at inducing apoptotic response.¹⁴³ However, this result may be an outcome of a tissue-specific phenomenon unique to the mammary gland as none of the previous studies utilized a breast/mammary cell line to conduct the experiments. Therefore, the current study emphasizes the importance of utilizing relevant *in vitro* and *in vivo* model systems that closely recapitulate the physiology of the tissue of interest.

A persistent increase in senescent mammary epithelial cells in the glands of E-R72 mice was observed, which has been shown to increase chronic inflammation mediated by elevated SASP and influx of proinflammatory macrophages compared to E-P72 mice. P21 is a major effector of senescence regulated by p53. Upregulation of p21 expression together with increased affinity of R72 to its p53 RE in the E-R72 mice compared to E-P72 mice, show that R72 plays a direct role in inducing senescence and consequently, SASP-driven chronic inflammation.

Upon analyzing a select set of genes, we observed that proinflammatory SASP was more active in the glands of E-R72 mice than E-P72 mice. This was demonstrated by significantly higher levels of; phosphorylated p65 (demonstrating more active NFkB pathway), proinflammatory cytokines *Tnfa* and *Il6*, chemoattractants *Ccl2* and *Ccl4*, senescence reinforcing *Pail*, matrix remodeling metalloproteinase *Mmp9* and angiogenic *Vegfa*. These findings are consistent with the gene expression profiles of several previous studies that have shown secretory components of SASP to include proinflammatory cytokines, chemoattractants, *Pail*, *Mmps* and angiogenic factors.⁹³ In our model, we found that *Mmp3* and *Il8* were not significantly different between the mammary glands of E-R72

and E-P72 mice showing that the differential effects of SASP were not mediated through these components. While some studies have shown *Il8* and *Mmp3* are significantly upregulated when SASP is active,^{93, 99, 106} the repertoire of secretory components of senescent cells differ depending on the cell type and biological context.^{103, 106, 107, 119, 131, 219} Therefore, we were able to identify a subset of genes that led to elevation of proinflammatory SASP in the mammary glands of E-R72 mice compared to E-P72 mice. SASP-driven chronic inflammation has been shown to enhance tumor development in hepatocellular carcinoma^{110, 131} and colorectal carcinoma⁹⁹ mouse models, as well as in xenograft and *in vitro* models of BrCa,^{113, 220, 221} further supporting the role of increased SASP-driven chronic inflammation in elevating tumor development in E-R72 compared to E-P72 mice.

Interestingly, comparison of the profiles of induced SASP factors in the above models revealed the existence of unique SASP factors showing that the induction of SASP factors are context dependent.¹¹¹ Therefore, next-generation sequencing of susceptible mammary glands of E-R72 and E-P72 mice will provide valuable information on what other SASP factors are upregulated in the susceptible glands of E-R72 mice compared to E-P72 mice. Moreover, gene-set enrichment and gene ontology analyses will enable identification of pathways and processes that are significantly different between the two variant models contributing to differences in tumor development.

Studies show that SASP-induced chemoattractant CCL2 plays a major role in influx of macrophages into mammary glands.²¹⁶ Therefore, it is possible that elevated expression of major chemoattractant CCL2 resulted in greater influx of macrophages into mammary glands of E-R72 mice. In addition, TNF α has been shown to increase chronic inflammation by establishing a positive feedback loop with activation of the NF κ B pathway.²²² Increased

association of R72 to the distal p53 RE of *Ccl2* promoter and p53 RE of TNF α , together with elevated levels of CCL2 and TNF α demonstrated a direct role of the R72 variant in inducing higher influx of proinflammatory macrophages and inflammation. Direct regulation of TNF α and *Ccl2* by the R72 variant of p53 was recently observed in livers of male R72 Hupki animals in C57/B6 background compared to P72 Hupki mice on a high-fat diet. Further, R72 Hupki mice show increased proinflammatory macrophage infiltration in the white adipose tissue.¹⁴⁰ Considering this report together with our results, it is apparent that R72 is able to regulate *Tnfa* and *Ccl2* expression to increase inflammation albeit potential differences due to animal background or tissue of interest. Since TNF α and CCL2 play an important role in maintenance of chronic inflammation, which is correlated with poor tumor presentation and outcomes in BrCa patients,²²³ inhibition of these factors may be beneficial in patients homozygous for R72.

Double-staining of macrophages with IBA1 and IL1 β showed a significantly greater influx of IBA1⁺IL1 β ⁺ proinflammatory macrophages in E-R72 mammary glands. Together with elevated proinflammatory components, this result showed increased protumorigenic chronic inflammation in the susceptible mammary glands of E-R72 mice compared to E-P72 mice. During chronic inflammation, influx of proinflammatory macrophages that produce reactive nitrogen species through induction of inducible Nitrous Oxide (iNOS) levels results in mutagenic oxidative DNA damage.²⁰⁸ In a model of colorectal cancer, reactive nitrogen species have been shown to initiate tumors by inducing DNA damage and accelerating loss of *Apc*.²²⁴ Interestingly, we observed increased expression of *iNos* in the susceptible mammary glands of E-R72 compared to E-P72 indicating that increased influx of

proinflammatory macrophages into mammary glands of E-R72 elevated production of reactive nitrogen species.

In the MMTV-*ErbB2/Neu* mice, wild-type *ErbB2/Neu* gene is expressed under MMTV-LTR (long terminal repeat) and the incidence of MMTV-*ErbB2/Neu*-driven mammary tumors are attributed to the activation of the tyrosine kinase activity of the receptor.¹⁸⁰ Sequence analyses in MMTV-*ErbB2/Neu* tumors have shown that somatic mutations and in-frame deletions in the extracellular portion of the ERBB2/Neu receptor results in constitutive activation of ERBB2/Neu tyrosine kinase activity.²²⁵ In a follow-up study, Siegel et al. provided a mechanistic explanation to the above as findings showed that somatic mutation of specific cysteine residues promoted dimerization of ERBB2/Neu receptors through disulfide bonds.²²⁶ In addition to mutations of *ErbB2/Neu*, *p53* mutant R172H has also been shown to provide proliferation advantage to MMTV-*ErbB2/Neu*-driven tumors. This was demonstrated by the observed reduction in tumor latency to 154 days from the average latency of 234 days and increase in aneuploidy and tetraploidy in tumor cells.^{182, 227} Interestingly, findings from human BrCa patients show that the R72 allele is more likely to mutate, which was associated with reduced survival.¹⁵⁸ Therefore, it is possible that the increase in proinflammatory macrophages that produce DNA-damaging reactive nitrogen species may have increased the transformation of *ErbB2/Neu*-overexpressing mammary epithelial cells by promoting somatic mutations of *ErbB2/Neu* and/or R72 alleles increasing the mammary tumor incidence in E-R72 animals compared to E-P72 mice. Hence, a next-generation sequencing of tumors will provide valuable information about how the genetic landscape is changed by each polymorphic variant.

Together with increased proinflammatory macrophage influx, a modest yet significant increase in CD31⁺ blood vessels was observed in the susceptible glands of E-R72 mice compared to E-P72 mice. We also observed CCL2 and IL1 β to be significantly upregulated in the susceptible glands of E-R72 mice compared to E-P72 mice. In addition, we observed increased levels of *Vegfa* and *Mmp9* in the susceptible mammary glands. Findings of Arendt et al. demonstrated macrophage recruitment and angiogenesis prior to tumorigenesis in a humanized mammary tumorigenesis model.²²⁸ In this model, pharmacological inhibition of CCL2 and IL1 β significantly decreased macrophage influx and angiogenesis in the precancerous mammary glands showing that CCL2 and IL1 β play important roles in influx of macrophages and angiogenesis.²²⁸ In a different study, increased VEGFA levels were shown to play a critical role in inducing angiogenesis, vascular permeability and vasodilation and MMP9 was shown to increase the bioavailability of VEGFA.²²⁹ Therefore, upregulation of CCL2, IL1 β , *Vegfa* and *Mmp9* as we observed provides a mechanistic explanation for elevated angiogenesis in the precancerous susceptible mammary glands of E-R72 mice compared to E-P72 mice.

In addition to susceptible mammary glands, mammary tumors found in E-R72 mice showed increased TAMs and CD31⁺ vasculature. Macrophages play an important role from the early stages of mammary tumor development. Therefore, an increase in macrophage infiltration into susceptible mammary glands of E-R72 mice indicate that this may have contributed to elevated levels of TAMs and intratumoral angiogenesis in the mammary tumors found in E-R72 mice compared to E-P72 mice. In a study conducted in the MMTV-*PyMT* mammary tumorigenesis model, which is closely related to the MMTV-*ErbB2/Neu* model, Lin et al. show that macrophage infiltration promotes malignant transformation and

tumor vasculature as this was significantly delayed when the macrophage load was depleted by deletion of *Csfl* expression.^{215, 230} Further, the previously-described study by Arendt et al. demonstrated reduction of macrophage influx by pharmacological inhibition of CCL2 and IL1 β which also decreased TAMs and intratumoral angiogenesis delaying tumor development.²²⁸ Given the role of TAMs and intratumoral angiogenesis in mammary tumor development, increased TAMs and intratumoral vasculature may have promoted significantly higher tumor proliferation in E-R72 mice compared to E-P72 mice.

Findings of the current study have parallels with the recent work by Kung et al. that show comparatively increased inflammation in the adipose tissue of R72 Hupki animals compared to P72 Hupki mice (C57Bl/6J background) when fed a high-fat diet (HFD). Findings show that R72 Hupki animals are more susceptible to obesity, associated inflammation, non-alcoholic fatty liver disease and insulin resistance when exposed to a HFD (8 weeks) compared to P72 mice.¹⁴⁰ Interestingly, increased number of CLSs in mammary glands of E-R72 animals than in E-P72 animals provided support for increased dysfunction of lipid metabolism in the mammary glands of E-R72 mice compared to E-P72 mice. Interestingly, CLS are commonly seen in obese women, BrCa patients and mouse models that show chronic inflammation in breast or mammary tissues.^{211, 214}

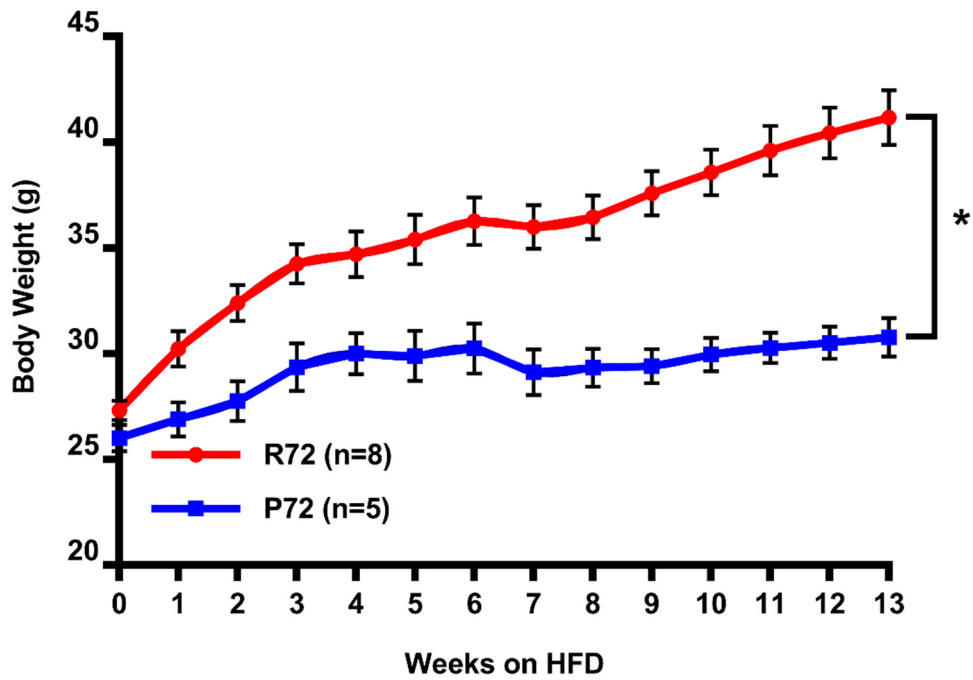


Figure V-1. Weekly body weights of male R72 (Red) and P72 (Blue) animals fed HFD (*p<0.05).

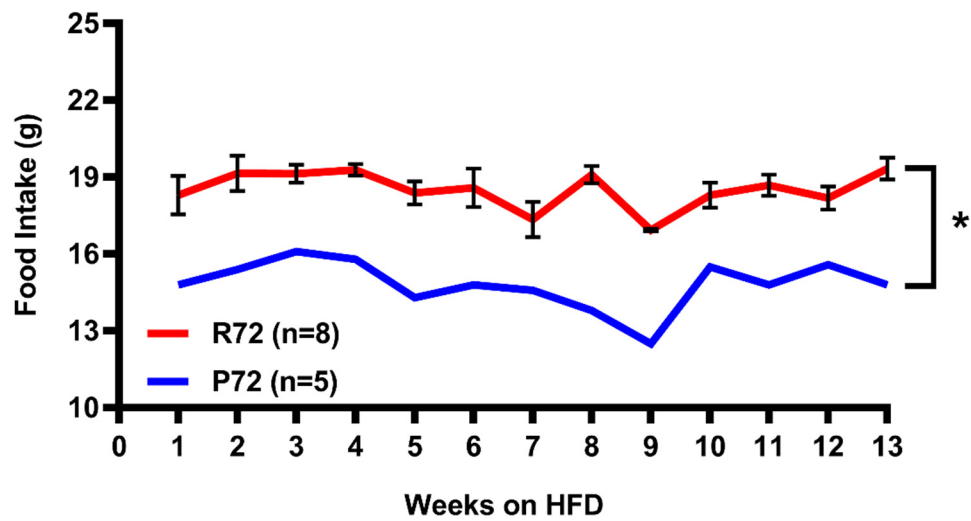


Figure V-2. Average food intake per male R72 and P72 animal fed HFD (*p<0.05).

Recently, we conducted a preliminary study in FVB codon 72 mice to investigate how the codon 72 variants affect fat accumulation. Ten weeks old R72 and P72 mice of both sexes were fed HFD (45%) for thirteen weeks and body weights and food intake were measured weekly. As shown in Figure V-1, R72 male mice showed significant weight gain compared to P72 male mice. Male R72 mice had a significantly higher food intake compared to P72 mice (Figure V-2) which suggested that differences in food intake may have resulted in the observed trends of body weights. Interestingly, R72 female mice had higher weight gain compared to P72 and had similar food intake (Figures V-3 and V-4). However, the body weight comparison was not statistically significant. Overall, the trends suggested R72 mice are prone to increased fat accumulation compared to P72 mice. Interestingly, differences in weight gain between male and female mice showed sexual dimorphism in fat accumulation that has been previously observed in HFD-fed mouse models of obesity.²³¹ Additional animals as well as determination of body fat percentage, lean mass, and expression of genes involved in fat metabolism are required to validate and provide further insight into the results obtained during this preliminary study.

Interestingly, a recent study by Yoshimoto et al. provides a link between obesity and SASP-driven hepatocellular carcinoma.¹³¹ Findings show that dietary and genetic-induction of obesity promoted hepatocellular carcinoma (HCC) development by increased production of deoxycholic acid (DCA), a gut bacterial metabolite, which caused DNA damage and triggered SASP in hepatic stellate cells. Blocking DCA production and/or induction of SASP significantly reduced development of HCC showing a mechanistic link between obesity-

induced tumor development. Therefore, it is indeed interesting to investigate how codon 72 variants respond to HFD and modify mammary tumorigenesis.

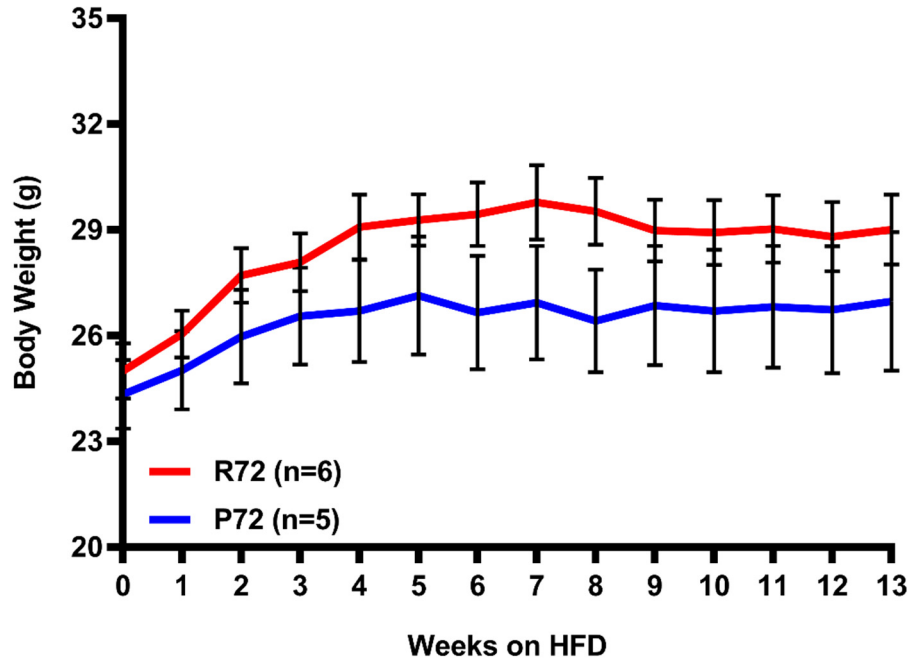


Figure V-3. Weekly body weights of female R72 (Red) and P72 (Blue) animals fed HFD.

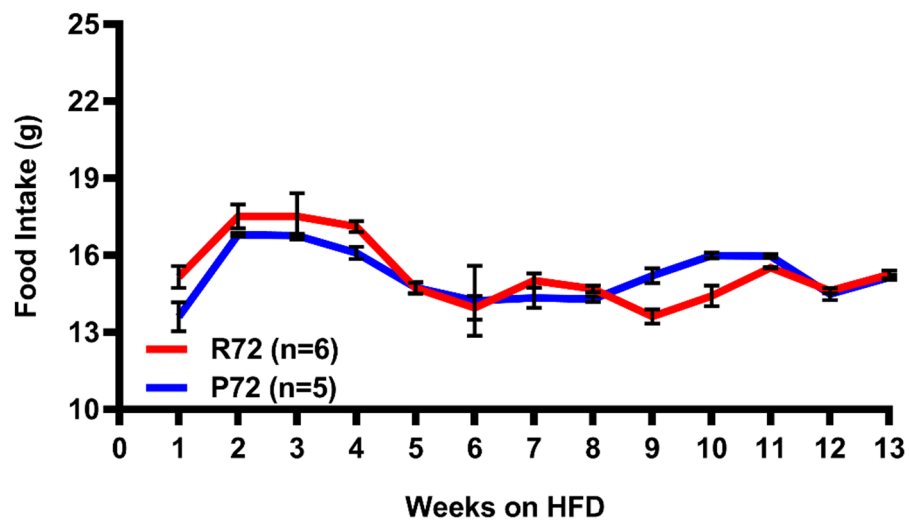


Figure V-4. Average food intake per female R72 or P72 animal fed HFD.

In recent years, obesity has been shown to increase the risk of post-menopausal BrCa, which is predominantly HR+HER- luminal A subtype.^{232, 233} While DMBA- and MMTV-*ErbB2/Neu*-driven mammary tumorigenesis provide valuable insight into how tumor susceptibility is modified by the codon 72 variants, the tumors found in these mice are HR-HER2- and HR-HER2+, respectively. Since these tumors do not represent the luminal A subtype, it is important to generate a model that closely recapitulate the relevant tumor presentation. Recently, Ando et al developed a transgenic mouse model that express human Ki-Ras^{G12V} selectively in the mammary epithelium post-lactation, which generated invasive ductal carcinomas within 3-9 months following Ki-Ras^{G12V} induction. Tumors arising in these mice closely recapitulated luminal A tumor characteristics such as, ER+PR+HER2-, expression of luminal markers (K8 and K18) and low proliferation index and responded positively to an aromatase inhibitor.²³⁴ While this is the most suitable model to study treatment efficacy and progression of luminal A subtype, the observed tumor incidence of 100% is not amenable to study tumor susceptibility.

Alternatively, rat models have been successfully used to study luminal A subtype. Administration of DMBA, MNU as well as chronic exposure to radiation and estrogen have been shown to develop ER+ lesions in rat models.²³⁵ The mammary tumor incidence of these models vary from 100% to 60% (at 40 weeks) in a background dependent manner.^{178, 236} Therefore, the generation of a rat model with codon 72 variants will permit investigation of how codon 72 variants will affect tumorigenesis of mammary tumors that closely recapitulate luminal A subtype.

Pregnancy has been shown to protect against post-menopausal luminal A subtype,^{188, 237} which can be closely recapitulated in ovariectomized rat models. Multiple rat models

have been successfully utilized to study pregnancy protection.^{177, 178, 236} Therefore, the generation of a rat model will also allow investigation of how codon 72 variants would affect pregnancy protection.

As mentioned in detail in the introduction, recent work shows that clearance or accumulation of senescent cells are determined by immune cells such as natural killer (NK) cells, macrophages and T cells. SASP factors include chemoattractants and activating cytokines that are responsible for recruiting immune cells.^{111, 115} Our study shows significant differences in recruitment of proinflammatory macrophages into the mammary glands of E-R72 and E-P72 mice. However, other immune cell populations were not identified. All of these cell populations are successfully isolated by flow cytometry-assisted cell sorting. Isolation of these cell populations in E-R72 and E-P72 mice to quantify the abundance and to determine the transcriptomic profiles by next-generation sequencing will provide more insight into differences in functional outcomes. Quantification of immune cell populations will inform whether the tissue microenvironment facilitates accumulation or elimination of senescent cells. Transcriptomes of immune cells will increase the resolution of what types of cells dictate the functional outcomes especially in heterogenous populations such as macrophages and T cell populations.^{166, 216} A similar approach could be adopted to identify immune cell populations in tumors as immune escape or creating an immune suppressive tumor environment is critical for tumor progression and metastasis.²²³

SASP factors, chronic inflammation and TAMs have been shown to increase cancer therapy resistance and metastasis.^{201, 223, 238} While MMTV-*ErbB2/Neu* mouse model has been shown to have pulmonary metastasis, this process has been shown to have a long lag period, which makes this model less desirable to study metastasis.^{180, 183} MMTV-*PyMT*

model has been successfully utilized to study metastasis and anticancer therapy response. The process of tumorigenesis in MMTV-*PyMT* model has been shown to closely recapitulate BrCa in humans and pulmonary metastasis has been shown to occur with a short lag period.^{183, 215, 239-241} Therefore, generating transgenic R72 and P72 mice with MMTV-*PyMT* will enable investigations to determine how codon 72 variants affect mammary tumor metastasis and anticancer therapy response.

SASP-mediated chronic inflammation is a driver of age-related pathologies, such as atherosclerosis, *Neurodegeneration*, sarcopenia and cancer.^{97, 195} Depletion of senescent cells and pharmacological inhibition of NFκB reduce inflammation and rescue the aging phenotype in multiple aging models,²⁴²⁻²⁴⁴ demonstrating the deleterious effects of senescent cell aggregation and SASP in age-related pathologies. While risk association of the p53 codon 72 SNP with age-related diseases is not extensively studied in human populations, a recent study in a patient cohort of sarcopenia shows that the R72 variant is associated with increased risk for development of the disease,²⁴⁵ indicating that R72 may modify the risk for age-related disease susceptibility through elevated chronic inflammation mediated by SASP. Additionally, this emphasizes the need for further studies investigating the association of the p53 codon 72 SNP with susceptibility to other age-related pathologies.

Chronic inflammation is also a hallmark of cancer.²⁰⁰ Interestingly, a recent human epidemiological study with a Canadian patient cohort shows that R72 is associated with significant risk for development of inflammatory irritable bowel disease (IBD), which is a major risk factor for colorectal cancer (CRC).²⁴⁶ Consistent with the positive association of R72 and IBD development, several studies on CRC patient cohorts from several countries,²⁴⁷⁻²⁵⁰ have shown that R72 increases CRC susceptibility, indicating that the R72-

mediated elevation of chronic inflammation may increase tumor susceptibility. On the other hand, P72 has also been shown to be associated with an increased risk of CRC in several patient cohorts, showing that risk associations may depend on unique environmental and genetic interactions found in distinct, but unrelated geographical locations.

Similarly, risk association of the p53 codon 72 SNP with BrCa is complex. Several epidemiological findings strengthen the increased association of R72 with BrCa.¹⁴² While the P72 variant is associated with increased risk for BrCa in Caucasian patient cohorts, which make up a preponderance of epidemiological studies, the R72 variant has been shown to increase risk of BrCa in Asian ethnicities.^{251, 252} This indicates that further comparisons in non-white populations need to be performed in order to understand how the codon 72 SNP modifies cancer susceptibility globally.

Findings reported herein showed that the p53 codon 72 polymorphic variants significantly modified susceptibility and kinetics of mammary tumorigenesis in a physiologically relevant *in vivo* model and provided evidence for a mechanistic link between p53 codon 72 variants and mammary tumor susceptibility. The proposed model given in Figure V-5 illustrates the overall findings, and how arginine variant of codon 72 p53 SNP may enhance mammary tumor development. These studies demonstrated that in addition to the substantial effect of p53 mutations, single nucleotide polymorphisms can have a profound effect on tumorigenesis. Given the adverse role of chronic inflammation in tumor susceptibility, progression and treatment response, genotyping of codon 72 variants may predict, at least in part, breast cancer susceptibility, disease progression and treatment outcome and warrant further investigation into the utility of codon 72 SNP as a biomarker.

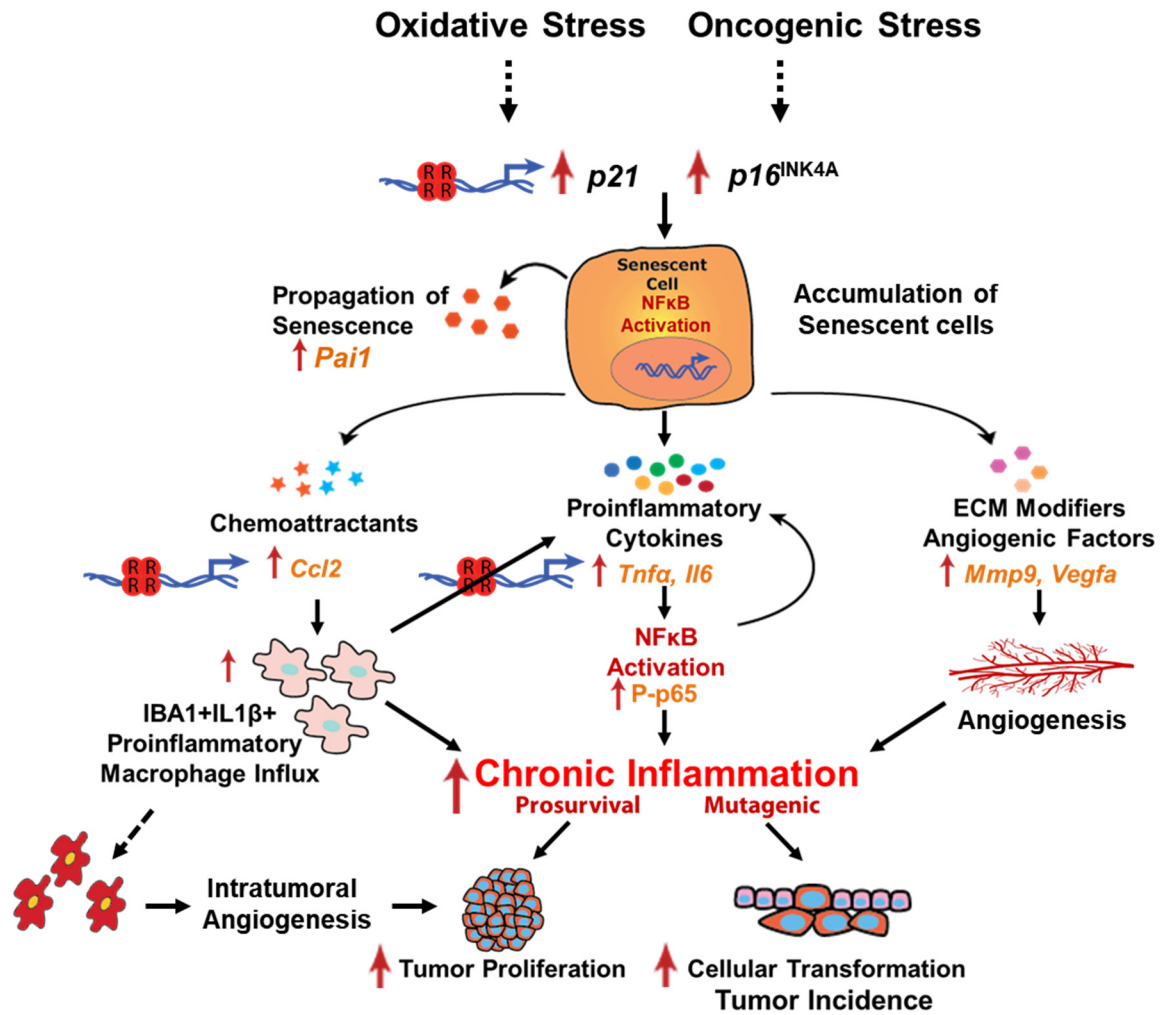


Figure V-5. Diagram of the proposed model of how R72 variant increase mammary tumor incidence and proliferation. Accumulation of senescent cells in the mammary glands of E-R72 animals contributed to increased chronic inflammation in the mammary tissue milieu through upregulation of proinflammatory SASP which, elevates influx of proinflammatory macrophages and angiogenesis. Increased influx of macrophages leads to mutagenic tissue environment by increasing oxidative stress via RNS, which may elevate cellular transformation and in turn, tumor incidence. R72 is likely to play a direct role in upregulating *p21*, *Ccl2* and *Tnfa* expression via higher affinity to the respective p53 REs. In addition to prosurvival functions of chronic inflammation, higher influx of macrophages may increase TAMs that enhance tumor vasculature contributing to increased tumor proliferation observed in the tumors arising in E-R72 mice.

REFERENCES

1. Fitzmaurice C, Allen C, Barber RM, Barregard L, Bhutta ZA, et al. Global, Regional, and National Cancer Incidence, Mortality, Years of Life Lost, Years Lived With Disability, and Disability-Adjusted Life-years for 32 Cancer Groups, 1990 to 2015: A Systematic Analysis for the Global Burden of Disease Study. *JAMA Oncol.* 2017;3(4):524-48.
2. Gage M, Wattendorf D, Henry LR. Translational advances regarding hereditary breast cancer syndromes. *J Surg Oncol.* 2012;105(5):444-51.
3. Siegel RL, Miller KD, Jemal A. Cancer statistics, 2016. *CA: a cancer journal for clinicians.* 2016;66(1):7-30.
4. DeSantis CE, Fedewa SA, Goding Sauer A, Kramer JL, Smith RA, Jemal A. Breast cancer statistics, 2015: Convergence of incidence rates between black and white women. *CA: a cancer journal for clinicians.* 2016;66(1):31-42.
5. Njiaju UO, Olopade OI. Genetic determinants of breast cancer risk: a review of current literature and issues pertaining to clinical application. *The breast journal.* 2012;18(5):436-42.
6. Stephens PJ, Tarpey PS, Davies H, Van Loo P, Greenman C, Wedge DC, et al. The landscape of cancer genes and mutational processes in breast cancer. *Nature.* 2012;486(7403):400-4.
7. Manolio TA. Bringing genome-wide association findings into clinical use. *Nat Rev Genet.* 2013;14(8):549-58.
8. Stracquadanio G, Wang X, Wallace MD, Grawenda AM, Zhang P, Hewitt J, et al. The importance of p53 pathway genetics in inherited and somatic cancer genomes. *Nature reviews Cancer.* 2016;16(4):251-65.
9. Cancer Genome Atlas N. Comprehensive molecular portraits of human breast tumours. *Nature.* 2012;490(7418):61-70.

10. Prat A, Perou CM. Deconstructing the molecular portraits of breast cancer. *Molecular oncology*. 2011;5(1):5-23.
11. Lane DP, Crawford LV. T antigen is bound to a host protein in SV40-transformed cells. *Nature*. 1979;278(5701):261-3.
12. Linzer DI, Levine AJ. Characterization of a 54K dalton cellular SV40 tumor antigen present in SV40-transformed cells and uninfected embryonal carcinoma cells. *Cell*. 1979;17(1):43-52.
13. Eliyahu D, Raz A, Gruss P, Givol D, Oren M. Participation of p53 cellular tumour antigen in transformation of normal embryonic cells. *Nature*. 1984;312(5995):646-9.
14. Eliyahu D, Michalovitz D, Oren M. Overproduction of p53 antigen makes established cells highly tumorigenic. *Nature*. 1985;316(6024):158-60.
15. Parada LF, Land H, Weinberg RA, Wolf D, Rotter V. Cooperation between gene encoding p53 tumour antigen and ras in cellular transformation. *Nature*. 1984;312(5995):649-51.
16. Eliyahu D, Goldfinger N, Pinhasi-Kimhi O, Shaulsky G, Skurnik Y, Arai N, et al. Meth A fibrosarcoma cells express two transforming mutant p53 species. *Oncogene*. 1988;3(3):313-21.
17. Finlay CA, Hinds PW, Tan TH, Eliyahu D, Oren M, Levine AJ. Activating mutations for transformation by p53 produce a gene product that forms an hsc70-p53 complex with an altered half-life. *Molecular and cellular biology*. 1988;8(2):531-9.
18. Finlay CA, Hinds PW, Levine AJ. The p53 proto-oncogene can act as a suppressor of transformation. *Cell*. 1989;57(7):1083-93.
19. Malkin D, Li FP, Strong LC, Fraumeni JF, Jr., Nelson CE, Kim DH, et al. Germ line p53 mutations in a familial syndrome of breast cancer, sarcomas, and other neoplasms. *Science*. 1990;250(4985):1233-8.
20. Lane D, Levine A. p53 Research: the past thirty years and the next thirty years. *Cold Spring Harb Perspect Biol*. 2010;2(12):a000893.

21. Johnson TM, Hammond EM, Giaccia A, Attardi LD. The p53^{QS} transactivation-deficient mutant shows stress-specific apoptotic activity and induces embryonic lethality. *Nature genetics*. 2005;37(2):145-52.
22. Brady CA, Jiang D, Mello SS, Johnson TM, Jarvis LA, Kozak MM, et al. Distinct p53 transcriptional programs dictate acute DNA-damage responses and tumor suppression. *Cell*. 2011;145(4):571-83.
23. Jiang D, Brady CA, Johnson TM, Lee EY, Park EJ, Scott MP, et al. Full p53 transcriptional activation potential is dispensable for tumor suppression in diverse lineages. *Proceedings of the National Academy of Sciences of the United States of America*. 2011;108(41):17123-8.
24. Walker KK, Levine AJ. Identification of a novel p53 functional domain that is necessary for efficient growth suppression. *Proceedings of the National Academy of Sciences of the United States of America*. 1996;93(26):15335-40.
25. Sakamuro D, Sabbatini P, White E, Prendergast GC. The polyproline region of p53 is required to activate apoptosis but not growth arrest. *Oncogene*. 1997;15(8):887-98.
26. Toledo F, Lee CJ, Krummel KA, Rodewald LW, Liu CW, Wahl GM. Mouse mutants reveal that putative protein interaction sites in the p53 proline-rich domain are dispensable for tumor suppression. *Molecular and cellular biology*. 2007;27(4):1425-32.
27. Dornan D, Shimizu H, Burch L, Smith AJ, Hupp TR. The proline repeat domain of p53 binds directly to the transcriptional coactivator p300 and allosterically controls DNA-dependent acetylation of p53. *Molecular and cellular biology*. 2003;23(23):8846-61.
28. Gu W, Roeder RG. Activation of p53 sequence-specific DNA binding by acetylation of the p53 C-terminal domain. *Cell*. 1997;90(4):595-606.
29. Dornan D, Shimizu H, Perkins ND, Hupp TR. DNA-dependent acetylation of p53 by the transcription coactivator p300. *The Journal of biological chemistry*. 2003;278(15):13431-41.

30. Yaffe MB, Schutkowski M, Shen M, Zhou XZ, Stukenberg PT, Rahfeld JU, et al. Sequence-specific and phosphorylation-dependent proline isomerization: a potential mitotic regulatory mechanism. *Science*. 1997;278(5345):1957-60.
31. Ranganathan R, Lu KP, Hunter T, Noel JP. Structural and functional analysis of the mitotic rotamase Pin1 suggests substrate recognition is phosphorylation dependent. *Cell*. 1997;89(6):875-86.
32. Lu KP, Hanes SD, Hunter T. A human peptidyl-prolyl isomerase essential for regulation of mitosis. *Nature*. 1996;380(6574):544-7.
33. Berger M, Stahl N, Del Sal G, Haupt Y. Mutations in proline 82 of p53 impair its activation by Pin1 and Chk2 in response to DNA damage. *Molecular and cellular biology*. 2005;25(13):5380-8.
34. Berger M, Vogt Sionov R, Levine AJ, Haupt Y. A role for the polyproline domain of p53 in its regulation by Mdm2. *The Journal of biological chemistry*. 2001;276(6):3785-90.
35. Mantovani F, Tocco F, Girardini J, Smith P, Gasco M, Lu X, et al. The prolyl isomerase Pin1 orchestrates p53 acetylation and dissociation from the apoptosis inhibitor iASPP. *Nat Struct Mol Biol*. 2007;14(10):912-20.
36. Kim MP, Zhang Y, Lozano G. Mutant p53: Multiple Mechanisms Define Biologic Activity in Cancer. *Front Oncol*. 2015;5:249.
37. Joerger AC, Fersht AR. Structure-function-rescue: the diverse nature of common p53 cancer mutants. *Oncogene*. 2007;26(15):2226-42.
38. Joerger AC, Ang HC, Veprintsev DB, Blair CM, Fersht AR. Structures of p53 cancer mutants and mechanism of rescue by second-site suppressor mutations. *The Journal of biological chemistry*. 2005;280(16):16030-7.
39. Ang HC, Joerger AC, Mayer S, Fersht AR. Effects of common cancer mutations on stability and DNA binding of full-length p53 compared with isolated core domains. *The Journal of biological chemistry*. 2006;281(31):21934-41.

40. Joerger AC, Ang HC, Fersht AR. Structural basis for understanding oncogenic p53 mutations and designing rescue drugs. *Proceedings of the National Academy of Sciences of the United States of America*. 2006;103(41):15056-61.
41. Olivier M, Hollstein M, Hainaut P. TP53 mutations in human cancers: origins, consequences, and clinical use. *Cold Spring Harb Perspect Biol*. 2010;2(1):a001008.
42. Kitayner M, Rozenberg H, Kessler N, Rabinovich D, Shaulov L, Haran TE, et al. Structural basis of DNA recognition by p53 tetramers. *Mol Cell*. 2006;22(6):741-53.
43. Friedman PN, Chen X, Bargonetti J, Prives C. The p53 protein is an unusually shaped tetramer that binds directly to DNA. *Proceedings of the National Academy of Sciences of the United States of America*. 1993;90(8):3319-23.
44. Stommel JM, Marchenko ND, Jimenez GS, Moll UM, Hope TJ, Wahl GM. A leucine-rich nuclear export signal in the p53 tetramerization domain: regulation of subcellular localization and p53 activity by NES masking. *EMBO J*. 1999;18(6):1660-72.
45. el-Deiry WS, Kern SE, Pietenpol JA, Kinzler KW, Vogelstein B. Definition of a consensus binding site for p53. *Nature genetics*. 1992;1(1):45-9.
46. Funk WD, Pak DT, Karas RH, Wright WE, Shay JW. A transcriptionally active DNA-binding site for human p53 protein complexes. *Molecular and cellular biology*. 1992;12(6):2866-71.
47. Beckerman R, Prives C. Transcriptional regulation by p53. *Cold Spring Harb Perspect Biol*. 2010;2(8):a000935.
48. Biegging KT, Mello SS, Attardi LD. Unravelling mechanisms of p53-mediated tumour suppression. *Nature reviews Cancer*. 2014;14(5):359-70.
49. Meek DW, Anderson CW. Posttranslational modification of p53: cooperative integrators of function. *Cold Spring Harb Perspect Biol*. 2009;1(6):a000950.
50. Hainaut P, Milner J. A structural role for metal ions in the "wild-type" conformation of the tumor suppressor protein p53. *Cancer Res*. 1993;53(8):1739-42.

51. Taira N, Yoshida K. Post-translational modifications of p53 tumor suppressor: determinants of its functional targets. *Histology and histopathology*. 2012;27(4):437-43.
52. Dai C, Gu W. p53 post-translational modification: deregulated in tumorigenesis. *Trends Mol Med*. 2010;16(11):528-36.
53. Das S, Raj L, Zhao B, Kimura Y, Bernstein A, Aaronson SA, et al. Hzf Determines cell survival upon genotoxic stress by modulating p53 transactivation. *Cell*. 2007;130(4):624-37.
54. Tanaka T, Ohkubo S, Tatsuno I, Prives C. hCAS/CSE1L associates with chromatin and regulates expression of select p53 target genes. *Cell*. 2007;130(4):638-50.
55. Espinosa JM. Mechanisms of regulatory diversity within the p53 transcriptional network. *Oncogene*. 2008;27(29):4013-23.
56. Timofeev O, Schlereth K, Wanzel M, Braun A, Nieswandt B, Pagenstecher A, et al. p53 DNA binding cooperativity is essential for apoptosis and tumor suppression in vivo. *Cell Rep*. 2013;3(5):1512-25.
57. Li T, Kon N, Jiang L, Tan M, Ludwig T, Zhao Y, et al. Tumor suppression in the absence of p53-mediated cell-cycle arrest, apoptosis, and senescence. *Cell*. 2012;149(6):1269-83.
58. Mendoza M, Mandani G, Momand J. The MDM2 gene family. *Biomol Concepts*. 2014;5(1):9-19.
59. Momand J, Wu HH, Dasgupta G. MDM2--master regulator of the p53 tumor suppressor protein. *Gene*. 2000;242(1-2):15-29.
60. Hu W, Feng Z, Levine AJ. The Regulation of Multiple p53 Stress Responses is Mediated through MDM2. *Genes Cancer*. 2012;3(3-4):199-208.
61. van den Bosch M, Bree RT, Lowndes NF. The MRN complex: coordinating and mediating the response to broken chromosomes. *EMBO Rep*. 2003;4(9):844-9.

62. Jackson SP, Bartek J. The DNA-damage response in human biology and disease. *Nature*. 2009;461(7267):1071-8.
63. Cimprich KA, Cortez D. ATR: an essential regulator of genome integrity. *Nat Rev Mol Cell Biol*. 2008;9(8):616-27.
64. McKinnon PJ. ATM and the molecular pathogenesis of ataxia telangiectasia. *Annual review of pathology*. 2012;7:303-21.
65. Banin S, Moyal L, Shieh S, Taya Y, Anderson CW, Chessa L, et al. Enhanced phosphorylation of p53 by ATM in response to DNA damage. *Science*. 1998;281(5383):1674-7.
66. Cheng Q, Chen J. Mechanism of p53 stabilization by ATM after DNA damage. *Cell cycle*. 2010;9(3):472-8.
67. Sluss HK, Armata H, Gallant J, Jones SN. Phosphorylation of serine 18 regulates distinct p53 functions in mice. *Molecular and cellular biology*. 2004;24(3):976-84.
68. Waldman T, Kinzler KW, Vogelstein B. p21 is necessary for the p53-mediated G1 arrest in human cancer cells. *Cancer Res*. 1995;55(22):5187-90.
69. Oren M. Relationship of p53 to the control of apoptotic cell death. *Semin Cancer Biol*. 1994;5(3):221-7.
70. Shay JW, Pereira-Smith OM, Wright WE. A role for both RB and p53 in the regulation of human cellular senescence. *Exp Cell Res*. 1991;196(1):33-9.
71. Sengupta S, Harris CC. p53: traffic cop at the crossroads of DNA repair and recombination. *Nat Rev Mol Cell Biol*. 2005;6(1):44-55.
72. Rinaldo C, Prodosmo A, Mancini F, Iacovelli S, Sacchi A, Moretti F, et al. MDM2-regulated degradation of HIPK2 prevents p53Ser46 phosphorylation and DNA damage-induced apoptosis. *Mol Cell*. 2007;25(5):739-50.

73. Taira N, Nihira K, Yamaguchi T, Miki Y, Yoshida K. DYRK2 is targeted to the nucleus and controls p53 via Ser46 phosphorylation in the apoptotic response to DNA damage. *Mol Cell*. 2007;25(5):725-38.
74. Sykes SM, Mellert HS, Holbert MA, Li K, Marmorstein R, Lane WS, et al. Acetylation of the p53 DNA-binding domain regulates apoptosis induction. *Mol Cell*. 2006;24(6):841-51.
75. Tang Y, Luo J, Zhang W, Gu W. Tip60-dependent acetylation of p53 modulates the decision between cell-cycle arrest and apoptosis. *Mol Cell*. 2006;24(6):827-39.
76. Smeenk L, van Heeringen SJ, Koeppl M, Gilbert B, Janssen-Megens E, Stunnenberg HG, et al. Role of p53 serine 46 in p53 target gene regulation. *PloS one*. 2011;6(3):e17574.
77. Biegging KT, Attardi LD. Deconstructing p53 transcriptional networks in tumor suppression. *Trends in cell biology*. 2012;22(2):97-106.
78. Leu JI, Dumont P, Hafey M, Murphy ME, George DL. Mitochondrial p53 activates Bak and causes disruption of a Bak-Mcl1 complex. *Nature cell biology*. 2004;6(5):443-50.
79. Fridman JS, Lowe SW. Control of apoptosis by p53. *Oncogene*. 2003;22(56):9030-40.
80. Attardi LD, Reczek EE, Cosmas C, Demicco EG, McCurrach ME, Lowe SW, et al. PERP, an apoptosis-associated target of p53, is a novel member of the PMP-22/gas3 family. *Genes & development*. 2000;14(6):704-18.
81. Ihrie RA, Marques MR, Nguyen BT, Horner JS, Papazoglu C, Bronson RT, et al. Perp is a p63-regulated gene essential for epithelial integrity. *Cell*. 2005;120(6):843-56.
82. Dusek RL, Bascom JL, Vogel H, Baron S, Borowsky AD, Bissell MJ, et al. Deficiency of the p53/p63 target Perp alters mammary gland homeostasis and promotes cancer. *Breast cancer research : BCR*. 2012;14(2):R65.
83. Barnum KJ, O'Connell MJ. Cell cycle regulation by checkpoints. *Methods in molecular biology*. 2014;1170:29-40.

84. Sherr CJ. G1 phase progression: cycling on cue. *Cell*. 1994;79(4):551-5.
85. Sherr CJ, Roberts JM. Inhibitors of mammalian G1 cyclin-dependent kinases. *Genes & development*. 1995;9(10):1149-63.
86. el-Deiry WS. p21/p53, cellular growth control and genomic integrity. *Curr Top Microbiol Immunol*. 1998;227:121-37.
87. Deng C, Zhang P, Harper JW, Elledge SJ, Leder P. Mice lacking p21CIP1/WAF1 undergo normal development, but are defective in G1 checkpoint control. *Cell*. 1995;82(4):675-84.
88. Mandal M, Bandyopadhyay D, Goepfert TM, Kumar R. Interferon-induces expression of cyclin-dependent kinase-inhibitors p21WAF1 and p27Kip1 that prevent activation of cyclin-dependent kinase by CDK-activating kinase (CAK). *Oncogene*. 1998;16(2):217-25.
89. Ohki R, Nemoto J, Murasawa H, Oda E, Inazawa J, Tanaka N, et al. Reprimo, a new candidate mediator of the p53-mediated cell cycle arrest at the G2 phase. *The Journal of biological chemistry*. 2000;275(30):22627-30.
90. Giono LE, Manfredi JJ. The p53 tumor suppressor participates in multiple cell cycle checkpoints. *J Cell Physiol*. 2006;209(1):13-20.
91. Carrier F, Smith ML, Bae I, Kilpatrick KE, Lansing TJ, Chen CY, et al. Characterization of human Gadd45, a p53-regulated protein. *The Journal of biological chemistry*. 1994;269(51):32672-7.
92. Hermeking H, Lengauer C, Polyak K, He TC, Zhang L, Thiagalingam S, et al. 14-3-3sigma is a p53-regulated inhibitor of G2/M progression. *Mol Cell*. 1997;1(1):3-11.
93. Munoz-Espin D, Serrano M. Cellular senescence: from physiology to pathology. *Nat Rev Mol Cell Biol*. 2014;15(7):482-96.
94. Hayflick L, Moorhead PS. The serial cultivation of human diploid cell strains. *Exp Cell Res*. 1961;25:585-621.

95. Zhang Y, Xiong Y, Yarbrough WG. ARF promotes MDM2 degradation and stabilizes p53: ARF-INK4a locus deletion impairs both the Rb and p53 tumor suppression pathways. *Cell*. 1998;92(6):725-34.
96. Serrano M, Hannon GJ, Beach D. A new regulatory motif in cell-cycle control causing specific inhibition of cyclin D/CDK4. *Nature*. 1993;366(6456):704-7.
97. Lasry A, Ben-Neriah Y. Senescence-associated inflammatory responses: aging and cancer perspectives. *Trends Immunol*. 2015;36(4):217-28.
98. Georgilis A, Gil J. Controlling secretion to limit chemoresistance. *Genes & development*. 2016;30(16):1791-2.
99. Kim SB, Bozeman RG, Kaisani A, Kim W, Zhang L, Richardson JA, et al. Radiation promotes colorectal cancer initiation and progression by inducing senescence-associated inflammatory responses. *Oncogene*. 2016;35(26):3365-75.
100. Takeuchi S, Takahashi A, Motoi N, Yoshimoto S, Tajima T, Yamakoshi K, et al. Intrinsic cooperation between p16INK4a and p21Waf1/Cip1 in the onset of cellular senescence and tumor suppression in vivo. *Cancer Res*. 2010;70(22):9381-90.
101. Dimri GP, Lee X, Basile G, Acosta M, Scott G, Roskelley C, et al. A biomarker that identifies senescent human cells in culture and in aging skin in vivo. *Proceedings of the National Academy of Sciences of the United States of America*. 1995;92(20):9363-7.
102. Georgakopoulou EA, Tsimaratou K, Evangelou K, Fernandez Marcos PJ, Zoumpourlis V, Trougakos IP, et al. Specific lipofuscin staining as a novel biomarker to detect replicative and stress-induced senescence. A method applicable in cryo-preserved and archival tissues. *Aging (Albany NY)*. 2013;5(1):37-50.
103. Rodier F, Campisi J. Four faces of cellular senescence. *J Cell Biol*. 2011;192(4):547-56.
104. Rinehart CA, Torti VR. Aging and cancer: the role of stromal interactions with epithelial cells. *Molecular carcinogenesis*. 1997;18(4):187-92.

105. Shelton DN, Chang E, Whittier PS, Choi D, Funk WD. Microarray analysis of replicative senescence. *Curr Biol.* 1999;9(17):939-45.
106. Krtolica A, Parrinello S, Lockett S, Desprez PY, Campisi J. Senescent fibroblasts promote epithelial cell growth and tumorigenesis: a link between cancer and aging. *Proceedings of the National Academy of Sciences of the United States of America.* 2001;98(21):12072-7.
107. Acosta JC, O'Loughlen A, Banito A, Guijarro MV, Augert A, Raguz S, et al. Chemokine signaling via the CXCR2 receptor reinforces senescence. *Cell.* 2008;133(6):1006-18.
108. Chien Y, Scuoppo C, Wang X, Fang X, Balgley B, Bolden JE, et al. Control of the senescence-associated secretory phenotype by NF-kappaB promotes senescence and enhances chemosensitivity. *Genes & development.* 2011;25(20):2125-36.
109. Salminen A, Kauppinen A, Kaarniranta K. Emerging role of NF-kappaB signaling in the induction of senescence-associated secretory phenotype (SASP). *Cellular signalling.* 2012;24(4):835-45.
110. Lujambio A, Akkari L, Simon J, Grace D, Tschaharganeh DF, Bolden JE, et al. Non-cell-autonomous tumor suppression by p53. *Cell.* 2013;153(2):449-60.
111. Ruhland MK, Coussens LM, Stewart SA. Senescence and cancer: An evolving inflammatory paradox. *Biochim Biophys Acta.* 2016;1865(1):14-22.
112. Rodier F, Coppe JP, Patil CK, Hoeijmakers WA, Munoz DP, Raza SR, et al. Persistent DNA damage signalling triggers senescence-associated inflammatory cytokine secretion. *Nature cell biology.* 2009;11(8):973-9.
113. Capell BC, Drake AM, Zhu J, Shah PP, Dou Z, Dorsey J, et al. MLL1 is essential for the senescence-associated secretory phenotype. *Genes & development.* 2016;30(3):321-36.
114. Kang C, Xu Q, Martin TD, Li MZ, Demaria M, Aron L, et al. The DNA damage response induces inflammation and senescence by inhibiting autophagy of GATA4. *Science.* 2015;349(6255):aaa5612.

115. Lujambio A. To clear, or not to clear (senescent cells)? That is the question. *Bioessays*. 2016;38 Suppl 1:S56-64.
116. Kortlever RM, Higgins PJ, Bernards R. Plasminogen activator inhibitor-1 is a critical downstream target of p53 in the induction of replicative senescence. *Nature cell biology*. 2006;8(8):877-84.
117. Kuilman T, Michaloglou C, Vredeveld LC, Douma S, van Doorn R, Desmet CJ, et al. Oncogene-induced senescence relayed by an interleukin-dependent inflammatory network. *Cell*. 2008;133(6):1019-31.
118. Hubackova S, Krejcikova K, Bartek J, Hodny Z. IL1- and TGFbeta-Nox4 signaling, oxidative stress and DNA damage response are shared features of replicative, oncogene-induced, and drug-induced paracrine 'bystander senescence'. *Aging (Albany NY)*. 2012;4(12):932-51.
119. Acosta JC, Banito A, Wuestefeld T, Georgilis A, Janich P, Morton JP, et al. A complex secretory program orchestrated by the inflammasome controls paracrine senescence. *Nature cell biology*. 2013;15(8):978-90.
120. Donehower LA, Harvey M, Slagle BL, McArthur MJ, Montgomery CA, Jr., Butel JS, et al. Mice deficient for p53 are developmentally normal but susceptible to spontaneous tumours. *Nature*. 1992;356(6366):215-21.
121. Jacks T, Remington L, Williams BO, Schmitt EM, Halachmi S, Bronson RT, et al. Tumor spectrum analysis in p53-mutant mice. *Curr Biol*. 1994;4(1):1-7.
122. Purdie CA, Harrison DJ, Peter A, Dobbie L, White S, Howie SE, et al. Tumour incidence, spectrum and ploidy in mice with a large deletion in the p53 gene. *Oncogene*. 1994;9(2):603-9.
123. Eischen CM, Weber JD, Roussel MF, Sherr CJ, Cleveland JL. Disruption of the ARF-Mdm2-p53 tumor suppressor pathway in Myc-induced lymphomagenesis. *Genes & development*. 1999;13(20):2658-69.
124. Schmitt CA, McCurrach ME, de Stanchina E, Wallace-Brodeur RR, Lowe SW. INK4a/ARF mutations accelerate lymphomagenesis and promote chemoresistance by disabling p53. *Genes & development*. 1999;13(20):2670-7.

125. Schmitt CA, Fridman JS, Yang M, Baranov E, Hoffman RM, Lowe SW. Dissecting p53 tumor suppressor functions in vivo. *Cancer Cell*. 2002;1(3):289-98.
126. Martin-Caballero J, Flores JM, Garcia-Palencia P, Serrano M. Tumor susceptibility of p21(Waf1/Cip1)-deficient mice. *Cancer Res*. 2001;61(16):6234-8.
127. Schlereth K, Beinoraviciute-Kellner R, Zeitlinger MK, Bretz AC, Sauer M, Charles JP, et al. DNA binding cooperativity of p53 modulates the decision between cell-cycle arrest and apoptosis. *Mol Cell*. 2010;38(3):356-68.
128. Xue W, Zender L, Miething C, Dickins RA, Hernando E, Krizhanovsky V, et al. Senescence and tumour clearance is triggered by p53 restoration in murine liver carcinomas. *Nature*. 2007;445(7128):656-60.
129. Sagiv A, Burton DG, Moshayev Z, Vadai E, Wensveen F, Ben-Dor S, et al. NKG2D ligands mediate immunosurveillance of senescent cells. *Aging (Albany NY)*. 2016;8(2):328-44.
130. Kang TW, Yevsa T, Woller N, Hoenicke L, Wuestefeld T, Dauch D, et al. Senescence surveillance of pre-malignant hepatocytes limits liver cancer development. *Nature*. 2011;479(7374):547-51.
131. Yoshimoto S, Loo TM, Atarashi K, Kanda H, Sato S, Oyadomari S, et al. Obesity-induced gut microbial metabolite promotes liver cancer through senescence secretome. *Nature*. 2013;499(7456):97-101.
132. Toso A, Revandkar A, Di Mitri D, Guccini I, Proietti M, Sarti M, et al. Enhancing chemotherapy efficacy in Pten-deficient prostate tumors by activating the senescence-associated antitumor immunity. *Cell Rep*. 2014;9(1):75-89.
133. Pribluda A, Elyada E, Wiener Z, Hamza H, Goldstein RE, Biton M, et al. A senescence-inflammatory switch from cancer-inhibitory to cancer-promoting mechanism. *Cancer Cell*. 2013;24(2):242-56.
134. Jackson JG, Pant V, Li Q, Chang LL, Quintas-Cardama A, Garza D, et al. p53-mediated senescence impairs the apoptotic response to chemotherapy and clinical outcome in breast cancer. *Cancer Cell*. 2012;21(6):793-806.

135. Petitjean A, Mathe E, Kato S, Ishioka C, Tavtigian SV, Hainaut P, et al. Impact of mutant p53 functional properties on TP53 mutation patterns and tumor phenotype: lessons from recent developments in the IARC TP53 database. *Hum Mutat.* 2007;28(6):622-9.
136. Beckman G, Birgander R, Sjalander A, Saha N, Holmberg PA, Kivela A, et al. Is p53 polymorphism maintained by natural selection? *Hum Hered.* 1994;44(5):266-70.
137. Kuehn BM. 1000 Genomes Project finds substantial genetic variation among populations. *JAMA.* 2012;308(22):2322, 5.
138. Puente XS, Velasco G, Gutiérrez-Fernández A, Bertranpetit J, King M-C, López-Otín C. Comparative analysis of cancer genes in the human and chimpanzee genomes. *BMC Genomics.* 2006;7:15-.
139. Kang HJ, Feng Z, Sun Y, Atwal G, Murphy ME, Rebbeck TR, et al. Single-nucleotide polymorphisms in the p53 pathway regulate fertility in humans. *Proceedings of the National Academy of Sciences of the United States of America.* 2009;106(24):9761-6.
140. Kung CP, Leu JI, Basu S, Khaku S, Anokye-Danso F, Liu Q, et al. The P72R Polymorphism of p53 Predisposes to Obesity and Metabolic Dysfunction. *Cell Rep.* 2016;14(10):2413-25.
141. Sellayah D, Cagampang FR, Cox RD. On the evolutionary origins of obesity: a new hypothesis. *Endocrinology.* 2014;155(5):1573-88.
142. Denisov EV, Cherdyntseva NV, Litviakov NV, Malinovskaya EA, Babyshkina NN, Belyavskaya VA, et al. TP53 Gene Polymorphisms in Cancer Risk: The Modulating Effect of Ageing, Ethnicity and TP53 Somatic Abnormalities. 2012. In: *Tumor Suppressor Genes* [Internet]. InTech. Available from: <http://www.intechopen.com/books/tumor-suppressor-genes/tp53-gene-polymorphisms-in-cancer-risk-the-modulating-effect-of-ageing-ethnicity-and-tp53-somatic-ab>.
143. Basu S, Murphy ME. Genetic Modifiers of the p53 Pathway. *Cold Spring Harb Perspect Med.* 2016;6(4):a026302.

144. Grochola LF, Zeron-Medina J, Meriaux S, Bond GL. Single-nucleotide polymorphisms in the p53 signaling pathway. *Cold Spring Harb Perspect Biol.* 2010;2(5):a001032.
145. Pim D, Banks L. p53 polymorphic variants at codon 72 exert different effects on cell cycle progression. *Int J Cancer.* 2004;108(2):196-9.
146. Frank AK, Leu JI, Zhou Y, Devarajan K, Nedelko T, Klein-Szanto A, et al. The codon 72 polymorphism of p53 regulates interaction with NF-kappaB and transactivation of genes involved in immunity and inflammation. *Molecular and cellular biology.* 2011;31(6):1201-13.
147. Salvioli S, Bonafé M, Barbi C, Storci G, Trapassi C, Tocco F, et al. p53 Codon 72 Alleles Influence the Response to Anticancer Drugs in Cells from Aged People by Regulating the Cell Cycle Inhibitor p21^{WAF1}. *Cell cycle.* 2005;4(9):1264-71.
148. Siddique M, Sabapathy K. Trp53-dependent DNA-repair is affected by the codon 72 polymorphism. *Oncogene.* 2006;25(25):3489-500.
149. Dumont P, Leu JI, Della Pietra AC, 3rd, George DL, Murphy M. The codon 72 polymorphic variants of p53 have markedly different apoptotic potential. *Nature genetics.* 2003;33(3):357-65.
150. Kung CP, Khaku S, Jennis M, Zhou Y, Murphy ME. Identification of TRIML2, a novel p53 target, that enhances p53 SUMOylation and regulates the transactivation of proapoptotic genes. *Mol Cancer Res.* 2015;13(2):250-62.
151. Murphy ME. Polymorphic variants in the p53 pathway. *Cell Death Differ.* 2006;13(6):916-20.
152. Zhu F, Dolle ME, Berton TR, Kuiper RV, Capps C, Espejo A, et al. Mouse models for the p53 R72P polymorphism mimic human phenotypes. *Cancer Res.* 2010;70(14):5851-9.
153. Azzam GA, Frank AK, Hollstein M, Murphy ME. Tissue-specific apoptotic effects of the p53 codon 72 polymorphism in a mouse model. *Cell cycle.* 2011;10(9):1352-5.

154. Whibley C, Pharoah PD, Hollstein M. p53 polymorphisms: cancer implications. *Nature reviews Cancer*. 2009;9(2):95-107.
155. Perez-Losada J, Castellanos-Martin A, Mao JH. Cancer evolution and individual susceptibility. *Integr Biol (Camb)*. 2011;3(4):316-28.
156. Tada M, Furuuchi K, Kaneda M, Matsumoto J, Takahashi M, Hirai A, et al. Inactivate the remaining p53 allele or the alternate p73? Preferential selection of the Arg72 polymorphism in cancers with recessive p53 mutants but not transdominant mutants. *Carcinogenesis*. 2001;22(3):515-7.
157. Bergamaschi D, Gasco M, Hiller L, Sullivan A, Syed N, Trigiante G, et al. p53 polymorphism influences response in cancer chemotherapy via modulation of p73-dependent apoptosis. *Cancer Cell*. 2003;3(4):387-402.
158. Bonafé M, Ceccarelli C, Farabegoli F, Santini D, Taffurelli M, Barbi C, et al. Retention of the p53 Codon 72 Arginine Allele Is Associated with a Reduction of Disease-Free and Overall Survival in Arginine/Proline Heterozygous Breast Cancer Patients. *Clinical Cancer Research*. 2003;9(13):4860.
159. Schneider-Stock R, Boltze C, Peters B, Szibor R, Landt O, Meyer F, et al. Selective Loss of Codon 72 Proline p53 and Frequent Mutational Inactivation of the Retained Arginine Allele in Colorectal Cancer. *Neoplasia*. 2004;6(5):529-35.
160. Hong Y, Miao X, Zhang X, Ding F, Luo A, Guo Y, et al. The role of P53 and MDM2 polymorphisms in the risk of esophageal squamous cell carcinoma. *Cancer Res*. 2005;65(20):9582-7.
161. Mitra S, Misra C, Singh RK, Panda CK, Roychoudhury S. Association of specific genotype and haplotype of p53 gene with cervical cancer in India. *Journal of clinical pathology*. 2005;58(1):26-31.
162. Katkoori VR, Jia X, Shanmugam C, Wan W, Meleth S, Bumpers H, et al. Prognostic significance of p53 codon 72 polymorphism differs with race in colorectal adenocarcinoma. *Clinical cancer research : an official journal of the American Association for Cancer Research*. 2009;15(7):2406-16.

163. Rogler A, Rogenhofer M, Borchardt A, Lunz J-C, Knoell A, Hofstaedter F, et al. P53 codon 72 (Arg72Pro) polymorphism and prostate cancer risk: association between disease onset and proline genotype. *Pathobiology*. 2011;78(4):193-200.
164. Marin MC, Jost CA, Brooks LA, Irwin MS, O'Nions J, Tidy JA, et al. A common polymorphism acts as an intragenic modifier of mutant p53 behaviour. *Nature genetics*. 2000;25:47.
165. de Ostrovich KK, Lambertz I, Colby JK, Tian J, Rundhaug JE, Johnston D, et al. Paracrine overexpression of insulin-like growth factor-1 enhances mammary tumorigenesis in vivo. *The American journal of pathology*. 2008;173(3):824-34.
166. Movahedi K, Laoui D, Gysemans C, Baeten M, Stange G, Van den Bossche J, et al. Different tumor microenvironments contain functionally distinct subsets of macrophages derived from Ly6C(high) monocytes. *Cancer Res*. 2010;70(14):5728-39.
167. Andrechek ER, Laing MA, Girgis-Gabardo AA, Siegel PM, Cardiff RD, Muller WJ. Gene expression profiling of neu-induced mammary tumors from transgenic mice reveals genetic and morphological similarities to ErbB2-expressing human breast cancers. *Cancer Res*. 2003;63(16):4920-6.
168. Park SW, Chen SW, Kim M, Brown KM, Kolls JK, D'Agati VD, et al. Cytokines induce small intestine and liver injury after renal ischemia or nephrectomy. *Lab Invest*. 2011;91(1):63-84.
169. Carron EC, Homra S, Rosenberg J, Coffelt SB, Kittrell F, Zhang Y, et al. Macrophages promote the progression of premalignant mammary lesions to invasive cancer. *Oncotarget*. 2017;8(31):50731-46.
170. Lopez-Arribillaga E, Rodilla V, Pellegrinet L, Guiu J, Iglesias M, Roman AC, et al. Bmi1 regulates murine intestinal stem cell proliferation and self-renewal downstream of Notch. *Development*. 2015;142(1):41-50.
171. Rijnkels M, Freeman-Zadrowski C, Hernandez J, Potluri V, Wang L, Li W, et al. Epigenetic modifications unlock the milk protein gene loci during mouse mammary gland development and differentiation. *PloS one*. 2013;8(1):e53270.

172. Tuominen VJ, Ruotoistenmaki S, Viitanen A, Jumppanen M, Isola J. ImmunoRatio: a publicly available web application for quantitative image analysis of estrogen receptor (ER), progesterone receptor (PR), and Ki-67. *Breast cancer research : BCR*. 2010;12(4):R56.
173. Schindelin J, Arganda-Carreras I, Frise E, Kaynig V, Longair M, Pietzsch T, et al. Fiji: an open-source platform for biological-image analysis. *Nature Methods*. 2012;9:676.
174. Schindelin J, Rueden CT, Hiner MC, Eliceiri KW. The imagej ecosystem: An open platform for biomedical image analysis. *Mol Reprod Dev*. 2015;82.
175. Schneider CA, Rasband WS, Eliceiri KW. Nih image to imagej: 25 years of image analysis. *Nat Methods*. 2012;9.
176. Cheon DJ, Orsulic S. Mouse models of cancer. *Annual review of pathology*. 2011;6:95-119.
177. Sivaraman L, Stephens LC, Markaverich BM, Clark JA, Krnacik S, Conneely OM, et al. Hormone-induced refractoriness to mammary carcinogenesis in Wistar-Furth rats. *Carcinogenesis*. 1998;19(9):1573-81.
178. Sivaraman L, Conneely OM, Medina D, O'Malley BW. p53 is a potential mediator of pregnancy and hormone-induced resistance to mammary carcinogenesis. *Proceedings of the National Academy of Sciences of the United States of America*. 2001;98(22):12379-84.
179. Medina D. Mammary developmental fate and breast cancer risk. *Endocrine-related cancer*. 2005;12(3):483-95.
180. Guy CT, Webster MA, Schaller M, Parsons TJ, Cardiff RD, Muller WJ. Expression of the neu protooncogene in the mammary epithelium of transgenic mice induces metastatic disease. *Proceedings of the National Academy of Sciences of the United States of America*. 1992;89(22):10578-82.
181. Scholzen T, Gerdes J. The Ki-67 protein: from the known and the unknown. *J Cell Physiol*. 2000;182(3):311-22.

182. Li B, Rosen JM, McMenamin-Balano J, Muller WJ, Perkins AS. neu/ERBB2 cooperates with p53-172H during mammary tumorigenesis in transgenic mice. *Molecular and cellular biology*. 1997;17(6):3155-63.
183. Ursini-Siegel J, Schade B, Cardiff RD, Muller WJ. Insights from transgenic mouse models of ERBB2-induced breast cancer. *Nature reviews Cancer*. 2007;7(5):389-97.
184. Costarelli V, Yiannakouris N. Breast cancer risk in women: the protective role of pregnancy. *Nursing standard*. 2010;24(18):35-40.
185. MacMahon B, Cole P, Lin TM, Lowe CR, Mirra AP, Ravnihar B, et al. Age at first birth and breast cancer risk. *Bull World Health Organ*. 1970;43(2):209-21.
186. Albrektsen G, Heuch I, Hansen S, Kvale G. Breast cancer risk by age at birth, time since birth and time intervals between births: exploring interaction effects. *British journal of cancer*. 2005;92(1):167-75.
187. Bruzzi P, Negri E, La Vecchia C, Decarli A, Palli D, Parazzini F, et al. Short term increase in risk of breast cancer after full term pregnancy. *BMJ*. 1988;297(6656):1096-8.
188. Meier-Abt F, Bentires-Alj M. How pregnancy at early age protects against breast cancer. *Trends Mol Med*. 2014;20(3):143-53.
189. Lambertini M, Santoro L, Del Mastro L, Nguyen B, Livraghi L, Ugolini D, et al. Reproductive behaviors and risk of developing breast cancer according to tumor subtype: A systematic review and meta-analysis of epidemiological studies. *Cancer treatment reviews*. 2016;49:65-76.
190. Yang XR, Chang-Claude J, Goode EL, Couch FJ, Nevanlinna H, Milne RL, et al. Associations of breast cancer risk factors with tumor subtypes: a pooled analysis from the Breast Cancer Association Consortium studies. *Journal of the National Cancer Institute*. 2011;103(3):250-63.
191. Medina D, Kittrell FS. p53 function is required for hormone-mediated protection of mouse mammary tumorigenesis. *Cancer Res*. 2003;63(19):6140-3.

192. Currier N, Solomon SE, Demicco EG, Chang DL, Farago M, Ying H, et al. Oncogenic signaling pathways activated in DMBA-induced mouse mammary tumors. *Toxicol Pathol.* 2005;33(6):726-37.
193. Medina D, Smith GH. Chemical carcinogen-induced tumorigenesis in parous, involuted mouse mammary glands. *Journal of the National Cancer Institute.* 1999;91(11):967-9.
194. Katz TA. Potential Mechanisms underlying the Protective Effect of Pregnancy against Breast Cancer: A Focus on the IGF Pathway. *Front Oncol.* 2016;6:228.
195. Campisi J. Aging, cellular senescence, and cancer. *Annu Rev Physiol.* 2013;75:685-705.
196. Garcia PB, Attardi LD. Illuminating p53 function in cancer with genetically engineered mouse models. *Semin Cell Dev Biol.* 2014;27:74-85.
197. Siddique M, Sabapathy K. Trp53-dependent DNA-repair is affected by the codon 72 polymorphism. *Oncogene.* 2006;25(25):3489-500.
198. Narita M, Nunez S, Heard E, Narita M, Lin AW, Hearn SA, et al. Rb-mediated heterochromatin formation and silencing of E2F target genes during cellular senescence. *Cell.* 2003;113(6):703-16.
199. Vaughan S, Jat PS. Deciphering the role of nuclear factor-kappaB in cellular senescence. *Aging (Albany NY).* 2011;3(10):913-9.
200. Hanahan D, Weinberg RA. Hallmarks of cancer: the next generation. *Cell.* 2011;144(5):646-74.
201. Qian BZ, Pollard JW. Macrophage diversity enhances tumor progression and metastasis. *Cell.* 2010;141(1):39-51.
202. Padala C, Tupurani MA, Puranam K, Gantala S, Shyamala N, Kondapalli MS, et al. Synergistic effect of collagenase-1 (MMP1), stromelysin-1 (MMP3) and gelatinase-B (MMP9) gene polymorphisms in breast cancer. *PloS one.* 2017;12(9):e0184448.

203. Folkman J. Fundamental concepts of the angiogenic process. *Curr Mol Med.* 2003;3(7):643-51.
204. Voronov E, Carmi Y, Apte RN. The role IL-1 in tumor-mediated angiogenesis. *Front Physiol.* 2014;5:114.
205. Gu H, Qiu W, Shi Y, Chen S, Yin J. Variant alleles of VEGF and risk of esophageal cancer and lymph node metastasis. *Biomarkers.* 2014;19(3):252-8.
206. VanCleave TT, Moore JH, Benford ML, Brock GN, Kalbfleisch T, Baumgartner RN, et al. Interaction Among Variant Vascular Endothelial Growth Factor (VEGF) and Its Receptor in Relation to Prostate Cancer Risk. *The Prostate.* 2010;70(4):341-52.
207. Pusztaszeri MP, Seelentag W, Bosman FT. Immunohistochemical expression of endothelial markers CD31, CD34, von Willebrand factor, and Fli-1 in normal human tissues. *J Histochem Cytochem.* 2006;54(4):385-95.
208. Balkwill F, Charles KA, Mantovani A. Smoldering and polarized inflammation in the initiation and promotion of malignant disease. *Cancer Cell.* 2005;7(3):211-7.
209. Yoshimura T. The production of monocyte chemoattractant protein-1 (MCP-1)/CCL2 in tumor microenvironments. *Cytokine.* 2017;98:71-8.
210. Martinez FO, Gordon S, Locati M, Mantovani A. Transcriptional profiling of the human monocyte-to-macrophage differentiation and polarization: new molecules and patterns of gene expression. *J Immunol.* 2006;177(10):7303-11.
211. Morris PG, Hudis CA, Giri D, Morrow M, Falcone DJ, Zhou XK, et al. Inflammation and increased aromatase expression occur in the breast tissue of obese women with breast cancer. *Cancer prevention research.* 2011;4(7):1021-9.
212. Hursting SD. Inflammatory talk: linking obesity, NF-kappaB, and Aromatase. *Cancer prevention research.* 2011;4(3):285-7.
213. Murano I, Barbatelli G, Parisani V, Latini C, Muzzonigro G, Castellucci M, et al. Dead adipocytes, detected as crown-like structures, are prevalent in visceral fat depots of genetically obese mice. *J Lipid Res.* 2008;49(7):1562-8.

214. Cha YJ, Kim ES, Koo JS. Tumor-associated macrophages and crown-like structures in adipose tissue in breast cancer. *Breast Cancer Res Treat.* 2018.
215. Lin EY, Li JF, Gnatovski L, Deng Y, Zhu L, Grzesik DA, et al. Macrophages regulate the angiogenic switch in a mouse model of breast cancer. *Cancer Res.* 2006;66(23):11238-46.
216. Brady NJ, Chuntova P, Schwertfeger KL. Macrophages: Regulators of the Inflammatory Microenvironment during Mammary Gland Development and Breast Cancer. *Mediators Inflamm.* 2016;2016:4549676.
217. Svensson S, Abrahamsson A, Rodriguez GV, Olsson AK, Jensen L, Cao Y, et al. CCL2 and CCL5 Are Novel Therapeutic Targets for Estrogen-Dependent Breast Cancer. *Clinical cancer research : an official journal of the American Association for Cancer Research.* 2015;21(16):3794-805.
218. Jackson JG, Pereira-Smith OM. p53 is preferentially recruited to the promoters of growth arrest genes p21 and GADD45 during replicative senescence of normal human fibroblasts. *Cancer Res.* 2006;66(17):8356-60.
219. Coppe JP, Patil CK, Rodier F, Sun Y, Munoz DP, Goldstein J, et al. Senescence-associated secretory phenotypes reveal cell-nonautonomous functions of oncogenic RAS and the p53 tumor suppressor. *PLoS Biol.* 2008;6(12):2853-68.
220. Barcellos-Hoff MH, Ravani SA. Irradiated mammary gland stroma promotes the expression of tumorigenic potential by unirradiated epithelial cells. *Cancer Res.* 2000;60(5):1254-60.
221. Tsai KK, Chuang EY, Little JB, Yuan ZM. Cellular mechanisms for low-dose ionizing radiation-induced perturbation of the breast tissue microenvironment. *Cancer Res.* 2005;65(15):6734-44.
222. Hayden MS, Ghosh S. Regulation of NF-kappaB by TNF family cytokines. *Semin Immunol.* 2014;26(3):253-66.
223. Jiang X, Shapiro DJ. The immune system and inflammation in breast cancer. *Molecular and cellular endocrinology.* 2014;382(1):673-82.

224. Shaked H, Hofseth LJ, Chumanevich A, Chumanevich AA, Wang J, Wang Y, et al. Chronic epithelial NF-kappaB activation accelerates APC loss and intestinal tumor initiation through iNOS up-regulation. *Proceedings of the National Academy of Sciences of the United States of America*. 2012;109(35):14007-12.
225. Siegel PM, Dankort DL, Hardy WR, Muller WJ. Novel activating mutations in the neu proto-oncogene involved in induction of mammary tumors. *Molecular and cellular biology*. 1994;14(11):7068-77.
226. Siegel PM, Muller WJ. Mutations affecting conserved cysteine residues within the extracellular domain of Neu promote receptor dimerization and activation. *Proceedings of the National Academy of Sciences of the United States of America*. 1996;93(17):8878-83.
227. Zelazny E, Li B, Anagnostopoulos AM, Coleman A, Perkins AS. Cooperating oncogenic events in murine mammary tumorigenesis: assessment of ErbB2, mutant p53, and mouse mammary tumor virus. *Experimental and molecular pathology*. 2001;70(3):183-93.
228. Arendt LM, McCreedy J, Keller PJ, Baker DD, Naber SP, Seewaldt V, et al. Obesity promotes breast cancer by CCL2-mediated macrophage recruitment and angiogenesis. *Cancer Res*. 2013;73(19):6080-93.
229. Ehling J, Bartneck M, Wei X, Gremse F, Fech V, Mockel D, et al. CCL2-dependent infiltrating macrophages promote angiogenesis in progressive liver fibrosis. *Gut*. 2014;63(12):1960-71.
230. Lin EY, Nguyen AV, Russell RG, Pollard JW. Colony-stimulating factor 1 promotes progression of mammary tumors to malignancy. *J Exp Med*. 2001;193(6):727-40.
231. Palmer BF, Clegg DJ. The sexual dimorphism of obesity. *Molecular and cellular endocrinology*. 2015;402:113-9.
232. Neuhouser ML, Aragaki AK, Prentice RL, Manson JE, Chlebowski R, Carty CL, et al. Overweight, Obesity, and Postmenopausal Invasive Breast Cancer Risk: A Secondary Analysis of the Women's Health Initiative Randomized Clinical Trials. *JAMA Oncol*. 2015;1(5):611-21.

233. Park YM, White AJ, Nichols HB, O'Brien KM, Weinberg CR, Sandler DP. The association between metabolic health, obesity phenotype and the risk of breast cancer. *Int J Cancer*. 2017;140(12):2657-66.
234. Ando S, Malivindi R, Catalano S, Rizza P, Barone I, Panza S, et al. Conditional expression of Ki-Ras(G12V) in the mammary epithelium of transgenic mice induces estrogen receptor alpha (ERalpha)-positive adenocarcinoma. *Oncogene*. 2017;36(46):6420-31.
235. Nandi S, Guzman RC, Yang J. Hormones and mammary carcinogenesis in mice, rats, and humans: a unifying hypothesis. *Proceedings of the National Academy of Sciences of the United States of America*. 1995;92(9):3650-7.
236. Blakely CM, Stoddard AJ, Belka GK, Dugan KD, Notarfrancesco KL, Moody SE, et al. Hormone-induced protection against mammary tumorigenesis is conserved in multiple rat strains and identifies a core gene expression signature induced by pregnancy. *Cancer Res*. 2006;66(12):6421-31.
237. Medina D. Pregnancy protection of breast cancer: new insights reveal unanswered questions. *Breast cancer research : BCR*. 2013;15(3):103.
238. Kitamura T, Qian BZ, Soong D, Cassetta L, Noy R, Sugano G, et al. CCL2-induced chemokine cascade promotes breast cancer metastasis by enhancing retention of metastasis-associated macrophages. *J Exp Med*. 2015;212(7):1043-59.
239. Cowen S, McLaughlin SL, Hobbs G, Coad J, Martin KH, Olfert IM, et al. High-Fat, High-Calorie Diet Enhances Mammary Carcinogenesis and Local Inflammation in MMTV-PyMT Mouse Model of Breast Cancer. *Cancers (Basel)*. 2015;7(3):1125-42.
240. Qiu TH, Chandramouli GV, Hunter KW, Alkharouf NW, Green JE, Liu ET. Global expression profiling identifies signatures of tumor virulence in MMTV-PyMT-transgenic mice: correlation to human disease. *Cancer Res*. 2004;64(17):5973-81.
241. Guy CT, Cardiff RD, Muller WJ. Induction of mammary tumors by expression of polyomavirus middle T oncogene: a transgenic mouse model for metastatic disease. *Molecular and cellular biology*. 1992;12(3):954-61.

242. Baker DJ, Wijshake T, Tchkonina T, LeBrasseur NK, Childs BG, van de Sluis B, et al. Clearance of p16Ink4a-positive senescent cells delays ageing-associated disorders. *Nature*. 2011;479(7372):232-6.
243. Osorio FG, Barcena C, Soria-Valles C, Ramsay AJ, de Carlos F, Cobo J, et al. Nuclear lamina defects cause ATM-dependent NF-kappaB activation and link accelerated aging to a systemic inflammatory response. *Genes & development*. 2012;26(20):2311-24.
244. Tilstra JS, Robinson AR, Wang J, Gregg SQ, Clauson CL, Reay DP, et al. NF-kappaB inhibition delays DNA damage-induced senescence and aging in mice. *The Journal of clinical investigation*. 2012;122(7):2601-12.
245. Di Renzo L, Gratteri S, Sarlo F, Cabibbo A, Colica C, De Lorenzo A. Individually tailored screening of susceptibility to sarcopenia using p53 codon 72 polymorphism, phenotypes, and conventional risk factors. *Dis Markers*. 2014;2014:743634.
246. Volodko N, Salla M, Eksteen B, Fedorak R, Huynh H, Baksh S. TP53 codon 72 Arg/Arg polymorphism is associated with a higher risk for inflammatory bowel disease development. *World Journal of Gastroenterology*. 2015;21(36):10358-66.
247. Dakouras A, Nikiteas N, Papadakis E, Perakis M, Valis D, Rallis G, et al. P53Arg72 homozygosity and its increased incidence in left-sided sporadic colorectal adenocarcinomas, in a Greek-Caucasian population. *Anticancer Res*. 2008;28(2A):1039-43.
248. Dastjerdi MN. TP53 codon 72 polymorphism and P53 protein expression in colorectal cancer specimens in Isfahan. *Acta Med Iran*. 2011;49(2):71-7.
249. Perez LO, Abba MC, Dulout FN, Golijow CD. Evaluation of p53 codon 72 polymorphism in adenocarcinomas of the colon and rectum in La Plata, Argentina. *World J Gastroenterol*. 2006;12(9):1426-9.
250. Schneider-Stock R, Boltze C, Peters B, Szibor R, Landt O, Meyer F, et al. Selective loss of codon 72 proline p53 and frequent mutational inactivation of the retained arginine allele in colorectal cancer. *Neoplasia*. 2004;6(5):529-35.

251. Alawadi S, Ghabreau L, Alsaleh M, Abdulaziz Z, Rafeek M, Akil N, et al. P53 gene polymorphisms and breast cancer risk in Arab women. *Med Oncol.* 2011;28(3):709-15.

252. Surekha D, Sailaja K, Rao DN, Padma T, Raghunadharao D, Vishnupriya S. Codon 72 and G13964C intron 6 polymorphisms of TP53 in relation to development and progression of breast cancer in India. *Asian Pac J Cancer Prev.* 2011;12(8):1893-8.